SPring-8 Upgrade Plan
Preliminary Report

RIKEN/JASRI

SPring-8

January, 2012

Contents

Contributors

Tetsuya Ishikawa, Shunji Goto, Hideo Kitamura, Noritaka Kumagai, Haruo Ohkuma, Hideo Ohno, Yoshitsugu Shiro, Masaki Takata, Hitoshi Tanaka, Ryotaro Tanaka
Hideo Ago, Hideki Aoyagi, Takao Asaka, Alfred Baron, Hideki Dewa, Hiroyasu Ego, Takahiro Fujita, Akihiko Fujiwara, Kenji Fukami, Kazuya Hasegawa, Yuji Higo, Naohisa Hirao, Yuka Ikemoto, Eiji Ikenaga, Kenichi Kato, Yoshiaki Kawano, Akio Kiyomichi, Yoshiki Kohmura, Masato Kotsugi, Naoki Kunishima, Mitsuhiro Masaki, Takemasa Masuda, Takahiro Matsumoto, Chikaori Mitsuda, Akira Mochihashi, Mitsuru Nagasono, Takeshi Nakamura, Tetsuya Nakamura, Toru Ohata, Yuichi Okayasu, Choji Saji, Yasunori Senba, Yoshito Shimosaki, Mari Shimura, Kouichi Soutome, Michihiro Sugahara, Kunihisa Sugimoto, Takashi Sugimoto, Motohiro Suzuki, Masamitsu Takahashi, Yukio Takahashi, Yusuke Tamenori, Takashi Tanaka, Yoshihito Tanaka, Masaru Takao, Hidenori Toyokawa, Takahiro Watanabe, Makina Yabashi, Masaki Yamamoto, Hiroshi Yamazaki, Koji Yonekura, Hirokatsu Yumoto

Chapter 1

Executive Summary

We propose upgrading the SPring-8 light source in the year 2019 in order to advance promising science and to support industrial innovations that will improve our life and contribute to a more sustainable society. The upgrade is expected to bring fundamental changes to photon science by providing (1) the highest ever brilliance and user capacity via unprecedented throughput, and (2) a unique combination with the X-ray Free Electron Laser (XFEL), SACLA. Further, the outstanding capabilities of the X-ray light source will be delivered within a highly energy-efficient facility. New scientific research enabled by the upgrade will be indispensable for developing sciences and technologies as well as creating new industrial fields that will solve diverse problems affecting human health, energy consumption, and other critical issues.

Photon science has contributed to a wide spectrum of fields in science, technology, culture and other areas. Taking advantage of its high brilliance and the short wavelength X-rays from a storage ring, scientists have been able to determine microscopic structures of functional materials and bio-molecules, which are indispensable for today's society. Because current observations are limited to certain layers of hierarchy in the key materials, our current knowledge is insufficient to create elaborate designs for advanced functional materials and for the development of versatile drugs. Demands for such functional materials have been increasing and will grow even faster due to the strong desire for a more "green" society. One sought-after key technology is self-organizing material fabrication with a low energy cost and high efficiency. Development of this technique is urgent but relies upon quick screening and precise determination of the structure and the dynamics of the synthesized materials. Current drug design, on the other hand, is facing difficulties because only the "static" structures of target proteins have been available. More efficient drug design requires a deeper understanding of the "dynamic" interactions among multiple proteins and on their temporal fluctuations. Further, a new scientific approach is needed that reveals valuable information from inhomogeneous systems since the methodologies currently used at synchrotron radiation facilities rely too much on the purity of materials under investigation. To accomplish these breakthroughs, it is extremely important

to illuminate high brilliant coherent X-ray beams on such systems so that the hierarchy and dynamics of these systems can be determined. This is why we strongly urge the upgrade of the SPring-8 light source.

SPring-8, the third generation light source, has served as one of the most powerful and reliable X-ray light sources in the world. Since operations started in 1997, a great number of achievements have been accomplished in both scientific and technological fields at the site. Moreover, SPring-8 has been one of the major pioneers in industrial uses for the light source, with beamlines dedicated to industrial applications. The performance of the light source has been continuously updated, achieving electron emittance of 3.4 nm.rad and brilliance in the order of 10^{20} [photons/sec/mm^2/mrad^2/0.1% B.W.] in the hard X-ray region. While users take full advantage of the performance from the third generation light source, they increasingly demand even higher performance in order to remain competitive with their research and innovation. Such demands are obviously common worldwide and several other new light sources have been constructed, some of which already exceed or plan to exceed the current emittance capabilities of SPring-8.

Our main goal is to provide world-leading brilliance by bringing the SPring-8 storage ring into a new *"ultimate"* configuration in order to best meet future scientific requirements. The ultimate storage ring, i.e., one in which the electron beam emittance reaches the diffraction limits of X-rays, would produce orders of magnitude higher brilliance and a higher degree of coherence than any existing storage ring. Such a high quality beam would certainly lead to significant scientific and social impacts as discussed in Chapters 2 to 4. Yet, it is worth noting that the energy consumption of the new facility would be less than that of the current SPring-8 facility, and existing resources, such as buildings, facilities, and equipment, would effectively be reused. In summary, the SPring-8 upgrade plan aims to achieve *an ultimate-performance energy-effective facility*. From the perspective of user experiments, major characteristics of the ultimate storage ring are: 1) The new ring would produce 1,000 times higher brilliance than the current SPring-8, and would significantly reduce the time and cost for experiments. 2) The increase in the degree of coherence would expand applications based on the coherent nature of light. The coherent X-ray imaging would allow observations of interacting systems in various length scales with a resolution, in principle, of an X-ray wavelength. 3) A short X-ray pulse option of around one pico-second would allow us to explore time domain studies with a wide range of time scales. SPring-8 after the upgrade would definitely open frontiers of new methodologies required for the future. Consider two orientations of scientific research as examples. First, the upgraded SPring-8 would have no equal for the comprehensive understanding of the hierarchy of interacting and inhomogeneous systems in science using coherent X-ray imaging and time-domain studies. Second, in a similar manner, there would be no other facility other than the upgraded SPring-8 better suited for statistical analysis using X-rays for understanding

the fundamental individual differences in the diversity of nature.

In 2011 the Japanese XFEL (SACLA) achieved successful lasing, and in 2012 user operations will commence. The roles for SACLA and the upgraded SPring-8 are clear since these two ultimate light sources are dedicated to completely different applications. The synergetic use of the two world-leading light sources will lead us to fruitful scientific frontiers by allowing an accumulation of complementary knowledge of scientific objects. First, SACLA enables ultra-fast measurements and atomic-resolution snapshots of local structures due to its high peak brilliance and femto-second pulse widths. While measurements using SACLA may severely damage samples, the peak brilliance of the upgraded SPring-8 would be orders of magnitude less, below the destruction threshold, but with an average brilliance still sufficiently high. Such performance of the upgraded SPring-8 would enable non-destructive or repeated data-accumulation on individual samples with an extremely short exposure time, complementarily to the measurements using SACLA. Second, SACLA offers an opportunity to investigate highly excited states in relatively simple matter samples, while the upgraded SPring-8 would be well-suited for the study of complex systems in the ground or at lower excited states. In addition to the separate use of the two facilities, X-ray (SACLA) pump-X-ray (SPring-8) probe experiments are planned to explore fundamental physics in the X-ray-excited states and their relaxation processes in matters. Thus, not only would the two world-leading light sources produce important results independently, the combination of the two would provide brand-new opportunities for future research in photon science.

The cost range of the upgrade is expected to be approximately 40 billion Japanese yen. This includes the upgrade of the storage ring, insertion devices, and beamlines. The existing buildings, including the accelerator tunnel and beamline hutches, would be reused in order to contain the total budget. The upgrade is planned to be executed in 2019, with an expected shutdown time of one year for minimizing the influence on users. The upgrade design discussed in this report takes all these conditions into consideration.

Chapter 2

Overview of the SPring-8 Upgrade Plan

2.1 Motivation for the SPring-8 upgrade

SPring-8 is one of the highest performance light source facilities in the world. Its mission is to support our society by producing a great quantity of important research in various fields such as science, industry and culture. In this section, we address the need for the SPring-8 upgrade.

Today, we enjoy the benefits of a modern society with abundant cultural activities, general security and a healthy lifestyle. Our comfortable life and activities are supported by advanced industries and medical services that have been established through years of accumulation of scientific knowledge. Continued development in science and technology is essential to sustain these benefits and achieve further improvements in the future. First, fundamental scientific research is applied to new technological applications. Then industry develops products to address social problems. After the twenty-first century, there are still many unresolved social and environmental problems, such as energy issues, global warming, and treatment for chronic disease and congenital disorders. Potential solutions are closely related to scientific and technological challenges yet to be resolved. The mission of research facilities is to address these social problems through new scientific inventions or discoveries.

Research using hard X-rays is based on physical and chemical processes at an atomic scale. For materials science, useful capabilities in new functional materials (e.g., high efficiency batteries, ultra-dense magnetic recording media, clean catalysts, and semiconductor memory chips) emerge as a result of the electronic nature of materials at the atomic scale. The key fabrication technology for future functional materials will be based on schemes of a self-organization mechanism for reducing energy consumption. For biological sciences, almost all biological activities, such as energy metabolism, gene maintenance and replication, and inter- and intra-cellular signal transduction proceed through the dynamical transition and collaboration of macromolecules. For example, potential drugs reactions can be understood through the dynamics of protein molecules. Thus, research revealing the structure and the dynamics of materials using hard

X-rays, have played and will continue to play key roles in the fundamental sciences during the next twenty years.

This is where SPring-8 comes into play. As SPring-8 is able to generate X-rays, especially hard X-rays of the highest brilliance, many scientists have come from all over the world in order to explore various kinds of research in key fields. From the viewpoint of users, higher brilliance allows *more precise observation during a shorter data acquisition time of smaller objects at a higher spatial resolution.* However, the reason why SPring-8 has attracted many users is not only because of its capabilities as a light source, such as high brilliance and stability, but also because we have contributed to society in two aspects. First, extensive research in fundamental sciences has been completed. As research outcomes have accumulated over the years, the resulting knowledge base will contribute to society through enabling future technological innovations. Second, a large amount of research executed at SPring-8 targets industrial applications in fields such as electronic devices, drugs, batteries, cosmetics, automobile tires, fibers, and polymers. SPring-8 has proved that synchrotron radiation is a useful tool not only for fundamental science but also for a wide variety of industrial applications. Increasing demands for using SPring-8 come from both scientific and industrial fields.

In order to meet the increasing light source requirements, the whole facility has continuously improved. Now, the available experimental time per user is already exhausted and little space remains for improving the capacity of the facility. On the other hand, a number of light sources have been constructed or upgraded in Asia, Europe, and the U.S., especially during the last ten years. Several of these facilities already exceed or plan to exceed current SPring-8 performance in key parameters.

We strongly recommend an upgrade of SPring-8 for the following reasons. In order to support a growing number of users and maintain competitiveness with their research requires improving the light source performance. The upgrade would benefit users from two perspectives. First, the upgrade aims to significantly improve the quality of light (as discussed in detail in the following sections) providing great new capabilities for cutting-edge research. Second, improved light source performance would provide additional opportunities for research by reducing the time required for each experiment. As will be shown, the brilliance of the newly designed facility is 1,000 times greater. It follows that acquisition time would be reduced by orders of magnitude, and with appropriate infrastructure development, more users would benefit from the new light source. Thus, all the research from cutting-edge sciences to industrial works could take advantage of the upgrade. In summary, we conclude that the upgrade of SPring-8 would benefit society by enabling profound new discoveries and technological innovations.

In the following sections, we first state the key concepts of our upgrade plan, also known as SPring-8 II, which provide a platform for world-leading research to be conducted in SPring-8 over the next twenty years. We then briefly introduce the pioneering science research that

would be achievable using the upgraded SPring-8. We then close the chapter by showing the superiority of our upgraded facility over other present and planned light source facilities.

2.2 Key concepts of the upgrade

In this section, we present the following key concepts for our upgrade plan and show how these concepts apply to future research:

1. An ultimate storage ring in hard X-ray regime.
2. Synergetic use with the X-ray Free Electron Laser.
3. An energy-efficient facility.

The following sections describe the details of each key concept.

2.2.1 Ultimate storage ring

The first and most important key concept for the upgrade is an ultimate storage ring in the hard X-ray region. We propose to upgrade SPring-8 to "ultimate" status by pushing the light source performance to its limits in two aspects, spatial coherence and brilliance. In the following sections, we present the vastly improved light source performance anticipated by upgrading SPring-8.

Diffraction limit

For the first goal of the ultimate ring, we plan to make the electron beam emittance comparable to the diffraction limit of X-rays so that the spatial coherence approaches unity. The degree of spatial coherence is determined by a product of the beam size and the divergence, known as photon emittance. In a storage ring, a circulating electron beam emits light. Its emittance is calculated from a combination of the electron beam emittance (defined in the same way as that of the photons it produces) and the photon emittance contributed by a single electron. Thus, as the electron emittance decreases, the photon emittance of light generated from a storage ring improves (i.e., decreases), and correspondingly the spatial coherence of light improves. However, the photon emittance has a minimum attainable value due to the diffraction properties of light. The intrinsic minimum product is called the diffraction limit, and is written as $\sigma_r = \lambda/4\pi$. For $\lambda = 0.1$ nm, for example, the diffraction limit is $\sigma_r \approx 10$ pm.rad. In the upgrade program, we propose to make the electron beam emittance in the same order as the diffraction limit, σ_r. The current electron emittance of SPring-8 is 3,400 pm.rad. We propose to reduce it by about

100 times with the upgrade to SPring-8 II, which would result in a dramatic improvement in the spatial coherence of the light.

Using an X-ray beam with such a large spatial coherence length would provide users with new opportunities for focusing experiments with nanometer-order probe beams. Moreover, the scanning coherent X-ray imaging (ptychography) method [1–3] would become much easier for users with orders of magnitude shorter acquisition time and for objects with various sizes. All these methods, not accessible in other facilities, would enable SPring-8 to complete world-leading research and to study more complex, smaller structures in materials that are important in various fields of science. In other words, the upgraded facility would be best suited to solve the hierarchy within various systems as summarized in Sections 2.3.1 and 3.1.

Ultimate brilliance

For the second goal of the ultimate ring, we plan to achieve ultimate brilliance from a storage ring. For this purpose, the huge improvement in electron beam emittance mentioned above works well. The reduction of emittance by a couple of orders of magnitude would bring the brilliance to a significantly higher level than what is currently available at SPring-8. In addition, we will develop insertion devices, especially in-vacuum undulators, in which making shorter undulator periods and narrowing the undulator gap will be key objectives. A combination of the improvement of insertion devices and a great reduction in the emittance of the electron beam is expected to increase the brilliance of SPring-8's light to an ultimately high level. Our plan is to provide high brilliance undulator radiation, in the X-ray region with energies up to 100 keV. Details of the accelerator development and the resulting spectra of light are presented in Chapters 5 and 6, respectively.

A great improvement in the brilliance practically enhances opportunities of experiments and effectively increases beamtime by a factor of around 1,000. This results in two important effects. First, it leads to a remarkable increase in the number of acceptable users. Second, it results in a significantly larger number of measurable samples per beamtime due to the shortening of the acquisition time. The latter effect will lead to a new statistical analysis using a synchrotron radiation source for the first time (see Sections 2.3.2 and 3.2).

2.2.2 Synergetic use with the X-ray Free Electron Laser, SACLA

The second key concept is to develop a facility where unique science and technology concepts are tested by using both SPring-8 II and SACLA, the new X-ray free-electron Laser (XFEL) facility. First, SPring-8 will have the option of using the XFEL linac as an injector for the newly designed storage ring (as discussed in detail in Section 5.2). This is advantageous because the new injector, having extremely low emittance beams, matches well with the new storage ring,

and it is also cost effective. The new injector provides very short electron bunches, which may also benefit the short X-ray pulse generation in the storage ring. Second, construction of the XFEL-SPring-8 experimental facility was completed in 2011. In this facility, an experimental hutch was built where the same sample can be illuminated by X-ray beams from both SPring-8 II and SACLA. Many frontiers of science cultivated by the synergetic use of these two light sources are surveyed and summarized in Section 2.3.3 and Chapter 4.

2.2.3 Energy-efficient facility

The third key concept of the upgrade of SPring-8 is to design an energy-efficient facility. As mentioned in Chapter 1, the upgrade plan aims not only to significantly improve the light source performance, but also to make it energy-efficient. First, we will fully utilize existing resources such as buildings and equipment. Although it imposes several major constraints on the new accelerator design as discussed in Chapter 5,the reuse of as many resources as possible is regarded as one of the most important bottom line benefits in the upgrade plan. Second, a new storage ring will be designed such that it consumes less energy than the current ring. Energy efficiency is a growing concern for current and future scientific projects. The newly designed light source will match the demand for a more sustainable society by yielding orders of magnitude higher performance with less energy consumption. As discussed in Chapter 5, the newly designed storage ring would reduce energy consumption by about 30 %, or even much more if we opted for an alternate design (see Table 5.8).The light brilliance generated by the new ring is estimated to be 1,000 times higher (see Fig. 6.1), and the increase of the flux at a sample could become even larger as indicated in Chapter 6. Thus, the upgrade plan proposes a considerably more energy-efficient facility.

Our strategy of reconstructing beamlines is to yield the best quality and highest brilliance beams at a maximum number of beamlines. In terms of beamline optical axes, we will keep the optical axes of normal undulator beamlines fixed, while bending beamline optical axes may eventually be moved by the new accelerator design. Additionally, plans call for mini-undulators with a short period (total length 10 cm) which generate a higher brilliance of X-rays than the existing standard undulators, due to the extremely low electron beam emittance.

2.3 Pioneering science using the upgraded SPring-8

In this section we show the expected benefits and the breakthrough in various fields of science using the new technologies achievable with the upgrade plan, which could never be achieved with the current SPring-8 configuration.

2.3.1 Resolving the hierarchy within systems using diffraction limited X-rays

The first new target in science for the next 20 years will be to clarify the hierarchical arrangement and its temporal evolution within systems that have spatial and temporal in-homogeneity. For such observations, SPring-8 II's beam would be a particularly effective tool, with its high brilliance, its high spatial coherence and its short time duration.

A diffraction limited hard X-ray beam could be achieved on the millimeter scale at SPring-8 II where the majority of X-rays are spatially coherent due to the extremely small emittance of the source in two dimensions (see details in Section 6.1). In Coherent Diffraction Imaging (CDI), a lens-less microscopy technique, an electron density distribution of an object in real space is retrieved from its recorded X-ray diffraction patterns. The observation of objects with a wide range of sizes, between millimeters and sub-micrometers, would be possible by scanning CDI (ptychography) method [1–3] for achieving a large field of view. The structural hierarchy of various biological and material samples could be elucidated for the first time using X-ray imaging as the main tool. CDI measurements are also planned at XFEL facilities, where hard X-rays with a slightly better spatial coherence are expected to be generated. However, an extremely high photon number within a short pulse duration, on the order of 10 fs, causes severe radiation damage to nearly all samples exposed. SPring-8 II would be the most powerful tool for elucidating the hierarchical organization within scientific objects using such ultimate, non-destructive imaging, since such research cannot be performed at existing XFEL facilities. The scientific outcomes expected from the research on these structural hierarchies is summarized in Section 3.1.

2.3.2 Statistical analysis using intense brilliance of X-rays

The second major target for science over the next 20 years will be to resolve the fundamental nature of individual differences using statistical analysis. For such a study, often more than 100 measurements are needed over the samples grown in the same conditions. The best way of obtaining statistically significant data over such a large number of samples would be to prepare samples with a very small size, which matches the focus size of the high intensity focused X-ray beam. SPring-8 II would provide an ideal beam for such experiments because the high degree of spatial coherence (see Section 6.1.5) enables diffraction-limited focusing and more than four orders of magnitude higher X-ray intensity to 50 nm focus size, compared with existing SPring-8 capabilities (see Section 6.3.3). More than four orders of magnitude higher throughput would completely change the conceptualization of the measurement schemes using synchrotron radiation (SR). Only well-characterized specimens, in terms of composition and so on, have been processed in conventional SR applications due to the long measuring times for

each specimen to obtain statistically significant data. SPring-8 II would remedy this problem. A new methodology using statistical analyses would clarify the fundamentally fluctuating nature of specimens. Namely, statistical analysis using SR measurements would be truly effective in science for the first time. This new approach would be especially powerful for research identifying local atmospheric environments by analyzing the nano-particles within the atmosphere, or in cell imaging to clarify the specific properties of specimens that are usually hidden by natural variations. This breakthrough due to the radical increase of the brilliance of SPring-8 II and the statistical analysis it facilitates is summarized in Section 3.2.

2.3.3 New Sciences enabled by two ultimate light sources

Aside from the previous two scientific targets, the upgraded SPring-8 engenders unique scientific capabilities arising from the synergy and complementary use with SACLA, the X-ray Free Electron Laser (XFEL). The construction of SACLA was completed in the 2010 fiscal year and its commissioning was successfully carried out in the 2011 fiscal year. Combined with the neighboring SACLA, SPring-8 II would be a unique ring source at which samples can be illuminated by the two different types of X-ray sources.

These two sources are complementary and can be used in a synergetic way as explained below. The X-ray beam from SACLA is characterized by extremely high peak brilliance, a billion times higher than that of SPring-8, a short pulse width, on the order of 10 fs and high spatial coherence. This source is attractive for many applications, e.g., allowing the fundamental processes of atomic movements to be elucidated on a femto-second time scale. On the other hand, the radiation damage to samples would, in most cases, be much less severe using SPring-8 II due to the much reduced peak brilliance, several orders of magnitudes lower than SACLA, although the brilliance averaged over time of SPring-8 II would be orders of magnitude larger. Moreover, the high repetition rate of approximately 100 MHz enables observations on a wide time scale, ranging from pico-seconds to minutes. Therefore, non-destructive measurements, especially for material sciences research, and the temporal evolution of various systems could only be effectively performed by SPring-8 II. The complementary use of SPring-8 II and SACLA (correlative imaging) would enable the observation of a wide field of view and a localized area of the same sample. The synergetic use of these two sources would enable the elucidation of the coherent optical processes in the X-ray region. The prospects for these new sciences are summarized in Chapter 4.

2.4 Status of Other Light Source Facilities

SPring-8 was constructed as one of three large third generation synchrotron radiation sources, together with the European Synchrotron Radiation Facility (ESRF, France/EU, 1995) and the

Advanced Photon Source (APS, USA, 1996). SPring-8 user operations started in 1997. The facility has provided a high brilliance X-ray beam and contributed to various breakthroughs in photon sciences by national and international researchers. Since 2000, medium sized, high quality rings have been constructed at various sites around the world. Two new projects under construction, the NSLS-II in the USA and the MAX-IV in Sweden, plan to exceed the emittance of the three large facilities, although the targeted X-ray ranges of the two new light sources are not exactly the same as those of the three facilities. Meanwhile, the 6-GeV light source, PETRA-III of DESY, began operations in 2009. The emittance of the PETRA-III reaches 1 nm.rad, smaller than SPring-8 and others, and now there are four large synchrotron radiation sources in the world. On the other hand, developments of XFELs, the fourth generation light source, are progressing in Japan (Hyogo, SACLA), USA (Stanford, LCLS) and Europe (Germany, Euro-FEL & FLASH). Additionally, compact FELs in the ultra-violet and soft X-ray regions are being developed at various sites around the world. To summarize, several sources having superior beam quality compared with SPring-8 and having completely different beam characteristics will be operational within the next ten years. The evolution of these sources has made a marked difference in both the quantity and quality of information obtained from experiments, as witnessed by the rapid development of X-ray and visible light sciences after the inventions of synchrotron radiation sources and lasers. Without doubt, the performance capabilities of the source are closely linked to the scientific achievements possible in the future. For our nation to maintain our stance in the forefront of science and technology, we need to lead in the development of synchrotron radiation sources. The purpose of the upgrade program is to maintain SPring-8's position as a center of excellence, leading the field of photon sciences during the next 10 to 20 years, only possible with innovative improvements in the accelerator and the light source quality. After this upgrade, SPring-8 II would have no equal in light-source performance. The diffraction-limited source in the hard X-ray region, in principle, would presumably have the highest performance in terms of brilliance. There are currently no definite proposals at other facilities for similar diffraction-limited sources in the hard X-ray region. The high brilliance in the hard X-ray region, one of the major merits of the large storage ring, would be maintained after the upgrade, giving SPring-8 II a significant advantage over medium size ring sources.

2.5 Contents of the report

In the following chapters, the results of various investigations for the upgrade of SPring-8 are presented. In Chapter 3, the scientific goals to be achieved during the next 10 to 20 years are listed. In Chapter 4, the pioneering areas of science that require the synergistic use of SPring-8 and SACLA are outlined. In Chapter 5, the list of technologies and the R&D required for

the accelerator components are summarized. Chapter 6presents estimates for the improved properties of the source and the X-ray beam at the sample position in an upgraded SPring-8. This report summarizes the discussions about the upgrade program that occurred during the fiscal years of 2008 and 2010 within our working group. In Appendix, the history of the activities of the working group is summarized. The names of participants in the working group and the committee members for the upgrade of SPring-8, belonging to RIKEN (Institute for Physical and Chemical Research), JASRI (JApan Synchrotron Radiation research Institute), Osaka University and International Medical Center of Japan, are listed before Chapter 1 of this report. This report will be published as the proposal from the SPring-8 facility as of 2011. We are grateful for any opinions or proposals from national or international researchers for further improvements to our proposal.

References

[1] J. M. Rodenburg *et al.*, Phil. Trans. R. Soc. Lond. A **339**, 521 (1992).

[2] J. M. Rodenburg *et al.*, Phys. Rev. Lett. **98**, 034801 (2007).

[3] H. M. L. Faulkner and J. M. Rodenburg, Phys. Rev. Lett. **93**, 023903 (2004).

Chapter 3

Scientific Vision for the Upgraded SPring-8

3.1 Comprehensive study of hierarchy in material and biological systems

3.1.1 SPring-8 II illuminates hierarchy and inhomogeneity

In material and biological systems, the hierarchy of structures is closely related to the function of these systems. To elucidate the relationship between the hierarchy and the function, the upgraded SPring-8 will play a vital role: coherent X-ray diffraction microscopy will allow imaging with a variable spatial resolution and field of view, and real-time observation with a variable temporal resolution will allow tracking the temporal development of systems with different characteristic time scales. In this chapter, we present the typical scientific targets for the study of hierarchical organization in systems, which are expected to be of great scientific importance and would be resolved using the upgraded SPring-8 facility in the next twenty years. We address most effective experimental techniques required at SPring-8 II for such scientific research.

All kinds of organisms, organic and inorganic materials have a certain degree of internal organization that is characterized by specific space and time scales. A good example is human body, in which various biological functional units are hierarchically organized, as shown in Fig. 3.1. All biological phenomenon such as thinking, sleeping, walking, eating, and so forth, are the results of combined functions of relevant organs such as brain, muscles, gastrointestinal tract etc. The functions of each organ also result from the combined functions of cells composing each organ. The cell functions are manifestations of functional collaboration of subcellular organelles and macromolecules. It is a simplified view of hierarchical layers in human body.

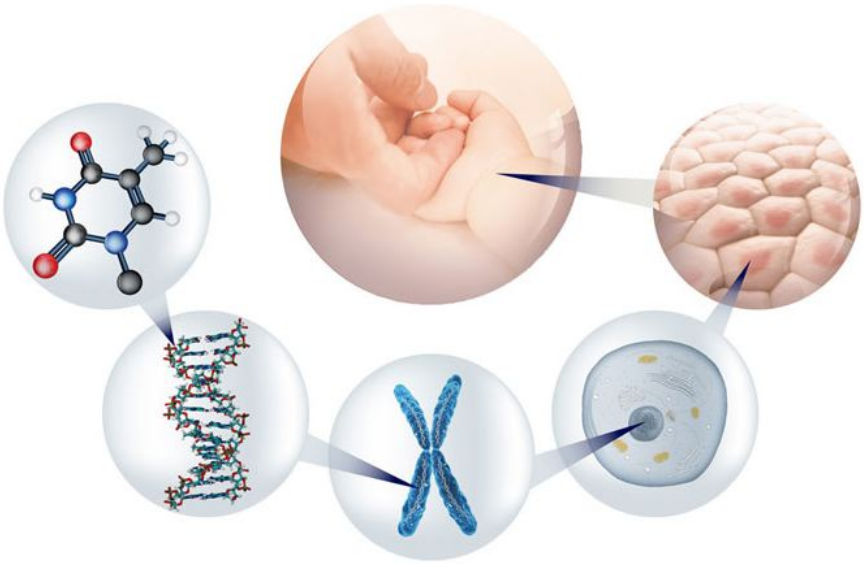

Figure 3.1: An example of hierarchy existing in the human body.

In addition, the layers do not function independently; even in a biological phenomenon there are dynamic and spatiotemporally regulated flows of inter- and intra-layer signals which allow the layers to function in a collaborative manner. Major entity of the dynamic flow of signal is a flow of molecules, such as ions, organic small molecules, macromolecules, and so forth. One of the essential contributor for the regulation of molecular flow of signal is proteins. Proteins themselves are belonging to a layer whose function is controlled spatiotemporally by other layers. Behind a biological phenomenon, there are many hierarchical layers interacting each other with spatiotemporal regulation. Therefore the major targets for biological science in the next two decades would be the understanding of the spatiotemporal collaboration of the layers behind a biological phenomenon and the clarificaion of dynamics and functions of each layer with subatomic resolution.

Inorganic materials are another example. Atoms and molecules correspond to the fundamental building blocks of materials. However, the nature of individual atoms and molecules is not always observable in matters at the macroscopic level. Actually, many layers of structural and functional units interact between the atomic and macroscopic scales. This hierarchy essentially contributes to the emergence of a wide variety of macroscopic properties of materials. A typical example could be seen in phase transition phenomena, one of the most fundamental but unresolved problems in physics. The general mechanism of phase transition could be studied using a hierarchy model: fluctuation of the electronic states–nucleation–clustering–macroscopic transition. To observe the spatial and temporal development of these hierarchical structures, which appear during the phase transition process, would be an exciting scientific topic using the SPring-8 II facility. This observation would greatly contribute to the comprehensive study of

the changes of physical properties caused by the phase transition. There are dozens of important topics such as high-Tc superconductivity, strongly correlated systems, quantum ordering. Additionally, in SPring-8 II, we could study systems in excited or non-equilibrium states, while those in ground or equilibrium states have been studied so far. When a material (or a device) exhibits some function, the system is in an excited or non-equilibrium state and this state evolves over a characteristic time scale.

The ultimate goal in material and biological science is the complete understanding of the hierarchies within systems, in other words, to explain the relationship between the activities and the functions at the top-level of a hierarchy and the properties of all the lower levels within the systems. This approach requires knowledge of the spatial and temporal structures at all the levels within a hierarchy. Using experimental techniques currently available, only a few particular levels of hierarchies could be studied. SPring-8 II offers new techniques for the seamless observation of these hierarchical structures, allowing a comprehensive understanding of the physical and biological phenomena. In the following subsections, we propose scientific subjects, unresolved today, where understanding the hierarchy of the system is an essential key and the upgraded SPring-8 would be a best suited facility for the research.

3.1.2 Static and dynamic structural biology

The minimum unit of life is a cell, which is separated from the outer space by lipid bilayer. Inside of the cell, there are various biological systems responsible for the fundamental activity of life, for instance, energy production, maintenance and duplication of genomic information on DNA, transcription of DNA into RNA, protein synthesis and so forth. Between the cells, there are inter-cellular signal transduction systems which are indispensable for functional unity of the biological body as a multi-cellular assembly. All of these biological systems are driven by biological macromolecules, such as a protein and a nucleic acid, whose function accompanies a dynamical motion, and sometimes accompanies a spatiotemporal cooperation of many biological macromolecules. To reveal the dynamical functions and collaboration of the biological macromolecules is one of the most attractive research areas using SPring-8 II, because it would help us to deeply understand the activities of life.

So far, synchrotron radiation has played an important role to study the three-dimensional structure of macromolecules by using X-ray crystallography. At present, only the static information is available using crystallography. The structure of biological macromolecules, however, helps us to clarify the mechanism of biological phenomenon with an atomic resolution. Highly brilliant synchrotron radiation boosted the throughput of the structure determination. The knowledge about the relationship between the structure and the function of biological macromolecule is accumulating rapidly, which results in the discovery of various useful drugs.

One example is G-protein coupled receptor (GPCR), which is the major target of the cur-

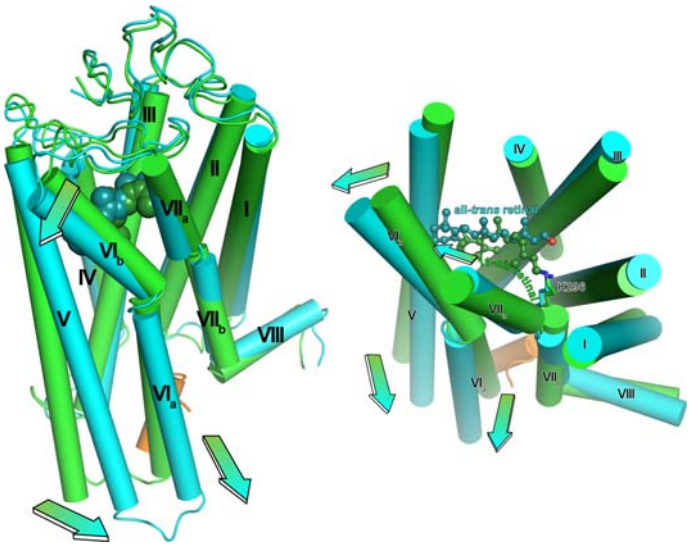

Figure 3.2: The structural comparison between the inactivated and activated states of rhodopsin as a G-protein coupled receptor (GPCR). The inactivated rhodopsin with 11-*cis*-retinal functioning as the inverse agonist is shown in green and the activated one with the all-*trans* retinal is shown in blue. Roman number shows the sequential number of α-helices from the N-terminal. The crystal structures provide the insight to the activation of rhodopsin essential for the eyesight. The structural change of retinal depending on photoreception induces the rearrangement of the transmembrane α-helices, resulting in the formation of the space for binding of the C-terminal part of Gα-protein (orange).

rently approved medicines [1]. The first crystal structure of GPCR was determined at SPring-8 one decade ago [2], and provided many insights into the signal transduction mechanism by GPCR (Fig. 3.2). After that, appearance of micro-beam MX beamlines, as well as development of techniques to improve the thermal stability of GPCR, has contributed to the structure determination of human GPCR, such as β_2 adrenergic receptor, A_{2A} adenosince receptor, chemokine receptor CXCR4, histamine H1 receptor [3–12]. Now, pharmaceutical companies are tackling to develope new drugs by using the structural information of GPCR [13, 14].

Since, there are still a lot of biological macromolecules whose structure is attracting researchers' interest from both scientific and applicative view points, the static structural study of biological macromolecule would definitely occupy one of the major area of synchrotron radiation research in the next few decades. Highly intense X-rays available at SPring-8 II would enable the structure determination using sub-micron crystal, and boosts the structure determination of challenging targets.

On the other hand, the direct and continuous observation of the structural transformation of biological macromolecule at atomic resolution has been the dream in the structural biology, because such a transformation is closely related with the dynamic function of the biological macromolecules (Fig. 3.3). Currently we need to imagine the dynamical motion of macromolecules

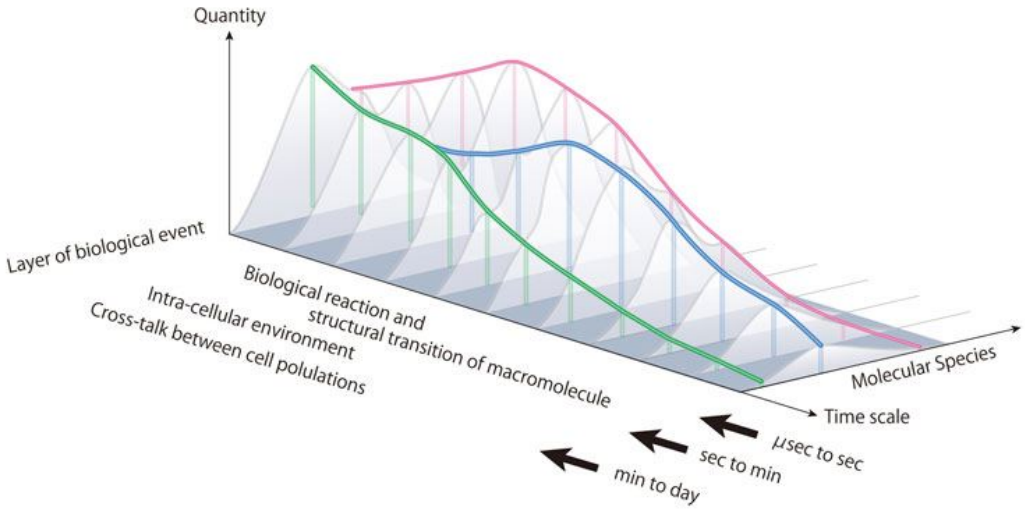

Figure 3.3: Dynamics of biological event. Life is composed of dynamic and layered biological events interacting closely each other and also having different time scale and spatial size. There must exist an optimized time and spatial resolution for observing each event. Such optimization would be easy using the upgraded SPring-8.

based on the stable intermediate state which appears in the time course of the structural transformation. For instance, the structural transformation of the calcium pump of sarcoplasmic reticulum, responsible for the ATP dependent Ca^{2+} transport, was determined at atomic resolution [15–17]. Another example is the molecular mechanisms of the pathogenesis of myopathy which were studied by means of the X-ray diffraction experiment of human muscle cells under different conditions at SPring-8. This study elucidated the effects of the myopathy-linked point mutation [18]. As such, the direct and continuous observation during the structural transformation would deepen our understanding of dynamical functioning of biological macromolecules.

The direct and continuous observation is also important for the understanding of the whole spatiotemporal collaboration of biological macromolecules driving the biological system. It would be an ambitious target for understanding the life in a comprehensive way (Fig. 3.4). The so-called "system biology" is a research area by which the whole map of the spatiotemporal collaboration of biological macromolecules could be described from the viewpoint of the gene expression. However, the spatiotemporal collaboration of biological macromolecules has been hardly studied from the structural aspect due to the technological difficulty. The direct and continuous observation of dynamical assemble/disassemble of macromolecules is informative even at low resolution to understand the collaboration of biological macromolecules. For example, the continuous small angle X-ray scattering measurement of the solution structure revealed that the periodic structural transformation of KaiC with a 24-hours cycle is the timing cue of the association/dissociation of other clock protein KaiA and KaiB [19]. These information were

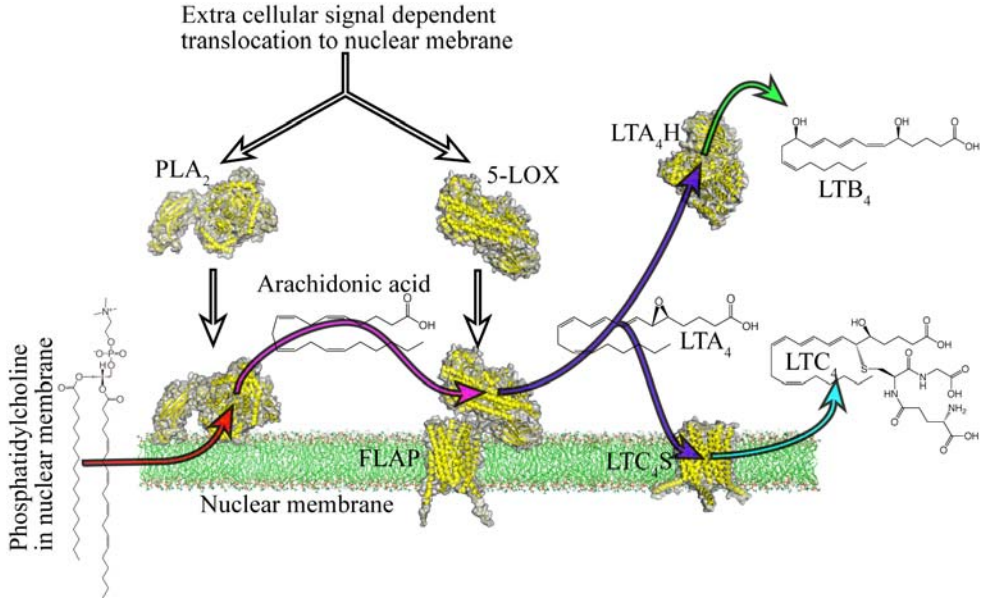

Figure 3.4: Spatiotemporal collaboration on the production of leukotrienes. Spatiotemporal collaboration of five proteins, that is, phospholipase A_2 (PLA_2); 5-lipoxygenase (5-LOX); five lipoxygenase activating protein (FLAP); leukotriene A_4 hydrolase (LTA_4H); leukotriene C_4 synthase (LTC_4S) produce leukotriene (LT) B_4 and LTC_4 as proinflammatory lipid mediators. The static structures of the proteins with an atomic resolution are available, but there is limited structural information on how structural transformation of the protein and the substrate proceeds during the catalysis and how the proteins collaborate to transport hydrophobic and reactive small molecules. Direct and continuous observation would make a definite contribution to solve these questions.

not detected by the static structural analysis until today.

The ultimate light from SPring-8 II with 1,000 times higher brilliance than the present SPring-8, and consecutive pulses with duration time of a few picoseconds would be suitable for the direct and continuous observation of biological event. It enables time-resolved Laue diffraction analysis using 2D or 3D micro-crystals, where a small size of the crystal is preferred in order to synchronize the biological events taking place inside. It also enables time-resolved solution scattering with a higher time resolution than currently available. The X-ray free-electron Laser (XFEL) facility, SACLA has a great advantage to provide the femtosecond snapshots of the biological systems, but it is difficult to observe the biological events continuously. SPring-8 II will compensate this point, and the combination of SPring-8 II and SACLA would be powerful for comprehensive understanding of life, and would contribute to the welfare of humankind through the various by-products such as the novel drugs.

3.1.3 Higher-order structures of relaxor ferroelectric

Materials science have been exploring the way to explain the properties of macroscopic materials on the basis of atoms and molecules, which are the smallest building blocks of materials. There are two extremes in this view. One is crystalline materials consisting of infinite regular array of atoms. The other extreme is amorphous materials in which atoms are uniformly distributed without periodicity. However, recent progress in materials science has revealed that intrinsic inhomogeneity or higher-order texture which connects the macroscopic materials and atoms often plays a significant role in the appearance of characteristic properties of materials. The higher-order structures sometimes show temporal fluctuations which are particularly prominent near the phase transition temperature. Such spatial or temporal fluctuations have already been studied in non-crystalline soft materials using coherent small angle X-ray scattering because the relatively large domain size and slow dynamics characteristic to soft materials fit the brilliance of the third-generation synchrotron light source. On the other hand, for the study of higher-order structures of crystalline materials, measurements at a large scattering angle is necessary in the geometry of Bragg diffraction rather than in the forward scattering. This leads to a demand for higher brilliance than that available with the existing light source.

A typical example of crystalline materials in which nm-scaled higher-order structures are important is found in a class of materials called relaxors. Since their discovery in 1958 [20], relaxors have attracted much attention both for their general scientific interest and technological importance. Relaxors are characterized by giant ferroelectric and piezoelectric responses, gentle temperature dependence of the dielectric susceptibility, and a distinctive dielectric relaxation in a low-frequency region. For the appearance of these complex dielectric properties, the intrinsic inhomogeneity of relaxors plays an essential role. From the structural viewpoint, the inhomogeneity of relaxors is originated from deeply buried domain structures. In the largest case,

relaxors show mm-sized domain structures observable with an optical microscope. Although each single domain is uniformly polarized, all the domains are randomly oriented to each other in the absence of external fields. The macroscopic ferroelectricity is achieved by the uniaxial orientation of the polarized domains complying with the applied electric fields. However, each domain that looks uniform at the mm-scale turns out to consist of many micro domains by observations at higher magnifications. These nested structures could eventually come down to atomic-scale polarization within a unit cell, through organization at the nm-scale. Generally, there is a scalable relationship between the spatial size of domains and the characteristic frequency of their dynamics. As the frequency of external electric fields is lowered, domain structures with a larger length scale start to contribute to the macroscopic dielectric response and thus lead to the giant ferroelectricity. Moreover, nonlinear ferroelectric responses shown by relaxors imply the presence of complex interplay between the domain structures belonging to different length scales [21]. Therefore, studying the higher-order domain structures and revealing the interaction among the buried domain structures are critical for understanding the complex ferroelectric properties of relaxors.

So far, inhomogeneous structures within relaxors have been studied by X-ray and neutron diffuse scattering methods [22] whereas inelastic scattering methods of neutrons and X-rays have been employed for the study of their dynamics on various time scales [23,24]. Beyond the existing techniques, coherent X-ray diffraction microscopy and X-ray photon correlation spectroscopy, by a highly brilliant light source, enables direct observations of higher-order domain structures and their low-frequency dynamics, respectively.

The roles of the higher-order structures are not limited to the ferroelectricity of relaxors. High magnetic resistivity of manganese oxides [25], shape memory effects of martensitic alloys [26] and superconductivity of high-T_c cuprates [27] also require explanation based on structural information bridging between the nanometer and micrometer scale rather than atomic scale structures within a unit cell. Further understanding of such complex materials strongly relies on the development of coherent X-ray diffraction microscopy, which widens the range of accessible spatial and temporal scales.

3.1.4 Nucleation and clustering

Nucleation and clustering are dynamic processes in which a state in a lower level of organization evolves into a more complicated structure. This is a universal phenomenon observed in a variety of systems including phase transition and crystallization. The cluster formation is sometimes energetically more favorable than uniform structures as seen in spontaneous formation of crystalline clusters in supersaturated solution. In other cases, clustering appears as a transient state from a stable uniform phase to another, for example, during a structural phase transition induced by temperature. So far, this process has mostly been described by macroscopic param-

eters, such as the total energy and diffusion coefficient. In such a mean-field model, however, important characteristics of clustering phenomena are unsatisfactorily described. In an atomistic view, clustering is initiated by nucleation whereby an initial distribution of stable nuclei is formed from the minimum number of diffusing units. After this stage, the clusters grow in size by adsorbing atoms or molecules on their surface from the environment. When the materials in the environment are nearly depleted, the average size of the clusters increases through coalescence of smaller clusters. Dynamical observation of the entire process from the nucleation in nm scale to clustering in larger scale has long been of great scientific interest and is still a challenging issue in modern materials science.

Clustering looks as if it were a one-way process on a macroscopic scale because of the huge number of atoms that are involved. On the atomic scale, however, structural fluctuation should be prevalent since the elemental processes of adsorption and desorption are reversible (see Fig. 3.5). Recently, dynamic scaling of fluctuation during the phase separation in a sodium borosilicate glass [28] and the development of long-range ordered phase out of a disordered Cu_3Au alloy [29] have been demonstrated using a third-generation X-ray source. With the increasing brilliance of the X-ray source, initial nucleation process prior to clustering in bulk would become accessible. At this stage, interesting phenomena, such as magic clusters having a preferred size [30] and bcc cluster in liquid fcc metal [31], are suggested. Dynamical feature of these initial nuclei is an open issue. The dynamics of nucleation and clustering would be more complex and profound for low-dimensional systems than for three-dimensional bulk because of the increased degree of freedom [32]. For example, on a surface, both three-dimensional clusters and monolayer islands could exist whereas the exchange of material amongst clusters is limited to two-dimensional surface diffusion. Since the atoms and the molecules always enter and leave the materials through their surfaces or interfaces, the dynamics of surfaces or interfaces is an important issue to understand and control physical and chemical phenomena occurring during the catalytic reactions, electrochemistry and crystal growth. Considering that the signals from the surfaces or interfaces is several-orders of magnitude weaker than those from the bulk matters, a highly brilliant light source would be required for promoting the re-

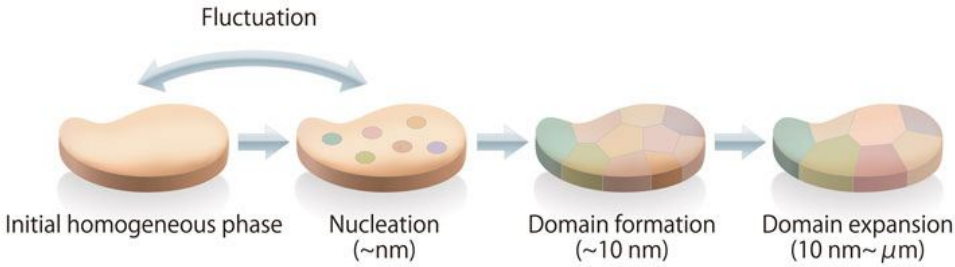

Figure 3.5: The schematic illustration of model for phase transition phenomenon.

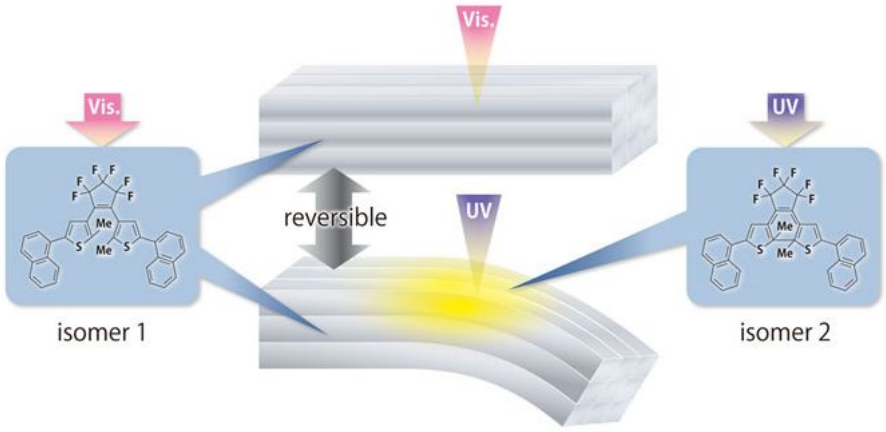

Figure 3.6: Plastic deformation of co-crystal of diarylethene by light irradiation

lated research using the time-resolved coherent X-ray diffraction microscopy or X-ray photon correlation spectroscopy [33].

3.1.5 Photochromism of functional organic materials at the molecular level

Organic materials are becoming one of the key materials for multi-function device having switching and light emitting function. Recently, great efforts have been made in the development of technologies to replace current devices with new organic and/or hybrid ones that have improved functions.

A photochromic crystal is one of the most important organic materials with useful applications such as organic light emitting displays, organic light-emitting diodes, organic transistors, organic solar cells, and molecular electronic devices [34–37]. Photochromism is a phenomenon where reversible transformation between two forms (isomer 1 and 2) of chemical species is induced by the light irradiation whilst chemical formula and molecular weight are unchaged during the transformations. When an isomer 1 absorbs light of a particular wavelength, it is transformed into isomer 2 through a conformational change driven by a change of its bonding structure or electronic state (see Figure 3.5). This structural phase transition results in a color change due to the change in its absorption spectrum or electronic state. The second isomer can also return to its original state (isomer 1), by irradiation with another specific wavelength of light, and will regain its original color or electronic state.

Photochromic materials are expected to broaden industrial applications. Azobenzene spiropyrans, and diarylethene are typical candidates for organic compounds exhibiting photochromism. These compounds exhibit a structural phase transition (cis/trans or open/close transformation) following light irradiation. Figure 3.6 shows an example where the photochromic compound

changes the shape by an exposure to light. This plastic deformation occurs because a conformational change takes place around the irradiated surface of a single crystal [38–40]. However, the flexible feature is sometimes lost under exposures at a high repeatition rate. Therefore more durable organic materials need to be developed for industrial applications. For understanding the mechanism of the durability to degrade, acquiring atomic-scale information as a function of time is highly required.

A high-energy synchrotron X-ray beam is one of the most powerful tools to monitor the durability of organic materials to degrade during repeated photochromic processes. Time-resolved measurements using the coherent and intense X-ray beam from SPring-8 II would enable us to trace the procedure where the atomic-scale structural change of a single organic molecule results in the large-scale morphological change of the material after the light irradiation [41]. Through such researches, a clearer understanding would be achieved for designing organic materials with improved durability and with various new functions.

3.2 Statistical characterization of inhomogeneous system

3.2.1 Access to inherent diversity

In the upgraded SPring-8, the throughput of analysis would be drastically improved, because the photon density on the sample would be raised to a 1000 times higher level than that of present SPring-8. To make best use of the light source property at the upgraded SPring-8, we here propose a scheme using the statistical characterization to access the diversity or inhomogeneity inherent in nature and in various systems.

The nature is highly diverse. A good example is individuality of humankind. More than five billion people live on the earth. Although all people share common features as human beings, there are no people exactly alike. That is, people have their individual specificity. This phenomenon is not just limited to human beings. There are inhomogeneous properties in all natural materials. For example, in the field of biology and environmental science, a large inhomogeneity and individual difference exists such as in cells, small tissues, or aerosol microparticles. Even if a specific trait is determined very precisely using a few specimens, one cannot conclude that it is a common feature of the system. To approach the essence of the natural materials, the statistical nature of observed properties should be elucidated. For this purpose, analyses of a huge number of specimens are indispensable.

Moreover, it is indispensable to analyze the individual specimen without averaging the information from multiple-specimens. Recent progresses in X-ray analysis techniques have enabled a detailed research at the micrometer to nanometer scale of single specimen. However, several hours of measurement time is usually required for one specimen. As a result, the number of ana-

lyzed sample is highly restricted,thus limiting the statistical significance. The ability to analyze a large amount of samples is crucial to obtain statistical information with high accuracy.

The upgrade of SPring-8 leads to the significant reduction in the measurement time and enable us to analyze a large number of analogous samples with inhomogeneous properties. By using X-rays from the diffraction limited ring at SPring-8 II, an X-ray beam could be focused to $\leq$ 50 nm without the use of a virtual source (See Section 6.3.3). We could expect that the photon densities on the sample would be improved by 1000 times higher than those currently available. This means that the throughput of measurement would be drastically improved assuming the present spatial resolution. This approach feasible with the upgraded SPring-8 would give us new opportunities to understand the essence of the natural materials with their hidden properties. In the following sections, we introduce several examples of such scientific targets: the statistical characterization in organisms, environmental science, and new materials design will be discussed.

3.2.2 Organisms

Living creatures are a classical example of systems displaying diversity. It is well known that humans show individual differences. A cell from one person whilst appearing similar in basic function to the same cell type of another would not be completely identical. The immunogenic properties of individual pathogens and the response they promote is another poignant example of this variation. The composition and density of intracellular signaling peptides and proteins is also different from cell to cell. These examples illustrate the diversity that exists at each level of the hierarchical organization within living creatures.

Recently, the presence and the quantity of metal elements inside cells has been reported to play a critical role in intracellular signaling and the outbreak of disease. Scanning X-ray Fluorescence Microscopy (SXFM) combines hard X-ray focusing techniques with fluorescence X-ray analysis and facilitates multiple elemental mapping at the cellular level. The high intensity beam focused into 10 nm size that would be made available at SPring-8 II using elaborate focusing systems (see Section 6.3.3) is well suited for elemental mapping with a high spatial resolution and a high sensitivity. Application of this technique to medical science would potentially play a major role in solving the problems our nation will confront in the future. A good example of the medical application is outlined here. By performing elemental mapping, scientists have obtained information about metals involved in drug metabolism and have conceived a novel strategy for anticancer chemotherapy [42]. By SXFM analysis, Shimura et al. [42] successfully found that Zn in cells increased according to Pt (cisplatin: anti-cancer drug) uptake. Further laboratory experiments suggested that Zn in cisplatin-treated cells was highly correlated with reduced Gulthathion (rGSH), and that Zn-biniding GSH was a key protein for drug resistant. The elemental mapping using SXFM [42] took more than 6 hours for 5~6 cells and

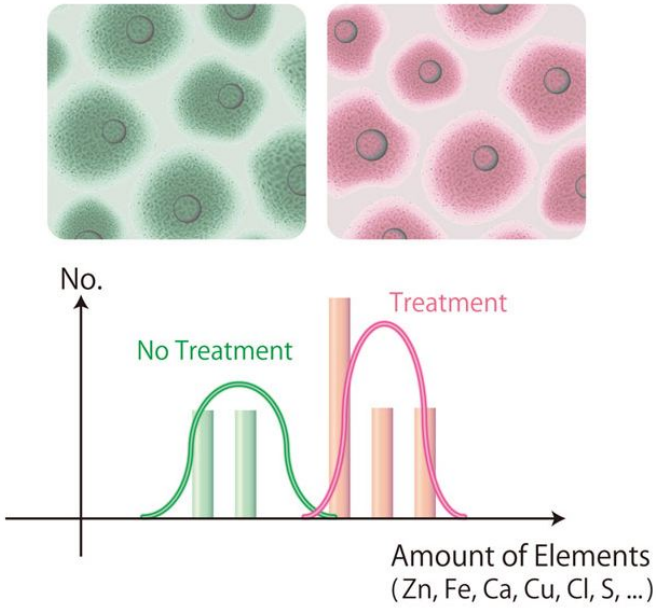

Figure 3.7: Schematic diagram showing that confidence of analysis is strongly dependent on the number of measurements. Histograms show the data with few number of measurements which approach the smooth curves by increasing the number of measurements.

more than10 repeats were required for the time-course analysis. X-ray focusing size was set wider in order to shorten the required time of experiments, resulting in lower resolution. With a higher resolution, they could investigate intracellular localization of each element as in conventional cell biology method, e.g. immunostaining using antibodies. Element mapping in a higher resolution is definitely required for the future cell biology.

In medical and biological sciences, it is important to detect a significant difference between specimens through repeated measurements, due to the individual variation of samples. The growth of cells is heavily dependent on their environment. As such, it is important to collect cells grown in a well-controlled environment and to investigate the diversity of these cells using statistical analysis. The confidence in the statistical analysis could be increased by performing more measurements. As noted above, various scientific discoveries have been made through the use of SFXM at SPring-8 beamlines. It is, however, important that more measurements could be made to increase the statistical significance of each experiment and overcome the problem of variation between biological specimens (see Fig. 3.7). The further development of medical and biological science would be facilitated by the realization of SPring-8 II with an highly brilliant and diffraction limited beam.

To elucidate the hierarchy and function existing within living systems, the detection of fluorescence X-ray signal from cells at the highest achievable sensitivity is essential. Moreover, high-resolution elemental mapping is required for clarifying the internal structure of the cell,

where the size of a cell, a nucleus and a mitochondrion are approximately 20, 10 and 1 micrometers, respectively. In the ideal case, a statistically significant result could be achieved from a 50 nm square region of biological sample, during a 1 millisecond exposure, by increasing the intensity of a focused beam by several orders of magnitude (see Section 6.3.3). Thus, the best SFXM station would be realized by focusing the intense and coherent beam from SPring-8 II with a high precision X-ray focusing system. A rapid measurement system is vital for measuring thousands of biological specimens per day and performing statistical analysis of all the measured data. The X-ray optics, detectors and data storage system need to be optimized to achieve such a high throughput.

To develop this new direction in elemental mapping of biological specimens using the synchrotron radiation, four key parameters need to be improved, namely, resolution, sensitivity, efficiency and the ease of handling both measured data and the sample itself. By upgrading SPring-8 into SPring-8 II, the first three parameters would be raised to an unrivaled level in the world, allowing innovative progress in medical and biological sciences.

3.2.3 Environmental science

Another important field of research where the statistical characterization would be powerful is the environmental science. In this section we describe a promising future prospect of research on the aerosol particles using a highest ever data-acquisition throughput using the upgraded SPring-8.

Aerosols, suspended particles in the atmosphere, are closely related to natural environments such as global warming, acid rains, and depletion of ozone layer, and eventually, human health. The size of aerosol particles ranges from a few nanometer,similar to the size of a molecule, to nearly 100 μm, comparable to the size of a pollen. The chemical composition of aerosols varies as well; aerosols with more than 3,000 different organic molecules have been reported. Particles of various sizes can absorb and/or scatter solar radiation and could become nuclei in the formation of clouds. The sizes and chemical compositions of individual particles could determine the climate. For example, a smoke dust strongly absorbs solar radiation and has been assumed to act as a warming gas. In contrast, sulfate and its organic compounds are more reflective to sun lights and have been assumed to cause cooling of the earth. The influence of aerosols on global warming has been pointed out in the IPCC report. The role of aerosols in climate change, however, still remains unresolved [43]. To understand the effects of aerosol particles to the natural environment in more detail, an analytical method of individual aerosol particle would be indispensable.

Most previous studies, such as by chromatography, have treated bulk aerosols, by evaluating the averaged characteristics of many aerosol particles. With this averaged approach, important information on distribution of compositions, sizes, and shapes of particles may have been lost.

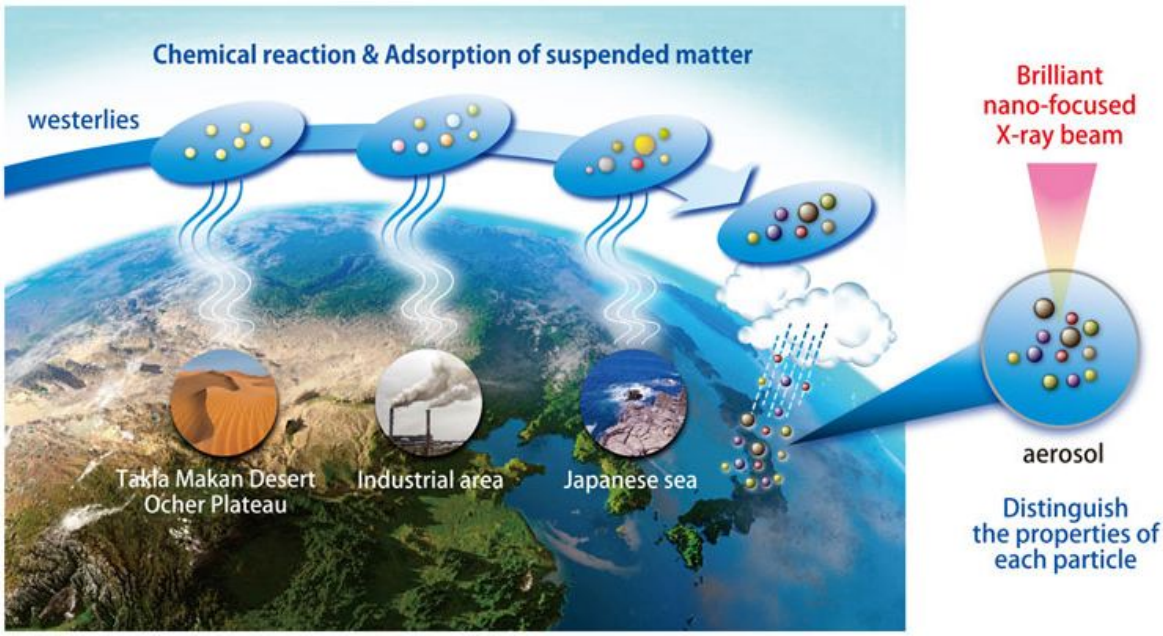

Figure 3.8: Proposed formation and transport mechanisms of yellow dust [48]

Several new techniques including X-ray fluorescent imaging using synchrotron radiation, electron microscopy, and mass spectrometry have recently been developed to analyze the properties of individual particles [44]. However, the measurable number of particles is still restricted due to the low data-acquisition throughput. Analysis of a large number of particles is required for the statistical characterization to clarify the role of these aerosol particles in the climate change. The highest ever throughput with the upgraded SPring-8 would be extremely powerful for making best use of this new experimental scheme.

Another important issue is to clarify the effect caused by the aerosol particles on the natural environment and the dependence on the mixing states of particles [45]. The mixing states of aerosol particles can be classified into two different states, external and internal mixtures [46]. In an external mixture, aerosol particles with different pure compositions are mixed, whereas, in an internal mixture, every particles have the same mixture of different composition. The conventional bulk analyses are not capable to distinguish these states. This problem could be overcome using the statistical analysis of a large number of particles.

Aerosol particles generally have a single composition when emitted in the primary source region. Then, the particles are transported in the atmosphere and changed into a mixing state, reacting with other particles and/or atmospheric components. Finally, the particles can reach an intermediate state between the external and internal mixture in the atmosphere. A thorough analysis of the mixing state would provide knowledge of the primary source region and the transportation pathways of the aerosol particles.

One of the key topics involving aerosols in the mixed state is yellow dust which are trans-

ported from the Chinese continent to Japan by the strong winds (Fig. 3.8). In 2010, an outbreak of the cattle disease, "foot-and-mouth disease" hit Japanese farmers. Yellow dusts originating from the deserts in China and Mongolia are considered to be a significant transport media of the infectious viruses [47]. To identify the primary source region and the transportation pathway of the dusts, it is necessary to analyze the yellow dusts in the mixed states. The statistical characterization of a large number of yellow dust particles would allow precise characterization of individual particles as well as the diverse properties of the particles. These results would contribute to the understanding of the mixed states of the aerosol particles, helping to unveil the effect of aerosols on the global and social environments.

The statistic characterization approach, which will be available with the upgraded SPring-8, would provide a new way to evaluate characteristics of various aerosol particles. It would contribute to resolve important issues in environmental science.

3.2.4 Quick and fine screening of synthesized materials

The statistical characterization would accelerate the research for developing useful functional materials by quick and fine screening of synthesized materials. SPring-8 II offers ideal X-ray beam properties for applying this approach to various kinds of materials. Despite of the huge demands for analyzing novel materials, homogeneous specimens with high purities and large volumes have been evaluated so far in most cases. For example, synchrotron X-ray experiments usually require specimens synthesized under well controlled conditions so that the analyzed results are attributed to known conditions. In a word, purification process is essential in order to characterize synthesized materials. This hinders the rapid progress of the materials research. Here, we propose two research methods to overcome these difficulties using the world-leading light source of the SPring-8 II, suited for the experiments using an intense nano-focused X-ray beam with a highest ever throughput. A fast data processing using a super-computer would accerelate the research speed.

The first method is useful to find new materials, forming small grains (sub-μm $\sim$ μm), inside the parent materials. Scanning microscopy experiment, acquiring X-ray spectra and/or X-ray diffraction signals, would be carried out on the samples using a nano-focused X-ray beam from the SPring-8 II. Unique signal from the novel material could be quickly and elaborately screened out of the huge datasets. Once the novel material is successfully located, more diverse information could be obtained from the same region of the sample, such as the electronic state, structures, magnetic properties and so on. Fig. 3.9 illustrates a scheme of this method. This approach would thus allow X-ray characterization of the newly-synthesized material without any purification process.

The second method makes best use of the combinatorial material synthesis. By changing the conditions and moving the synthesizing spot as a function of time, the properties of material is

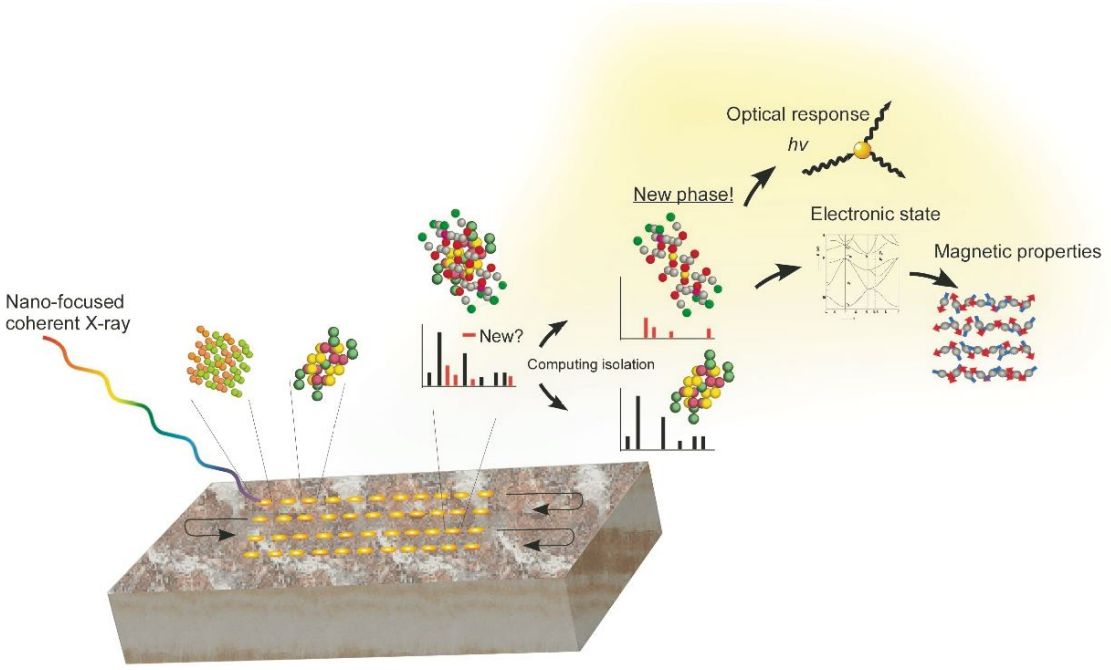

Figure 3.9: Concept of quick and fine screening of the newly synthesized materials which have a texture. A nano-focused beam would make it possible to discover the new material.

varied as a function of position at the sample substrate. More than hundred regions with different compositions of materials would be produced on a single substrate, by changing the parameters controlling the process of the material synthesis. However, we have been able to measure only a few regions due to the limited beamtime at the present SPring-8. The upgraded SPring-8, on the other hand, would allow us to characterize hundreds of regions on the samples in a short beamtime. Novel materials with new structures and new properties could be discovered from the huge data sets. An in-situ measurement with the combinatorial synthesis would be even more effective for synthesizing materials having ideal properties. The "process and characterize" scheme would become practical.

References

[1] J. P. Overington *et al.*, Nat. Rev. Drug Discov. **5**, 993 (2006).

[2] K. Placzewski *et al.*, Sicence **289**, 739 (2000).

[3] D. M. Rosenbaum *et al.*, Science **318**, 1266 (2007).

[4] D. M. Rasmussen *et al.*, Nature **450**, 383 (2007).

[5] V. Cherezov *et al.*, Science **318**, 1258 (2007).

[6] T. Warne *et al.*, Nature **454**, 486 (2008).

[7] V. P. Jaakola *et al.*, Science **322**, 1211 (2008).

[8] B. Wu *et al.*, Science **330**, 1066 (2010).

[9] D. M. Rosenbaum *et al.*, Nature **469**, 236 (2011).

[10] S. G. F. Rasmussen *et al.*, Nature **469**, 175 (2011).

[11] F. Xu *et al.*, Science **332**, 322 (2011).

[12] T. Shimamura *et al.*, Nature **475**, 65 (2011).

[13] http://www.heptares.com/news/15/74/Drug-discovery-collaboration-focused-on-gpcr.html

[14] http://www.receptos.com/pdfs/Receptos-010611-b.pdf

[15] T. Toyoshima *et al.*, Nature **405**, 647 (2000).

[16] T. Toyoshima and H. Nomura, Nature **418**, 605 (2002).

[17] T. Toyoshima and T. Mizutani, Nature **430**, 529 (2004).

[18] J. Ochala *et al.*, Proc. Natl. Acad. Sci. USA **107**, 9807 (2010).

[19] Y. Murayama *et al.*, EMBO J. **30**, 68 (2011).

[20] G. A. Smolenskii and A. I. Agronovskaya, Sov. Phys. Tech. Phys. A **3**, 1380 (1958).

[21] G. Burns and F. H. Dacol, Phys. Rev. B **28**, 2527 (1983).

[22] G. Xu, J. Phys. Soc. Jpn **79**, 011011 (2010).

[23] K. Hirota, Z.-G. Ye, S. Wakimoto, P. M. Gehring and G. Shirane, Phys. Rev. B **65**, 104105 (2002).

[24] K. Ohwada, K. Hirota, H. Terauchi, T. Fukuda, S. Tsutsui, A. Q. R. Baron, J. Mizuki, H. Ohwa and N. Yasuda, Phys. Rev. B **77**, 094136 (2008).

[25] Y. Moritomo, A. Asamitsu, H. Kuwahara and Y. Tokura, Nature **380**, 141 (1996).

[26] W. Hu, K. Hayashi, T. Yamamoto, N, Happo, S. Hosokawa, T. Terai, T. Fukuda, T. Kakeshita, H. Xie and M. Suzuki, Phys. Rev. B **80**, 060202(R) (2009).

[27] J. M. Tranquada, B. J. Sternlieb, J. D. Axe, Y. Nakamura and S. Uchida, Nature **375**, 561 (1995).

[28] A. Malik, A. R. Sandy, L. B. Lurio, G. B. Stephenson, S. G. J. Mochrie, I. McNulty and M.Sutton, Phys. Rev. Lett **81**, 5832 (1998).

[29] A. Fluerasu, M. Sutton and E. M. Dufresne, Phys. Rev. Lett. 94 (2005) 055501.

[30] G. Rosenfeld, A. F. Becker, B. Poelsema, L. K. Verheij and G. Comsa, Phys. Rev. Lett. **69**, 917 (1992).

[31] Y. C. Shen and D. W. Oxtoby, Phys. Rev. Lett. **77**, 3585 (1996).

[32] M. Zinke-Allmang, L. C. Feldman and M. H. Grabow, Surf. Sci. Rep. **16**, 377 (1992).

[33] M. S. Pierce, K.-C. Chang, D. Hennessy, V. Komaicky, M. Sprung, A. Sandy and H. You, Phys. Rev. Lett. **103**, 165501 (2009).

[34] G. Smets, J. Breaken, and M. Irie, Pure Appl. Chem. **50**, 845 (1978).

[35] M. Irie, Adv. Polym. Sci. **94**, 28 (1990).

[36] H. Finkelmann, E. Nishikawa, G. G. Pereira, and M. Warner, Phys. Rev. Lett. **87**, 015501 (2001).

[37] Y. Yu, M. Nakano and T. Ikeda, Nature **425**, 145 (2003).

[38] S. Kobatake, S. Takami, H. Muto, T. Ishikawa, and M. Irie, Nature **446**, 778 (2007).

[39] R. O. Al-Kaysi and C. J. Bardeen, Adv. Mater. **19**, 1276 (2007).

[40] M. A. Garcia-Garibay, Angew. Chem. Int. Ed. **46**, 8945 (2007).

[41] Y. Ishibashi, M. Fujiwara, T. Umesato, H. Saito, S. Kobatake, M. Irie, and H. Miyasaka, J. Phys. Chem. C **115**, 4265 (2011).

[42] M. Shimura *et al.*, Cancer Res. **65** 4998 (2005).

[43] *Climate Change: 2007 Synthesis Report*, Contribution of Working Groups I, II and III to the Fourth Assessment Report of the Intergovernmental Panel on Climate Change, Core Writing Team, R. K. Pachauri and A. Reisinger (Eds.) IPCC, Geneva, Switzerland (2007).

[44] For example, J. Aerosol Res., **19**, 4–40 (2004) (in Japanese).

[45] K. Okada, J. Aerosol Res. **19**, 21 (2004) (in Japanese).

[46] P. Winkler, J. Aerosol Sci. **4**, 373 (1973).

[47] *Study of Global Cycle of Air-Polluting Yellow Dusts*, Science Council of Japan (2010) (in Japanese).

[48] *Dust and Sandstorms, 2nd version*, Ministry of the Environment of Japan (2008): http://www.env.go.jp/en/earth/dss/pamph/pdf/full.pdf

Chapter 4

Synergy with X-ray Free-Electron Laser

4.1 Introduction

At SPring-8, a synchrotron light source and an X-ray Free Electron Laser (XFEL) are neighboring each other in the same campus. This provides SPring-8 with a unique opportunity for synergetic experiments using the two different kinds of light sources. To exploit this opportunity to its full potential, it is essential to upgrade SPring-8 so that it can deliver a diffraction limited beam with ultra high brilliance matching the XFEL.

One of the promising techniques that would be enabled by the synergetic use of a synchrotron light source and XFEL is correlative imaging, where, e.g. the 1st step analysis is performed using SPring-8II beam which dramatically enhances the efficiency of the measurements using XFEL. Such technique would be powerful for atomic resolution imaging. Although the light from XFEL is considered to be useful for solving the three dimensional atomic structure of nanocrystals, the number of nanocrystals needed for a complete dataset would be larger than ten thousand if the crystal orientation is completely random [1]. The number of necessary images is expected to be greatly reduced by using nanocrystals with a pre-determined orientation using the SPring-8 II beam.

Synergetic experiments using SPring-8 II and XFEL would allow pioneering scientific experiments in the imaging of non-crystalline samples as well. Using both sources, the imaging capability in different length scale and comprehensive understanding of them could be achieved. The high-resolution imaging in general has the severe drawback of radiation damage to the sample. This is why combined measurements would be useful, where a large area of the sample such as a whole cell is imaged with SPring-8 II, followed by a successive very high-resolution imaging of a particular region such as an organelle within the cell using the XFEL. For the large area imaging, multiple coherent X-ray diffraction images with overlapping fields of view (ptychography method [2–4]) would be powerful. On the other hand, the high-resolution image of a local area could be extracted from an extended object by using the keyhole imaging method [5].

These two measurements would provide key insights, e.g., about the organization inside the cell.

The XFEL pulsed beam contains a huge number of photons, 5×10^{11} photons per pulse, in an extremely short temporal duration of less than 100 femtoseconds. By using a delayed beam from SPring-8 II, unique X-ray pump-probe experiments could be performed. For example, the XFEL beam is used as a pump beam which excites specific elements into highly ionized states or many hole states [6]. SPring-8 II beam, on the other hand, is used as the probe beam to analyze using signals of, such as X-ray diffraction and/or energy dispersive EXAFS, with varied delay time. For each measurement at different time delay, materials under investigation need to be unchanged even after repeated excitation. This condition is easily fulfilled for gaseous or liquid samples. Even for crystalline or homogeneous amorphous materials, movement of the illuminated position has proven to be effective for obtaining consistent pump-probe data [7]. With extremely high spatial coherence of XFEL and SPring-8II, pump and probe experiments on a 10 nm area of the sample would be possible. This technique would enable us to measure a sharp initial distribution of the ionization state and its temporal evolution, which are especially important for surface science applications.

4.2 Atomic resolution imaging

4.2.1 Correlative imaging in protein nanocrystallography

Protein crystallography provides the 3D structural information of proteins indispensable for rational drug design and high-level medical services. However, many important proteins for industrial application are yet to be analyzed due to the difficulty in producing large single crystals. Thus, microfocus beamlines, allowing structural determination from microcrystals with dimensions more than 1 micrometer, are rapidly developed. However, mainly due to the radiation damage during data collection, analysis of protein nanocrystals with dimensions less than 1 micrometer is difficult to date.

Protein nanocrystallography using XFEL is a promising approach to overcome this problem [1]. In this method, intense X-ray pulses with ultra short durations, less than 100 fs, enables one to collect a 'still' diffraction pattern from a single nanocrystal before its destruction. However, the current system in protein nanocrystallography needs tens of thousands of still images from different single nanocrystals with random orientations to reconstruct a full data set. Furthermore, the liquid jet apparatus utilized in the current system produces a droplet containing small numbers of nanocrystals in a stochastic Poisson process. This indicates a limited crystal hit rate in the data collection, typically of around 20%. The first XFEL nanocrystallography experiment on the photosystem I protein consumed 10.3 billion nanocrystals to reconstruct a

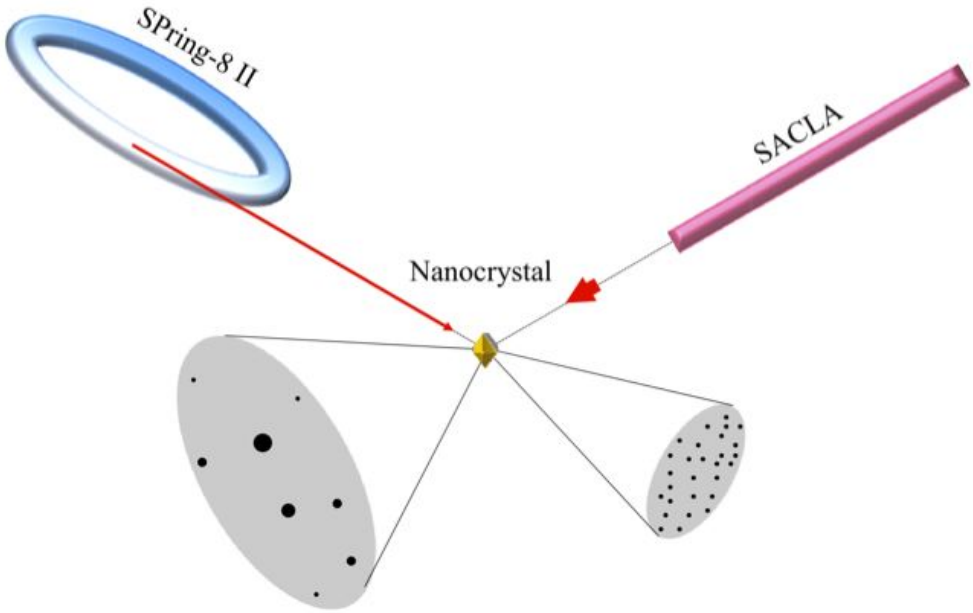

Figure 4.1: Schematic illustration of correlative diffractometry proposed for protein nanocrystallography where oscillation image using SPring-8 II and a high-resolution still image using SACLA are successively taken. In typical cases, a few hundred nanocrystals with random orientations would be enough to reconstruct a complete data set.

full data set at 8.5 Å resolution [1]. In addition, the liquid jet apparatus requires preliminary optimization of operating conditions which may consume over ten times the amount of crystals than that required for the actual experiment. Thus the current protocol would be unrealistic for most of the important proteins to be analyzed.

A complementary use of SPring-8 II and SACLA could reduce the required number of nanocrystals dramatically (see the schematic diagram in Fig. 4.1). This new system adopts a deterministic approach in which a precise determination of crystal parameters, using a nano-focused continuous X-ray beam from the storage ring, allows us to utilize most of the partially recorded reflections in the still images captured from the XFEL. Nanocrystals are mounted using a conventional cryogenic method that ensures much higher success rates in data collection. After the centering of a single nanocrystal, by X-ray scanning or a detection of fluorescence, one or a few oscillation diffraction patterns, including fully recorded reflections, are taken using the SPring-8 II X-rays with a small scanning angle that is larger than the crystal mosaicity. Radiation damage should be minimized by reducing the X-ray dose and/or using a liquid helium cryostat. Subsequently, the XFEL pulse irradiates the same nanocrystal from the opposite direction to take a high-resolution still diffraction pattern. This combination of taking two different kinds of shots from a single nanocrystal using SPring-8 II and SACLA is repeated on many independent nanocrystals with random orientations. Fully recorded reflections in the oscillation

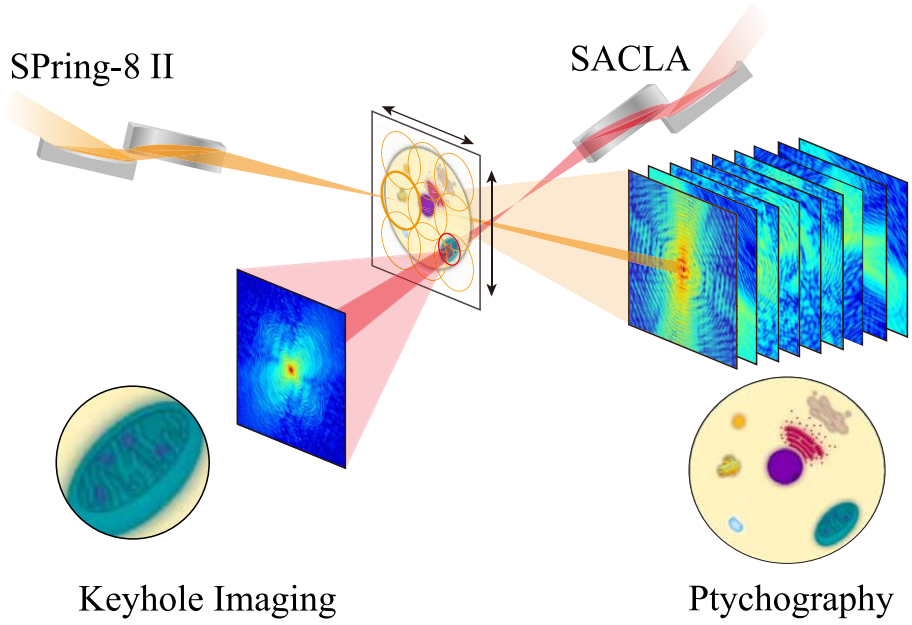

Figure 4.2: Schematic illustration of combined coherent diffractive imaging taking data for a wide area using SPring-8 II and for a specific local area using SACLA.

images are favorable in the determination of precise crystal parameters, thereby serving as a useful guide for the data reconstruction.

Alternatively, we could combine a complete low-resolution data set from SPring-8 II and many independent still data from SACLA. Even in this case, only the complementary use of SPring-8 II and SACLA allows the protein nanocrystallography at high resolution, suggesting the importance of the nano-focused continuous X-ray beam of SPring-8 II.

4.2.2 Coherent diffractive imaging of non-crystalline samples

Coherent diffractive imaging [8] (CDI) with iterative phasing methods offers X-ray imaging with extraordinarily high spatial resolution. The spatial resolution of CDI is limited, in principle, only by the X-ray wavelength and the largest recorded scattering angle. The use of highly focused incident X-ray beams is effective for collecting large angle diffraction data with a high signal-to-noise ratio [9]. A diffraction limited hard X-ray beam of SPring-8 II matched with the numerical aperture of the total reflection mirrors with ultimate surface roughness [10], makes it easy to increase the flux density by orders of magnitudes and improve the achievable resolution of CDI. On the other hand, the field of view becomes narrow as the X-ray spot size becomes small. In addition, the radiation damage of samples due to high-density radiation doses would be serious. For biological samples, the acceptable dose is limited by the radiation damage of the sample, thus limiting the spatial resolution to around 10 nm [11].

A new strategy for high-resolution and large-field-of-view CDI is provided by synergetic

experiments using SPring-8 II and XFEL (see the schematic diagram in Fig. 4.2). Using SPring-8 II, ptychographic CDI [2–4] would be carried out using a focused synchrotron X-ray beam, in which a probe is scanned across the sample and the diffraction pattern would be measured at each beam position. Using XFEL, keyhole CDI [5] would be performed using a tightly focused single pulse, in which a finite expanding beam would be used to define a finite extent for the exit wave field of the object. For example, a 10-um-sized cell would be observed by ptychographic CDI with a 10-nm resolution in SPring-8 II. The shape of the cell and the spatial distribution of the organelles would be observed. Successively the region of interest, e.g. the nucleus or mitochondrion of the cell, would be measured by keyhole CDI with a resolution of less than a nanometer. Although keyhole CDI with XFEL destroys the area of the sample irradiated by X-rays, a coherent diffraction pattern could be collected faster than the relevant damage processes [12] as thermalization of the ejected electrons through collisional electron cascades is not completed within the time frame of a single XFEL pulse [13, 14]. This approach could also be used as a tool for studying the dynamics of various materials. For example, spatial distribution of catalytic nanoparticles, their individual nano-mesoscale structures, and the atomic-scale catalytic reactions they perform could be visualized. To realize this combined technique, various elementary techniques are necessary as follows: the mirror figuring and alignment technique, the positioning technique for alignment of X-rays from both X-ray sources at the same sample position, and the stabilization technique of optical systems. In addition, the illumination function must be defined beforehand or be derived in parallel to the object reconstruction. It is important to establish the technique for characterizing the X-ray probe beam [15, 16].

4.3 X-ray pump-probe experiment

X-ray free electron lasers (XFEL), such as LCLS and SACLA, would stimulate various pioneering research exploring the highly excited states in atoms, molecules, and materials. The FELs can create a specific excited state in one shot. XFEL-SPring-8 Experimental Facility, constructed in 2011, would offer an unique chance of X-ray pump-probe experiments, by overlaying the two X-ray beams from two ultimate sources on the same sample position with an appropriate time delay (see schematic diagram in Fig. 4.3).

4.3.1 Exploring elementary processes in highly-excited matters

In XFEL-irradiated systems, it is predicted that multiple inner shell electron excitation, producing multiple core-hole state and/or multiple photon excitation, occurs in addition to the simple inner shell electron ejection. The highly excited states must induce secondary process, which includes Auger process in sequence, leading to a Coulomb explosion. However, nobody has

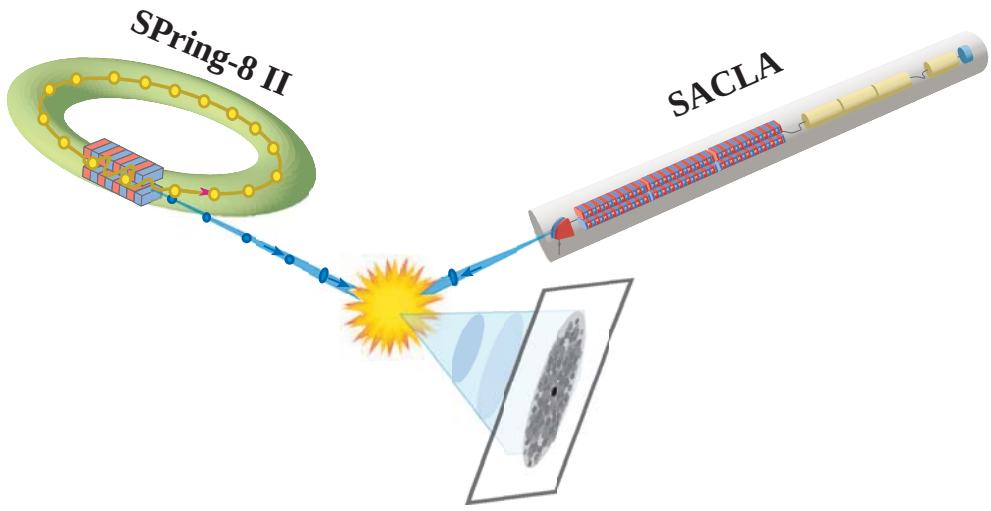

Figure 4.3: Schematic illustration of x-ray pump and x-ray probe experimental setup at SPring-8 campus.

observed the real process and experimental evidence is highly sought after. The advanced synchrotron radiation source, SPring-8 II, will become one of the most powerful tools for this observation. For this purpose, the following four features of SPring-8 II would be powerful: wide tunability of X-ray photon energy, ultra-short pulse, ultra-high brilliance, and high spatial coherence.

The energy tunability is important for probing the X-ray excited states using spectroscopic methods which require X-rays with different energy from the pumping X-rays. The two features, ultra-short pulse and ultra-high brilliance, are important for monitoring the X-ray excited states, which generally have a short life-time and relax to a ground state through higher energy intermediate states in less than picoseconds. Higher energy states in general have higher relaxation rates. Thus, SPring-8 II should provide a short pulse close to a sub-picosecond timescale. For example, the SPring-8 II SR with a sub-picosecond pulse duration would help to monitor the transient states of multiply-charged ions of neon (observations of product ions is reported by the LCLS group [6]). The high spatial coherence would help cultivating the new scientific frontier. The ultra-intense X-rays would produce new states or new phases in crystalline materials due to the proximity of the wavelength of the X-rays and the lattice constant. In the highly-excited transient state, the sample crystal may no longer keep its periodic atomic arrangements. The excited state cannot be expressed by applying perturbation theories. New states or new phases in crystalline materials are easily detectable by observing coherent diffraction patterns at a particular Bragg spot. The superior spatial coherence of SPring-8 II (Section 6.1.5) is indispensable for quantitative evaluations of the unknown states of materials.

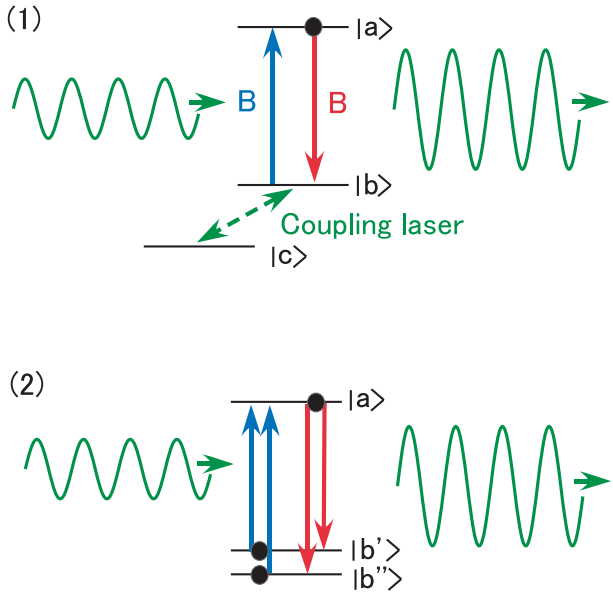

Figure 4.4: Schematic diagram of laser without inversion. (1) In normal laser condition, population inversion condition is indispensable. If an atom in which the laser field (coupling laser) is coupled to two levels rather than to one lower level, that is, the atom is prepared in a "coherent superposition" of the two lower levels of $|b'\rangle$ and $|b''\rangle$ as shown in (2), the two dipole moments for absorption are destructively interfered and canceled. On the other hand, the dipole moment for emission contributes to amplification. Therefore lasing without population inversion is achieved.

4.3.2 Coherent optical processes in the hard X-ray region

Combination of the two X-ray sources and a visible laser, makes it possible to conduct another challenging experiment, the coherent amplification of X-rays achieved in a coherent atomic system as described below. When a coherent visible (or infrared) laser is strongly coupled with the two levels of excited states in gas phase atoms, the resulting destructive interference of transition moments modifies the absorption coefficient. This phenomenon is well known as EIT (Electromagnetically Induced Transparency), which gives reduced absorption coefficient at a limited energy window [17]. At the ALS beamline, where femto-second SR pulses are generated by a laser slicing method, EIT was observed in the soft X-ray region with a high peak power femto- or pico-second pulsed laser [18]. The beams for pumping and probing should have pulse durations shorter than that of the coupling laser in this experiment. We can potentially realize EIT in the X-ray region, by modifying the population of the excited states using X-ray excitation with SACLA. One of the requirements to achieve a conventional laser is the population inversion, which requires the same value of Einstein's B coefficients between absorption and emission processes. However, if only the absorption coefficient becomes zero, the population inversion would not be required any more. Therefore, X-ray pumping to the excited states leads to the induced emission and coherent amplification of radiation. By using SACLA and SPring-8 II as

the pump and probe X-ray beams, respectively, “laser without inversion” [19] may be achieved in the hard X-ray region (as schematically shown in Fig. 4.4). The coherent X-ray process may be also useful for the development of temporally- and spatially-coherent intense X-ray beams, by using the monochromatized SPring-8 II SR as a seeding light.

In summary, the SPring-8 II SR with a short pulse duration and a high spatial coherence would contribute to the probing of high energy transient systems produced by XFEL irradiation. It would open the research fields that elucidate ultrafast dynamics in highly excited states and coherent phenomenon in the X-ray region.

References

[1] H. N. Chapman *et al.*, Nature **470**, 73 (2011).

[2] J. M. Rodenburg *et al.*, Phil. Trans. R. Soc. Lond. A **339**, 521 (1992).

[3] J. M. Rodenburg *et al.*, Phys. Rev. Lett. **98**, 034801 (2007).

[4] H. M. L. Faulkner *et al.*, Phys. Rev. Lett. **93**, 023903 (2004).

[5] B. Abbey *et al.*, Nat. Phys. **4**, 394 (2008).

[6] L. Young *et al.*, Nature **466**, 56 (2011).

[7] Y. Tanaka *et al.*, Jpn. J. Appl. Phys. **48** 03A001 (2009).

[8] H. N. Chapman and K. A. Nugent, Nat. Photo. **30**, 833 (2010).

[9] Y. Takahashi *et al.*, Phys. Rev. B **80**, 054103 (2009).

[10] H. Mimura *et al.*, Nat. Phys. **6**, 122 (2010).

[11] M. R. Howells *et al.*, J. Electron Spect. **170**, 4 (2009).

[12] R. Neutze *et al.*, Nature **406**, 752 (2000).

[13] N. Timneanu *et al.*, Chem. Phys. **29**, 277(2001).

[14] B. Ziaja *et al.*, J. Appl. Phys. **97**, 064905 (2005).

[15] H. M. Quiney *et al.*, Nat. Phys. **2**, 101 (2006).

[16] P. Thibault *et al.*, Science **321**, 379 (2008).

[17] K. J. Boller *et al.*, Phys. Rev. Lett. **66**, 2593 (1991).

[18] T. E. Glover *et al.*, Nat. Phys. **6**, 69 (2010).

[19] D. Braunstein and R. Shuker, Phys. Rev. A **68**, 013812 (2003).

Chapter 5

Accelerator Design

5.1 Accelerator Overview

New science and scientific schemes proposed and discussed in the previous chapters would greatly benefit from an upgrade of the light source. One of the examples is that significant increase in light brilliance may open an opportunity to implement new observations of inhomogeneous objects via statistical analyses. Another example is a coherent diffraction imaging that relies on transverse coherent characteristic of the light. For the purpose, the SPring-8 upgrade plan aims at significant improvement in light source qualities, especially in brilliance and coherence [1,2]. The keyword is the diffraction limit in the X-ray region. The quality of radiation, either synchrotron radiation emitted from a bending magnet or undulator radiation from an insertion device, depend on that of the source, which in our case is electron bunches. The quality of electron bunches can be measured by so-called emittance, of which definition is a product of a bunch size and a divergence angle. If the electron emittance were negligibly small, the quality of radiation would be dominated by the intrinsic product of radiation size and its divergence. The intrinsic product is referred as a diffraction limit, known to be $\lambda/4\pi$, where λ is the wavelength of the light. For the existing SPring-8, however, the emittance of electron beams stored in a storage ring has exceeded the diffraction limit of light by orders of magnitudes, thereby the quality of light is dominated by the electron emittance, which is most likely the case for other storage rings as well.

As the electron emittance approaches the diffraction limit of the light, the spatial coherent fraction approaches the unity, and the brilliance comes close to the maximum given by so-called zero-emittance beam. The goal of the SPring-8 upgrade plan is to achieve the electron emittance that is equivalent to the diffraction limit of light in the X-ray region. Such a goal has been regarded as "ultimate" in storage rings, originally coined by Ropert [3]. Note that the diffraction limit, $\lambda/4\pi$, is proportional to the wavelength of light, or inversely proportional to the photon energy. So the diffraction limit becomes smaller as the electron energy becomes

higher to generate higher photon energies. Moreover, the equilibrium emittance in a storage ring is proportional to the square of the electron energy (see Eq.(5.1)); lower energy electrons intrinsically yield better emittance for a given lattice. In consequence, one finds it more difficult to achieve the diffraction limited ring for higher electron/photon energies, although it is extremely important to challenge the future scientific opportunities in the hard X-ray region.

In this chapter, major requirements and constraints for upgrading the SPring-8 accelerator complex, and the basic concept and approach for meeting the user demands are described. Important details of individual accelerator components and the related physics are presented in a separate report [1].

5.1.1 Scope of SPring-8 II Accelerator Complex

Figure 5.1 shows the current view of the SPring-8 site. On the site, there are two main accelerators; a storage ring called SPring-8 (top right in Fig.5.1) , and a linac-based XFEL called SACLA (left). The current SPring-8 accelerator complex is composed of a 1 GeV linear accelerator (linac), a 8 GeV booster synchrotron, and a 8 GeV storage ring. The upgrade plan mainly focuses on modifying the whole part of the storage ring including insertion devices and beamlines. As an injector, we plan to make use of the XFEL linac that generates an unnormalized emittance of tens of pm.rad.

The newly designed storage ring features a multi-bend lattice with damping wigglers, which allows us to reduce natural emittance by two orders of magnitudes or more compared with the current SPring-8 double-bend lattice without damping wigglers. The final natural emittance will reach or come close to the diffraction limit of light in the X-ray region. In order to realize the goal, new technology developments will be indispensable and is discussed in the report. Note that some detailed verifications of the technology developments are still open at the moment, and the R&D are underway. In the following sections, we shall begin with a new lattice design that is expected to bring the emittance down to the regime of diffraction limit. The technologies that support the lattice design are then briefly overviewed in the report. Some of more detailed discussion on the technologies are found in Ref. [1].

5.1.2 Basic Constraints and Design Criteria

At the SPring-8 upgrade, the new storage ring will not be built in a new building, but is planned to replace the existing accelerator system. Therefore the new storage ring lattice has to fit in the existing SPring-8 tunnel. The constraints for the upgrade plan are summarized in the following.

Considering cost-effectiveness and influences on current and future users, the following constraints are set in the SPring-8 upgrade design:

1) The new storage ring will be built in the existing tunnel.

Figure 5.1: SPring-8 Accelerator Complex; SPring-8 (right top) and SACLA (left).

2) Existing insertion device beamlines should stay in existing hutches.

3) Shutdown time should be about a year.

In addition to the three major constraints, it is required that the new ring should provide an adequate beam stability for user experiments. Although the brilliance and the coherence of light may be the first figure of merit for the new design, we regard the stability as equally important criterion as the light qualities. Since the beam dynamics in a storage ring tends to be less stable as a newly designed lattice approaches the diffraction limit in terms of beam dynamics and technological challenges, it is an important strategy in a design to find a good compromise between the light quality and the stability.

A top-up operation is as well one of key features for recent storage rings. SPring-8 has provided the top-up operation since 2004 so that the heat loads are kept stable and the constant flux of light are provided to beamlines. A flexibility of the filling pattern is also an important feature. The flexibility will be determined by wakefield calculations and a beam loading effect in cavities. The bottom line is that the advantages of the current SPring-8 should be maintained, while the accelerator performances are significantly upgraded. The currently available features are already taken for granted.

Nowadays to built an energy-efficient and environmentally friendly facility is a crucial matter to accommodate with a sustainable society. In the design of a new storage ring at the SPring-8 site, we shall strive to construct an energy-concious accelerator facility, still meeting high demands for future sciences.

5.1.3 Design Goals for the Upgraded Accelerator

The SPring-8 upgrade plan sets an ultimate goal that the new storage ring would provide extremely high quality electron beams of which emittance reaches the diffraction limit of light in the X-ray region. The diffraction limit corresponds to 10 pm.rad for 10 keV photons, for example. When the electron beam quality reaches the level, the brilliance is almost saturated as presented in Fig. 5.2 and the coherent fraction gets close to unity. In Fig. 5.2, the brilliance is calculated at the photon energy of 10 keV under conditions that the electron energy is 6 GeV, the current 100 mA, coupling ratio 0.02, energy spread 0.12 %, and betatron functions 1.0 meter in both horizontal and vertical axes as an example. As one can see, the brilliance effectively increases as the electron emittence decreases from a few nm.rad to tens of pm.rad. Although there would still be gain in the brilliance and the coherent fraction beyond the diffraction limit until the electron emittance reaches zero, the effectiveness would become smaller while the difficulty and costs would become much higher. Therefore, the diffraction limit is set as a *reasonable* ultimate goal for the SPring-8 upgrade.

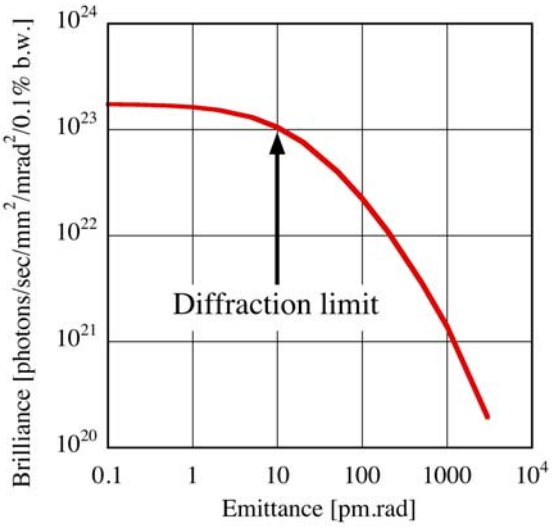

Figure 5.2: Brilliance vs Emittance. Brilliance is estimated at 10 keV, of which diffraction limit corresponds to 10 pm.rad. Electron energy of 6 GeV, current of 100 mA, coupling ratio of 0.01, energy spread of 0.12 %, and betatron functions of 1.0 meter in horizontal and vertical axes are assumed.

A short X-ray pulse generation is also an option of the upgrade. In general, storage rings have been regarded as high average brilliance/flux light sources, while linac based light sources such as XFELs and ERLs are likely expected to provide high peak brilliance/flux. The reason is that a natural bunch length, i.e., an equilibrium bunch length determined by stochastic nature of beam dynamics in a storage ring, is normally longer than that can be generated by linear accelerators. Furthermore, it is often required that the bunch duration should be lengthened by external devices in order to suppress the intra-beam scattering effect; otherwise low emittance

of stored bunches are deteriorated by mutual collisions between electrons. We have considered a possibility of generating short X-ray pulses without affecting the extremely low emittance, since the short time scale in a range of subpico- to pico-second is of great importance especially when pump-and-probe experiments are demonstrated (see Chapter 4).

In the present chapter, the conceptual design of the accelerator system as well as critical issues for materializing the design are presented. The resulting performance of the design as a light source is summarized in Chapter 6.

5.2 Conceptual Design of the Accelerator

5.2.1 Storage Ring Lattice

The goal of the upgrade plan is to realize a "diffraction limited" hard X-ray source and an ultimate target value of the emittance is set to be 10 pm.rad, about 1/300 of the current value. Such a small emittance cannot be realized by the present storage ring lattice of the double-bend type and hence its drastic modification is inevitable.

The equilibrium horizontal emittance, ϵ, is written as,

$$\epsilon = C\frac{E^2}{N^3}, \tag{5.1}$$

where C is a constant determined by a lattice, E is an electron energy, and N is the number of bending magnets (see, for example, [4, 5] for detailed definition). The constant C can be minimized by employing the theoretical minimum emittance (TME) lattice [4]. However, to decrease the constant C is not enough for approaching extremely small emittance. Thus, we plan to modify both the electron energy E and the number of bending magnets N.

We carried out feasibility studies of converting the lattice from the double-bend type, i.e. $N = 2$, to a multi-bend type, $N > 2$, having the arc structure close to the TME [3, 6–11]. Due to the constraint that the ring circumference is fixed and the number and positions of straight sections for insertion devices are unchanged, the new lattices have to keep roughly the same cell length and the existence of four long straight sections. Starting from the double-bend lattice we increased the number of bending magnets in a unit cell one by one and checked linear and nonlinear beam dynamics issues [12–14].

All the newly designed lattices assume the electron energy of 6 GeV. The decrease of the energy from 8 GeV should give an emittance reduction by a factor of ~2 according to Eq.(5.1). In addition, the lower energy helps relax required magnet strengths, allow a higher beam current, make an energy spread narrower, and maximize damping wiggler effects, although the harmful effects of intrabeam scattering and shortening of Touschek beam lifetime must also be considered. The decrease of the electron energy relies on developments of insertion devices. Shorter

period undulators have made it possible to generate higher photon energies for a given electron energy, which has supported recent projects of new light sources. Even further advances will be expected in the future. At present, we choose the beam energy of 6 GeV as a most possible candidate for the challenging goal, and in what follows beam parameters are calculated at this energy. More detailed discussion on the choice of electron energy will be presented in Section 5.4 and Ref. [1].

Unit Cell

Figure 5.3 shows the present double-bend lattice of the SPring-8 storage ring. The natural emittance is ϵ = 3.4 nm.rad at 8 GeV, while the effective one at the normal straight section (with dispersion leakage) is $\epsilon_{\rm eff}$ = 3.7 nm.rad. When we lower the beam energy from 8 to 6 GeV and impose the achromat condition, the emittance becomes about ϵ = 4 nm.rad.

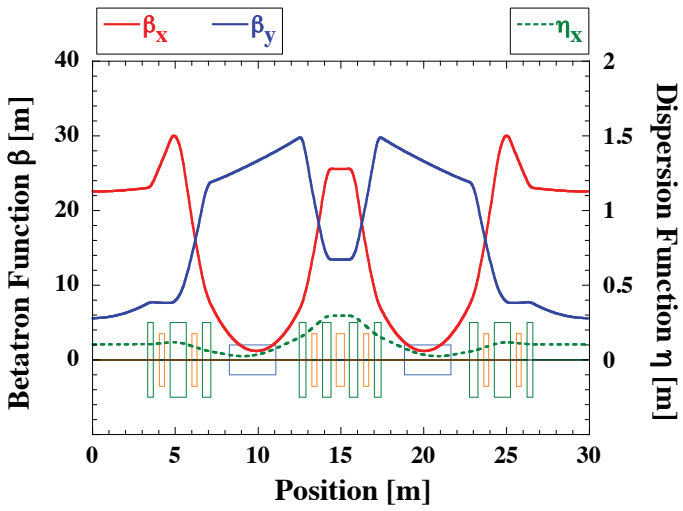

Figure 5.3: The present double-bend lattice of the SPring-8 storage ring. The lattice functions and magnet arrangement (blue: bending, green: quadrupole, orange: sextupole) are shown for a unit cell.

By changing the lattice structure to multi-bend type and increasing the number of bending magnets N, we can reduce the emittance as shown in Fig. 5.4. This procedure of emittance reduction has, however, a practical limit at some value of N, since the cell length is fixed and as we require a smaller emittance the focal length of quadrupole magnets becomes shorter and hence their strengths become stronger, yielding large natural chromaticities. Then, strong sextupole magnets are required and the dynamic aperture shrinks. For example, the horizontal dynamic aperture calculated at β_x = 20 m with 10 μm (rms) alignment errors of sextupole magnets is about ±15 mm for N = 2, and it shrinks to ±10 mm for N = 3 and to ±2 mm for N = 6. By considering the achievable emittance, required magnet strengths and the resulting dynamic aperture, we have currently chosen a 6 bend lattice (N = 6) as the most promising

candidate for an upgraded storage ring lattice. Figure 5.5 shows the lattice functions of the 6 bend achromat optics. The betatron functions at normal straight sections are about 1 m in both horizontal and vertical directions. This is for maximizing the brilliance of synchrotron radiation and for allowing a small minimum gap of insertion devices. In Fig. 5.5 we also show the arrangement of bending, quadrupole and sextupole magnets. The design of quadrupole and sextupole magnets must be as compact as possible, having an optimized pole shape and capability of generating high field gradient. The interference of reciprocal magnetic fields must be considered and a suitable design of the vacuum chamber is needed.

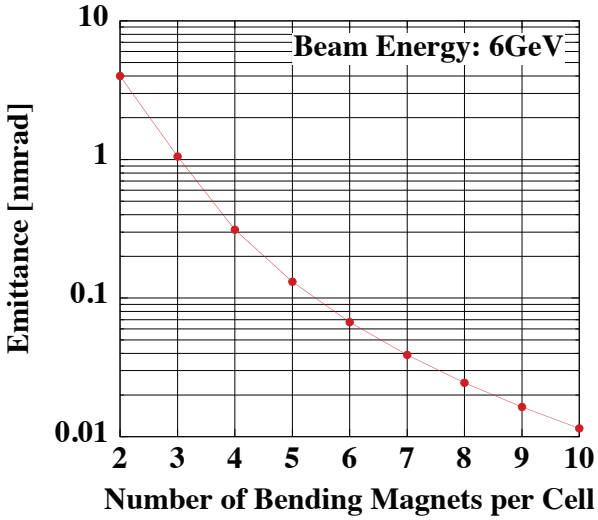

Figure 5.4: Typical values of the emittance for the SPring-8 storage ring calculated by assuming a multi-bend achromat optics and the same cell length. The beam energy is 6 GeV and the ring circumference is fixed at the present value of 1436 m.

Long Straight Section

In the SPring-8 storage ring there are four magnet-free long straight sections (LSS's). A quarter of the ring is composed of 11 unit cells and one LSS. Since the betatron functions at normal straight sections are set to be small, being about 1 m in both horizontal and vertical directions as shown in Fig. 5.5, we will use one of the LSS's for beam injection by extending the present beam transport line by about 170 m. The LSS has a simple lattice structure composed of weak qudrupole magnets to suppress local chromaticites in this section. The betatron phase advance in LSS is set to be $2\,\pi n$, where n is an integer, and so the LSS becomes "transparent" and the betatron functions at both ends are automatically matched to the unit cell. The straight section having a large horizontal betatron function is used for the beam injection. The rest can be used to install damping wigglers to control the beam emittance. When necessary in the future, other devices can also be installed in these sections.

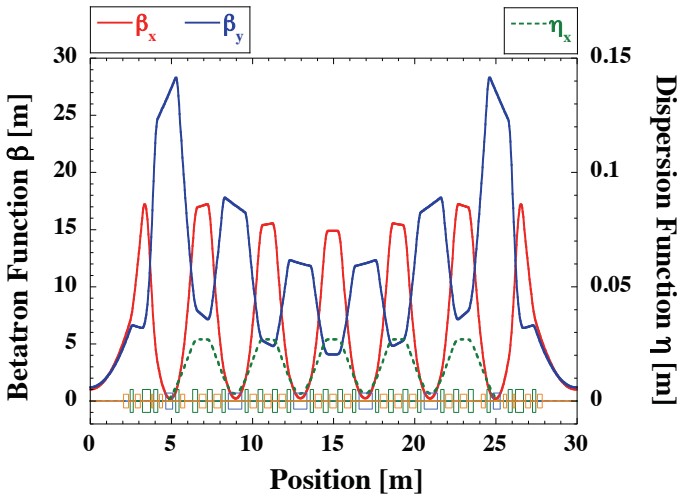

Figure 5.5: 6 bend lattice. The lattice functions and magnet arrangement (blue: bending, green: quadrupole, orange: sextupole) are shown.

Dynamic Aperture

As mentioned above, when we increase the number of bending magnets to achieve a smaller emittance value, the natural chromaticities become large, especially in the horizontal direction, and strong sextupole magnets are required for the chromaticity correction. Then the dynamic aperture shrinks and the momentum acceptance becomes small, and it becomes difficult to inject a beam with high efficiencies and to keep a stored current constant even in the top-up operation. To solve this problem and enlarge the dynamic aperture, we developed a method of optimizing sextupole strengths [12] by using an isolated resonance Hamiltonian [15] so that resonance excitations are suppressed for both on- and off-momentum electrons. In the optimization procedure we also took account of the high-order (nonlinear) dispersions [16] and chromaticities [17] to keep the momentum acceptance as large as possible.

We further incorporated an idea that dominant effects of nonlinear sextupole fields cancel when the betatron phase relation is properly set. In the unit cell of the 6 bend lattice the horizontal betatron phase between two bending magnets is close to π, and one can arrange sextupole positions and strengths so that their nonlinear effects cancel to a certain extent as in the case of (non-)interleaved sextupole scheme [18–20]. This scheme of cancellation can also be applied to the case between cells [11]. In our case the strengths of some sextupole magnets in the arc were fixed according to the former cancellation scheme, and the betatron phase advance of the unit cell was optimized according to the latter scheme: the horizontal tune difference is $\Delta\nu_x = 12.527$ per 4 cells and the vertical one is $\Delta\nu_y = 1.557$ per 2 cells, or $\Delta\nu_x = 35.450$ and $\Delta\nu_y = 9.563$ for a quarter of the ring (superperiod of the lattice structure of the whole ring). Though the cancellation of sextupole fields is not perfect, we found this is effective for maximizing the dynamic aperture.

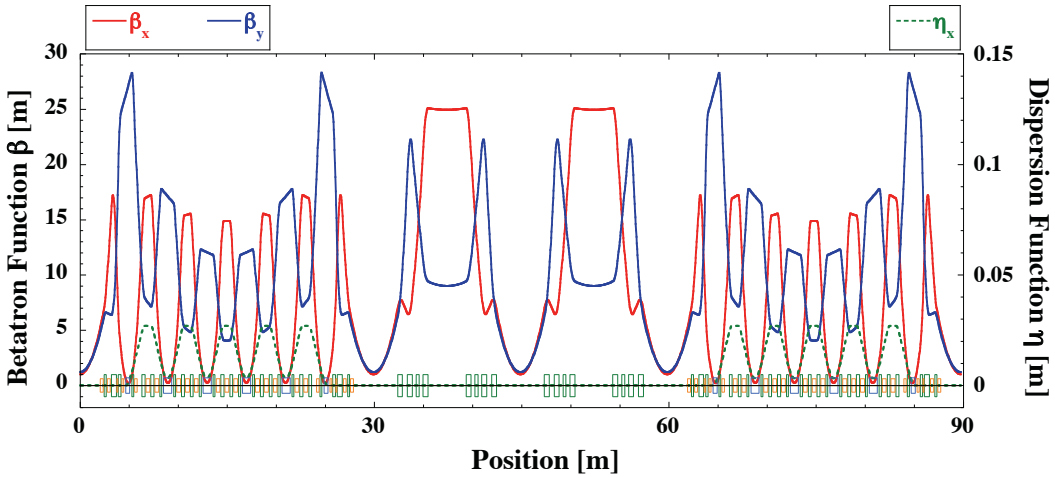

Figure 5.6: Typical lattice functions for three cells including the LSS (middle). In this example the betatron phase advance of the LSS is 2π in both horizontal and vertical directions.

In Fig. 5.7 we show the dynamic aperture calculated at the high-beta section of LSS. Since the sextupole magnets are strong, the dynamic aperture is sensitive to the sextupole misalignment. We checked the dependence of the dynamic aperture on the sextupole misalignment and found that the tolerance is about 10 μm. It is then needed to develop a very precise alignment and correction method. For checking magnet misalignment and for calibrating beam position monitors in the early stage of the beam commissioning, a "detuned" (or relaxed) optics having weaker quadrupole strengths will be useful. Since the sextupole magnets are also weaker in this optics, the dynamic aperture is robust against machine errors. Examples of such a "detuned" optics have been obtained, and these will be refined and used in discussing the commissioning scenario.

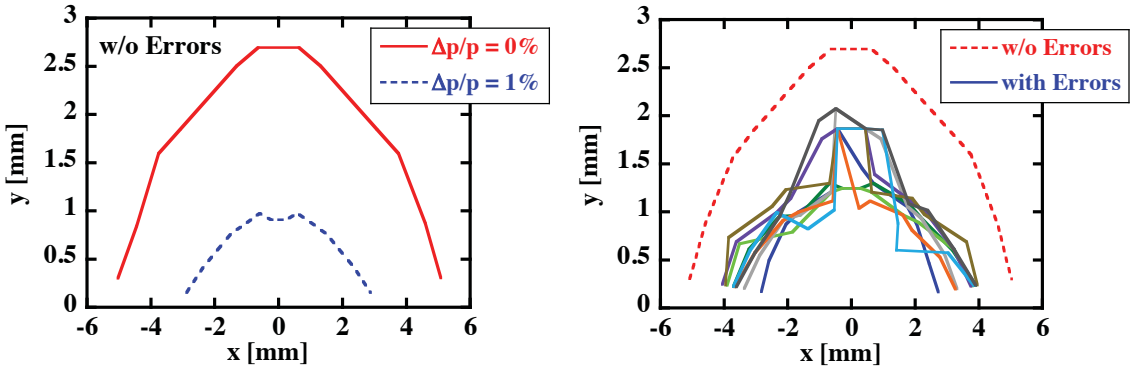

Figure 5.7: The dynamic aperture for the ideal ring without errors (left) and for the ring with sextupole misalignment (right) calculated at the high-beta section of LSS, where β_x = 24.9 m and β_y = 9.0 m. The sextupole misalignment was distributed according to the Gaussian distribution of σ = 5 μm with the cutoff at 2σ.

The momentum acceptance is about 2 % (see Fig. 5.7) and the Touschek beam lifetime is calculated to be about 0.1 h at the bunch current of 0.1mA and the emittance coupling ratio of 2%. To increase the beam lifetime and to relieve the intrabeam scattering effects, we plan to introduce a harmonic cavity system that allows us to control the bunch length.

Main parameters of the new storage ring are summarized in Table 5.1, where we also show parameters for the present ring for comparison.

Table 5.1: Main parameters of the storage ring.

	New Ring	Present Ring
Lattice Type	6 Bend	Double-Bend
Unit Cell Length [m]	29.92	29.92
Ring Circumference [m]	1435.95	1435.95
Beam Energy [GeV]	6	8
Natural Emittance [pm.rad]	67	3400
Energy Spread [%]	0.096	0.109
Dispersion Func. [m] at Straights	0	0.107
Betatron Func. [m] at Straights (H/V)	1.0 / 1.2	22.6 / 5.6
Betatron Tune (H/V)	141.80 / 38.25	40.14 / 18.35
Natural Chromaticity (H/V)	-473 / -199	-88 / -42
Momentum Compaction Factor	1.55×10^{-5}	1.68×10^{-4}
Radiation Loss [MeV/turn]	4	9
Number of Magnets per Cell (Bending / Quadrupole / Sextupole)	6 / 26 / 23	2 / 10 / 7
Bending Field [T]	0.70	0.68
Max. Strength of Quadrupoles [m^{-1}]	1.52	0.40
Max. Strength of Sextupoles [m^{-2}]	120	6.2

Damping by Insertion Devices

As we lower the beam energy, the damping effect due to insertion devices on the emittance is enhanced. This is demonstrated in Fig. 5.8, where the emittance (left axis) and the relative energy spread (right axis) is plotted as a function of the field strength of undulators installed in the normal straight section. We assumed that the number of undulators is 28, the same number as in the present situation at SPring-8, and they are all cryo-undulators of the same planar type having a period of 14.4 mm and a length of 3 m. By changing the gap of the undulators, one can vary their magnetic field up to 2.04 T, which corresponds to the photon energy of 5 keV.

From Fig. 5.8, we see that as we close the gap, the emittance is drastically reduced. When users require the photon energy at around 5 to 10 keV (indicated by dashed lines in the figure), the emittance will be around 30 pm.rad. In the present case, the minimum emittance that can be achieved by the damping effect of undulators is about 23 pm.rad (when all of the undulators are operated at the minimum gap, or at the maximum field of 2.04 T).

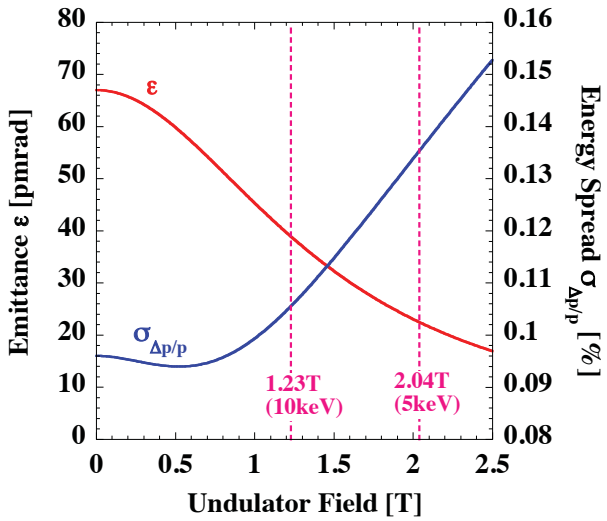

Figure 5.8: The effect of undulators on the emittance and the relative energy spread. In this calculation, 28 undulators, each having a period of 14.4 mm and a length of 3 m, are distributed in normal straight sections where $\beta_x = 1.0$ m and $\eta_x = 0$.

The emittance can further be reduced by using the damping wigglers. As shown in Fig. 5.6, the LSS has some magnet-free spaces and they can be used for installing damping wigglers. For definiteness, we assume that nine damping wigglers, each having a period of 50 mm and a length of 3 m, are installed in the low-beta sections of LSS and all of the undulators in the normal straight sections are operated at their maximum field of 2.04 T. Figure 5.9 shows the emittance and the energy spread calculated as a function of the magnetic field of the damping wigglers. As seen from this figure, the emittance of less than 20 pm.rad, being close to our ultimate goal of the "diffraction limit", can be obtained when the damping wiggler field is around 2 to 3 T.

The damping wigglers can also play another role in user operation: they can be used to keep the emittance constant when users change the gap of their undulators independently. Such a feed-forward control of the emittance will be important for keeping the light source performance during user operation.

5.2.2 Technology Developments

The basic lattice design for the upgraded SPring-8 has been overviewed in the previous section 5.2.1. The six-bend lattice has mainly been studied, for which linear and nonlinear optics

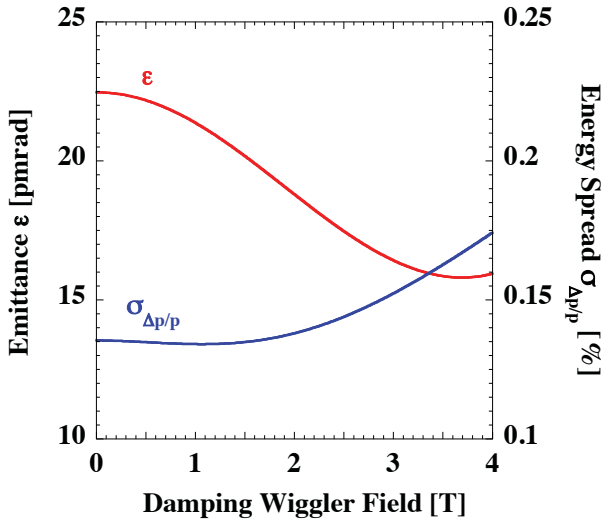

Figure 5.9: The effect of damping wigglers. In this calculation, nine damping wigglers are placed in the low-beta sections of LSS where β_x = 1.0m and η_x = 0. Each damping wiggler has a period of 50 mm and a length of 3 m.

have been optimized. The resulting performances as a light source are summarized in Chapter 6, which will presumably meet demands for future sciences. However, we have to verify the feasibility of the lattice in terms of technologies beforehand. It is especially because the lattice aims at the ultimate performance as a storage ring under several constraints. Such a challenging upgrade imposes not only an advanced lattice design via manipulation of nonlinear beam dynamics but also extensive technological developments in almost every component such as an injection device, magnets, RF systems, and monitors.

A design of an extremely small emittance ring naturally results in the following technical challenges. First, a dynamic aperture becomes smaller as natural chromaticities become larger and sextupoles that compensate it have stronger magnetic gradients. An injector, therefore, needs to accommodate such a small acceptance. Next, required magnetic fields for multipole magnets, especially sextupoles, will quickly increase as the number of bending magnets is increased. Thus, development of multipole magnets is one of key issues. As a combination of the two natures, i.e., small dynamic apertures and high magnetic gradients off an axis, an accuracy of sending electron beams in each magnet has to be very high. For the purpose, a monitor system attached to a magnet assembly needs further development. An intra-beam scattering (IBS) effect also comes into play. As transverse emittances are made small, the IBS effect starts to dominate the final emittance. To avoid it, RF systems should take care of a longitudinal bunch distribution of electrons to suppress the emittance blowup.

These technical challenges have been recognized in our design, too. It is no more reasonable for us to fix the lattice first, then develop hardwares afterward based on the lattice. Instead, it is frequently necessary to go back and forth between the lattice and hardware designs. Otherwise,

the feasibility of hardware is not secured.

Thus, the lattice design shown in the previous section is actually the consequence of the iteration process between the lattice design and the extensive hardware studies, although the hardware developments still have to be continued via R&D's. One good example is that the packing factor is so high and simultaneously the integrated magnetic fields of multipole magnets are so high that the magnets should be carefully distributed in order to avoid extremely high magnetic gradients that are technologically impossible. (The packing factor is the ratio of space occupied with magnets to the total.) The lattice design shown in Fig.5.6 already considers such an iteration. In the following, the requirements for technology developments and our approach to them are overviewed.

Injection Schemes

The first requirement for a design of the new injection system is to accommodate the small dynamic apertures presented in Fig.5.7. Under assumption that the sextupole alignment tolerance is ± 10 μm, dynamic apertures are estimated to be about 2.5 mm in horizontal and 1 mm in vertical directions at the betatron function of ~25 m. This aperture is ten times smaller than that of the current ring. Also the natural bunch length of the SPring-8 II ring is a few ps, one fifth of the current values of the rings. The injection to such small acceptances requires low emittance and short bunch beams from an injector.

The top-up operation is also an important feature for the injection system. Since the top-up operation was introduced to SPring-8 in 2004, the new type of injection has brought significant changes to user experiments. Heat loads on X-ray optics are kept stable, and flux at samples do not decrease any more as time elapses. Now the new feature is taken for granted, and should be maintained at the next ring. More precisely, we should satisfy the following strengths in terms of the injection system (in the order of appearance in the following):

(1) low injection beam loss to the narrow aperture for radiation safety and low damage on insertion device,

(2) a variety of filling patterns with a variety of bunch current,

(3) minimum perturbations on stored beam,

(4) a high purity single bunch; currently, the bunch purity of SPring-8 is in the order of 10^{-10} or a single electron level,

(5) a stored current stability of the order of 0.01 %.

The requirement on the beam parameters and candidates for the new injector are compared in Table 5.2. The booster synchrotron, i.e., the current injector to the SPring-8 ring, has large

emittance and long bunches that do not fulfill the requirements, unless large amount of efforts including budgets are to be put into the renewal. The SACLA linac, on the other hand, produces extremely high quality beam in emittance and bunch length with an adequate repetition rate. Therefore we choose the SACLA linac as the best candidate for the injector of the SPring-8 II. Although further discussion on the choice of the injector will be necessary, the parameters of the SACLA linac are expected to meet the requirement (1). For the same purpose, the injection point would be moved from the current injection point at the normal straight section to one of the four 25-m long straight sections (LSS). At LSS, the horizontal betatron function can be adjusted to be more than 20 m for a large dynamic aperture, while that at the normal straight sections is fixed at ~1 m for insertion devices. By choosing the SACLA linac and the LSS as the injection point, it is expected that the injected beams fit in the small dynamic apertures without significant losses.

Table 5.2: Parameters of candidates for injector

Parameters (rms)	Requirement	SACLA	Booster Synchrotron
Emittance	≤1 nm.rad	0.05 - 0.1.nm rad	100 nm.rad
Beam size at β_H = 25m	≤0.17 mm	0.035 - 0.05 mm	1.5 mm
Energy spread	≤0.2 %	0.1 %	0.1 %
Bunch length	≤10 ps ≤25-50 ps [1]	< 1 ps	< 60 ps
Repetition rate	a few Hz	60 Hz	1 Hz
Bunch charge	0.25 nC[2]	0.25 nC	> 0.25 nC

[1] with higher harmonic RF

[2] for 100 mA with on-axis injection

An off-axis injection is preferred for the requirement (2). SPring-8 has currently provided the bunch current of 3.0 mA at maximum, which corresponds to the bunch charge of 14.4 nC. Such a high charge needs to be built up by multiple injections at the same bucket via the off-axis injection. For the off-axis injection, the incident beam is guided to the aperture by an injection device, while the stored beam is kept in the aperture without being considerably affected. Since the expected dynamic aperture for the new ring is a few mm, the distance between the injected and the stored beams should be a little less than that. It follows that the strong position dependence of the kick field needs to be given by the injection device. Therefore well-known off-axis injection schemes with bump orbit formation are not necessarily appropriate, as far as we consider the requirements mentioned above. The pulsed quadrupole magnet [21] is one candidate for such an injection device. However, the scheme excites a quadrupole oscillation on stored beams, which lasts for the damping time after the injection.

Note that the pulsed field of a magnet lasts at least for several hundreds of nano-seconds due to its inductance, thereby all the stored beams during this period suffer the quadrupole oscillation. Although a counter pulsed quadrupole may solve this problem, the installation space at matched betatron phase and the precise adjustment of the strength and the pulse shape would be required. A pulsed sextupole may be another solution, because it is superior in regard to the quadrupole oscillation due to no quadrupole field at the stored beam. Nevertheless, the question is whether it is feasible to manufacture such a magnet for matching the small dynamic aperture like our case; it would require very strong sextupole fields to deflect incident beams, leaving stored beams unkicked just a few mm away. Thus, the schemes with pulsed magnets do not seem to fulfill the requirement (3) in our case.

As a result, we propose to introduce a new injection scheme based on a bucket-by-bucket injection (BBI) using a variable field fast kicker [22]. The fast kicker is composed of two stripline electrodes and each is excited with a TEM mode by a high pulse power driver. The fast kicker produces a deflecting field with a time duration of about 3-4 ns, which can separate only one bucket from adjacent buckets that are separated by 2 ns. The length of the kicker is 0.2-m long for fast kick pulse, thus several kickers will be installed to the ring to obtain necessary amount of kick for the injection.

The fast kicker is designed such that the kick field can be continuously controlled from dipolar to quadrupolar field by adjusting the power and polarity of the input to the kicker. With the quadrupolar kick field, the injection beams are guided to off-axis of the fast kicker where there is a quadrupole-like deflecting field, while store beams feels no significant deflecting field on the axis as in Fig.5.10 . Although the quadrupolar field on the axis excites the quadrupole oscillation on the store beam, it only occurs in one bucket that are being injected. Thus, the quadruple oscillation is no more a problem and the requirement (3) is fulfilled. Also, with BBI scheme, the satellite bunches in injection beams are naturally rejected by the fast kicker as expected and the requirement (4) should be fulfilled by the BBI scheme. The requirement (5) will be maintained as far as the new injection system including the new injector catch up with the required repetition rate (~3 Hz) estimated by the beam lifetime.

Here, we would like to emphasize one more important feature for the new injection system. We find it important to prepare an option of on-axis injection. Since the dynamic aperture is expected to be small, the on-axis injection can be very effective especially at early stages of commissioning, or for some advanced operations in the future. The concept of taking advantage of the on-axis injection for the small dynamic aperture is referred as "swap-out" coined by the APS [23]. Note that we designed the BBI fast kicker so that the apparatus also enables a *bucket-by-bucket* on-axis injection by changing kick fields inside the fast kicker to dipolar field. The scheme is schematically drawn in Fig. 5.10. Only the single apparatus can switch between on- and off-axis injections, both of which work for a single bucket. It is another advantage of the

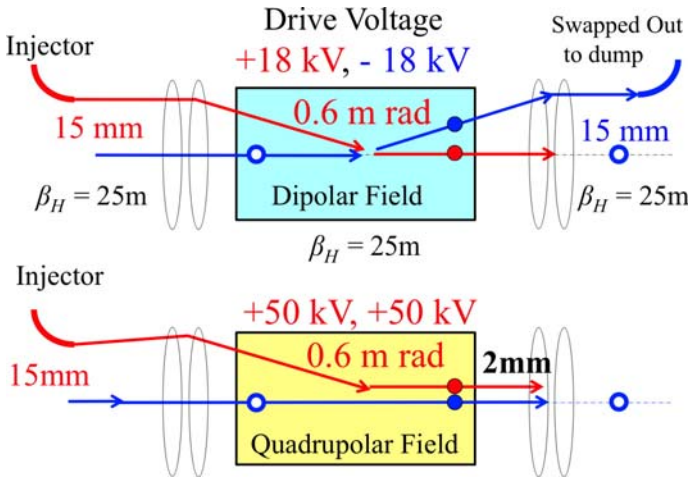

Figure 5.10: Top: On-axis injection with dipole kick by fast kicker (boxes). Bottom : Off-axis injection with quadrupole kick. The kickers are excited just at the injection bucket.

BBI fast kicker compared with pulsed multipole magnets.

The prototype of the fast kicker is now under construction for the feasibility study of the BBI injection scheme [1].

Magnet System

A magnet configuration in a cell of the newly designed 6 bend lattice is drawn in Fig.5.11. The magnets marked ”B” and ”D” are dipole magnets, where ”B” has a half length of ”D”. Quadrupole and sextupole magnets are distributed in segments ”A”, ”C”, ”E”, and ”F”. Some space is found in segments ”C”, where we are considering a possibility of installing mini-undulators. The new lattice does not only need three times more bending magnets than the existing lattice has, but also a lot more quadrupole and sextupole magnets in between. Moreover, the integrated field strengths of quadrupole and sextupole magnets intrinsically become much higher than the present ones as we proceed to the extremely small emittance ring (see Table 5.1). The issue in regard to the strong multipole magnets as well as the high packing factor is one of the common challenges in developments of extremely small emittance ring. It is obviously the case for us, too.

Our first approach is to define acceptable minimum distances between neighboring magnets for the lattice design. By that, we can take full advantage of extending longitudinal magnet lengths that helps mitigate the field gradient of each magnet. In order to determine the minimum distances, it is assumed that an overlap of magnetic fields from two neighboring magnets in a drift space in between is to be accepted, if necessary. Meanwhile, a significant intrusion of

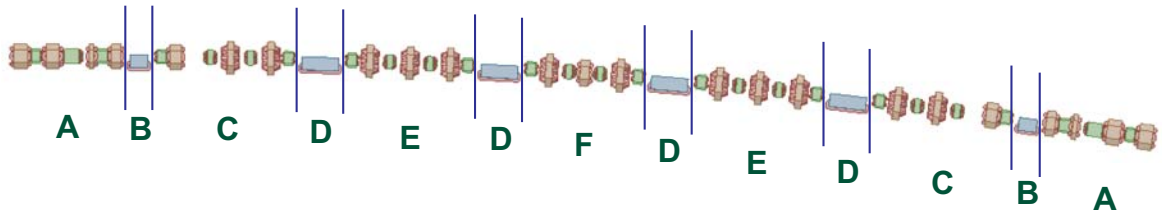

Figure 5.11: A magnet configuration design for a normal cell (*color*). In this figure, *blue*, *green* and *brown* magnets represent dipole, quadrupole and sextupole magnets, respectively. None of steering magnets are drawn in the figure. Electron beam propagates from right to left.

magnetic field from one magnet into the other should be avoided. Also, the magnets that are close with each other are carefully designed so that the total length of each magnet including coils and its support should not exceed that of the core itself [1].

Throughout such an iteration between the lattice and magnet designs, the lattice has been fixed at the moment as presented in Section 5.2.1 and drawn in Fig. 5.11. The resulting maximum field gradients of sextupole magnets are estimated to be somewhere between 10,000 and 14,000 T/m^2, which is still high. Taking vacuum enclosures into consideration, we define a bore diameter as 26 mm. Good field regions of all the magnets are designed to be ±3 mm both in horizontal and vertical directions because the dynamic aperture of the ring is estimated to be approximately ±2 mm in horizontal, and ±1 mm in vertical axes (Fig.5.7). The specifications and total numbers of dipole, quadrupole, and sextupole magnets are summarized in Table 5.3.

Since the required magnetic fields listed in Table 5.3 are high, even if a shape of a magnetic pole is optimized with a pure iron (e.g., JIS C 2504 SUY-0), field saturation in the core cannot be avoided. Thus, unique core materials are required to avoid the saturation in a core.

Saturated magnetic flux density of an iron alloy with cobalt is much higher than that of the SUY-0. Field calculation for multipole magnets are performed and are compared by using the code ”MAFIA” for two core materials, an ideal magnetic iron alloy, ”Steel1010”, and the Co-Fe alloy. As discussed in detail in Ref [1], the Co-Fe alloy is adopted as a possible magnet core material for high gradient quadrupole and sextupole magnets, and R&D, including an optimization of mixing rate of cobalt, is planned.

As a consequence, there is no plenty of space prepared for steering magnets. Some quadrupole magnets may function as steering magnets by attaching extra coils. The maximum kick angle is designed to be 0.5 mrad both in horizontal and vertical directions.

The alignment of magnets, especially that of sextupole magnets, is also one of the most critical issues for verifying the feasibility of the new ring. As discussed in Section 5.2.1, it is critical to keep a closed orbit in the vicinity of the center of sextupole magnets; otherwise, the dynamic aperture considerably shrinks to prevent orbiting beams from being stably stored.

Table 5.3: Specification and total number of dipole, quadrupole, and sextupole magnets

Parameter	Dipole	Quadrupole	Sextupole
Center field	0.7 [T]	36-50 [T/m]	<14,000 [T/m^2]
Length [m]	0.41,0.82	0.2–0.5	0.1–0.4
Gap or bore size [mm]	26	26	26
Good field region [mm]	±3	±3	±3
Field tolerance	10^{-4}	10^{-4}	10^{-4}
Total number	264	1144	1012

According to Fig. 5.7, the tolerance, that is an acceptable error between the closed orbit and the sextupole magnetic center, has to be ±10 μm or less in both horizontal and vertical directions. In order to solve the issue, we need to develop an integrated strategy including the alignment scheme of magnets and commissioning procedures. Up to now, several scenarios have been proposed and discussed. The discussion on the integrated strategy is summarized in the section of Diagnostics and Instrumentations below.

Vacuum System

The new ring would be operated at a top-up mode as the current SPring-8 is. Yet, it would be important to sustain a reasonable beam lifetime in order to meet the requirement on the current stability. Another advantage of the long lifetime is that the beam current does not quickly decrease while some mechanical or other problems interferes the top-up operation. As discussed in the section of RF system, the Touschek lifetime is expected to be around an hour, which is close to the lowest accepted for the stable top-up operation. Therefore, it is required that the vacuum lifetime, i.e., the beam lifetime determined by vacuum conditions, should be enough longer than the Touschek lifetime so that the overall lifetime is not significantly deteriorated from the Touschek lifetime. Another concern for the vacuum system is that a bore radius of magnets is 26 mm at minimum due to high magnetic fields required for the low emittance lattice. Thus, considerably thinner vacuum chambers than the present ones have to be developed for securing enough height of light slots.

The vacuum related beam lifetime is described by cross sections, and is mainly contributed by the three factors; 1) Rutherford scattering : σ_r, 2) Møller scattering : σ_m and 3) Bremsstrahlung : σ_b; $\sigma(Z_i) = \sigma_r(Z_i) + Z_i\sigma_m + \sigma_b(Z_i)$. Electron beam will be annihilated in vacuum ducts if the orbiting electron scatters with an angle of above a critical value ϕ_c or above a critical energy loss γ_c. In general, H_2 and CO are considered to be dominant residual gas components in pre-baked vacuum ducts during operation.

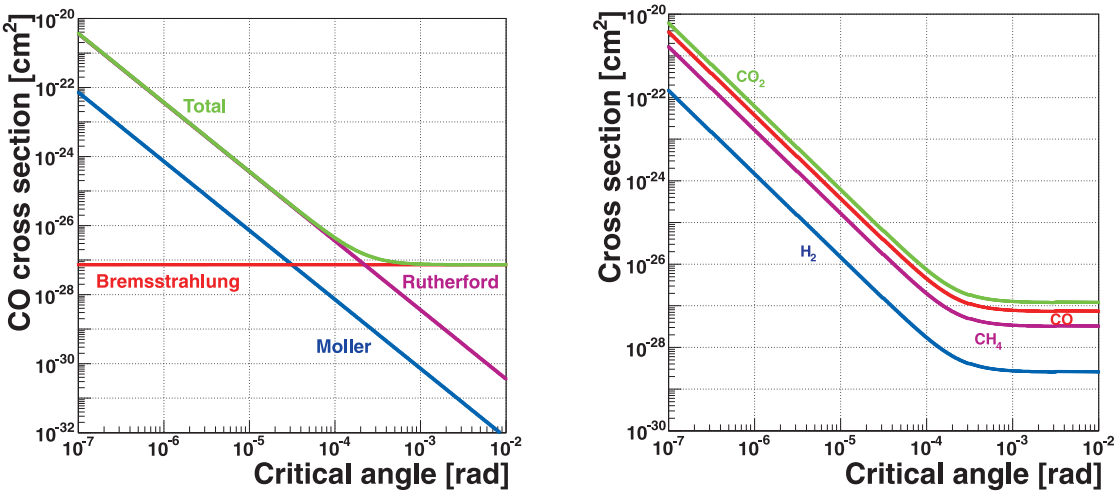

Figure 5.12: Calculated cross sections of the electron scattering with CO molecule (*left*) and with prominent residual gas molecules (*right*). An electron energy of 6 GeV is assumed.

Figure 5.12 represents calculated cross sections of the electron scattering with CO molecules (*left*) and with prominent residual gas molecules, H_2, CH_4, CO and CO_2 (*right*) assuming the electron energy of 6 GeV. It is found that the Rutherford scattering is the major factor to determine the lifetime when a critical scattering angle is less than $\phi_c \sim 10^{-4}$ rad. As shown in Fig. 5.12 (*right*), the cross section becomes smaller as the atomic number (Z_i) of the scattered residual gas particle becomes smaller. Electron beam lifetime, τ_i [s], which is caused by the scattering with a residual gas atom (Z_i) is described as

$$\frac{1}{\tau_i} = cn_i\sigma(Z_i) = c\frac{P_i}{k_B T}\sigma(Z_i), \tag{5.2}$$

where P_i residual gas pressure in Pa, n_i density in m^3 and T temperature in K. k_B is the Boltzmann constant, 1.38×10^{-23} J/K. The minimum critical angle for the new ring discussed in Section 5.2 is estimated to be 8×10^{-5} rad. Figure 5.13 summarizes the relation between the vacuum lifetime and the partial pressure for the individual four residual gas components; H_2, CH_4, CO and CO_2 at $\phi_c = 8 \times 10^{-5}$ rad.

From Fig. 5.13, it is found that a reasonably achievable beam lifetime is estimated to be around 10^5 sec., i.e. 28 hours, under assumption that the reliably achievable pressure is a fraction of 10^{-9} Pa. Now a contribution from the Touschek effect to the beam lifetime (τ_t) is estimated to be about an hour under the assumption that an appropriate RF system functions as a bunch stretcher. Therefore, assuming that the total beam lifetime (τ) is determined by the vacuum system and the Touschek effect, the total beam lifetime is

$$\frac{1}{\tau} = \frac{1}{\tau_v} + \frac{1}{\tau_t} \rightleftharpoons \tau \cong 0.97 \quad \text{[hours]}, \tag{5.3}$$

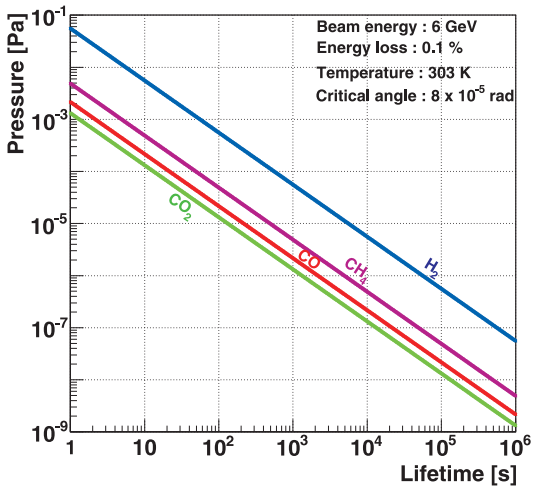

Figure 5.13: Calculated electron scattering cross sections and partial pressures for four prominent residual gas molecules. Electron energy of 6 GeV, energy loss (γ_c/γ) of 0.1 %, and temperature of 303K are assumed.

which is not significantly smaller than the original Touschek lifetime as expected. As an option, the longer Touschek lifetime, such as 3 hours, is also considered via an adjustment of the coupling ratio, especially in a commissioning stage. In the case, the overall lifetime is estimated to be 2.7 hours according to Eq.(5.3).

RF system

The role of an RF acceleration system of a storage ring is to generate a sufficient beam-accelerating voltage and compensate for beam energy loss caused by synchrotron radiation at bending magnets and insertion devices. The RF system of the current SPring-8 storage ring has stably generated a voltage of 16 MV at a frequency of 508.58 MHz and accelerated electron beams with a current of 100 mA [24].

In upgrading the storage ring for the SPring-8 II, a beam energy would be lowered to 6 GeV but a beam current would be increased up to 300 mA. Radiation losses at bending magnets, undulators and damping wigglers are respectively estimated to be 4.0, 2.0 and 4.0 MeV/turn, so the total is 10 MeV/turn. In practical user operations in the future, we plan to keep the total radiation loss at 8 MeV/turn by adjusting damping wiggler gaps depending on the status of insertion devices. The reason is that an equilibrium emittance with radiation dampings should be constant irrespective of user settings of insertion devices. Thus, the possible radiation loss ranges from 8 to 10 MeV, and we suppose the new RF system should be able to provide the accelerating voltage of 16 MV as a possibly maximum value that we have to care. In terms

of the RF frequency, the same frequency as the current one, 508.58 MHz, is chosen. Refer in detail the section of timing system below.

New RF stations for the acceleration would be distributed at three normal straight sections. The normal straight section is 4 m long each (Section 5.2.1), so the whole length of the RF cavities at each station has to be no more than 4 m in total including the whole assembly. The existing cavities in the SPring-8 storage ring does no more fit in it. Further, the increased stored current excites strong coupled-bunched instabilities from impedances of parasitic resonant modes, while the current RF cavities in SPring-8 ring have no countermeasure for the strong instabilities [25]. Thus, we have designed a new RF cavity that meets the new requirements. The TM020 mode is selected as a beam-accelerating mode since it has a shunt impedance sufficient for the beam acceleration. The shunt impedance is 6.8 MΩ and a beam-accelerating voltage of 16 MV is generated with 24 cavities, i.e., 8 cavities at each station. The TM020 mode also enables a compact damping structure for the harmful parasitic resonance. The detailed design is presented in Ref. [1].

Table 5.4 summarizes the major parameters for the new RF system. The accelerating voltage of 16 MV and the shunt impedance of 6.8 MΩ at 24 cavities result in the total cavity-wall loss of 1.6 MW. The stored current of 300 mA and the accelerating voltage of 10 MeV/turn correspond to the beam loading of 3.0 MW. In consequence, it is required to supply RF power of about 5 MW with the RF cavities. The requirement for RF power sources is again beyond the capability of the existing ones. For the sake of cost-effectiveness and a smooth transition from the current to the new systems, we are going to reinforce the existing power sources, instead of replacing with completely new ones. The total power of 5 MW will be supplied by six klystrons, each of which will have a rated output of 1 MW, an efficiency of better than 60% and a gain of more than 50 dB. Two klystrons will be situated at each station, and each klystron drives four cavities (i.e., 8 cavities per station). Correspondingly, the power supplies will be upgraded so that each can be enough to drive two 1 MW klystrons. The DC power supplies should have a voltage ripple of less than 0.5 % peak-to-peak to decrease the noises on the RF power output from the klystrons.

The coupling between an RF cavity and an external waveguide circuit must be adjusted in order not to cause a useless power-reflection from the cavity with variable beam loading. We have been developing a new RF input coupler with a coupling tuner to avoid coupling discrepancy. The optimum coupling coefficient of the SPring-8 II cavity is 2.9 at a beam current of 300 mA. The tuner will cover the necessary coupling range and be adjusted according to the various beam current without interrupting the continuous RF feed [1].

In order to achieve the diffraction limited beam both in the horizontal and the vertical directions, it is crucial to avoid the emittance growth due to the intra-beam scattering (IBS).

Table 5.4: Main parameters of fundamental RF system.

RF frequency [MHz]	508.58
harmonic number	2436
energy loss [MeV/turm]	10.0
at bending magnets	4.0
at undulators	2.0
at damping wigglers	4.0
acceleration voltage [MV]	16
RF accelerating stations	3
1 MW klystrons	6
RF cavities	24
total cavity-wall loss [MW]	1.6
beam loading power [MW]	3.0

Figure 5.14 shows the dependences of the emittance growth and the beam lifetime on the bunch length. The emittance grows remarkably and the beam lifetime becomes short as the bunch length reaches a natural length of about 5 ps. It is essential to lengthen the bunch longer than 20 ps in order to mitigate the IBS and keep the low emittance as well as enough beam lifetime. We, therefore, plan to introduce a 3.5th harmonic system for the bunch lengthening at another RF station. Because a harmonic voltage needs to be about 3.5 MV at a beam accelerating voltage of 16 MV, we would use two super-conducting single-cell cavities resonating at 1780.03 MHz. Table 5.5 shows the parameters of the harmonic cavity. The cavities should be operated at 2 K in temperature, and their wall loss would be reduced to about 4 W.

Table 5.5: Parameters of the Harmonic Cavity

frequency [MHz]	1780.03
harmonics	3.5
mode	TM010
unloaded Q	10^9
R/Q [Ω]	80
Number of cavity	2

Two types of cavity operations are under consideration: (1) active operation driven by an external RF power source and (2) passive operation driven by a beam-induced power [27].

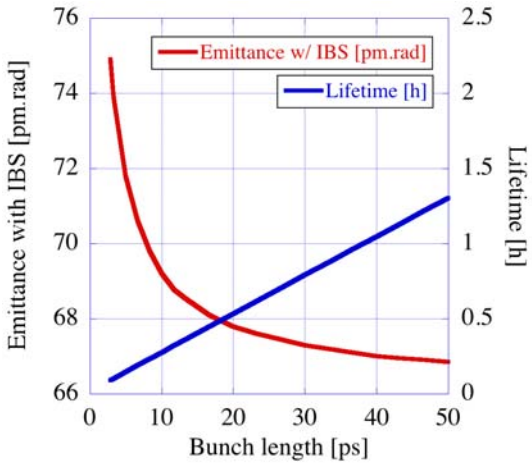

Figure 5.14: Dependence of the emittance and the beam lifetime on the bunch length. (elegant calculation [26] at a bunch current of 0.1 mA)

Figure 5.15 shows the bunch lengths in the active and the passive operations by the double RF model calculation [28]. In the active operation, the bunch extends to 50 ps and becomes 10 times longer than the natural bunch length. In order to succeed the active operation, however, an RF system must have stabilities of less than 0.1 degree in phase and of less than 1% in voltage. In the passive operation, a bunch length can be extended to 25 ps or more. The resulting bunch length is half of that obtained in the active operation, but is sufficient to meet the minimum requirement that the beam lifetime should be over half an hour. No external RF components other than the super-conducting cavities are necessary, so the RF system becomes simple and inexpensive. Since a frequency tuner is the only knob to control the cavity voltage, the passive operation is less flexible than the active operation, though.

Due to the harmonics of multiples of half integer, we can simultaneously compress a beam to a length of 4 ps and store long and short bunches bucket by bucket (Section 5.3). Damping higher-order-modes (HOM) in the cavity and 2 K cooling system are the matters with both the active and the passive operation. We should develop a HOM coupler or a HOM absorber that are fit to the cavity in a cryo-module and construct the cooling system.

Diagnostics and Instrumentations

One of the most challenging issues in technology developments for the SPring-8 upgrade is to develop new diagnostics that enable a precise observation of an electron orbit at each magnet position. In the following, the challenging issue is first addressed, then our strategy to approach the issue is presented.

As shown in Fig. 5.7, the alignment error of sextupoles must be less than ±10 μm. Otherwise, the dynamic aperture of the ring shrinks and there is a chance that the beam is no more

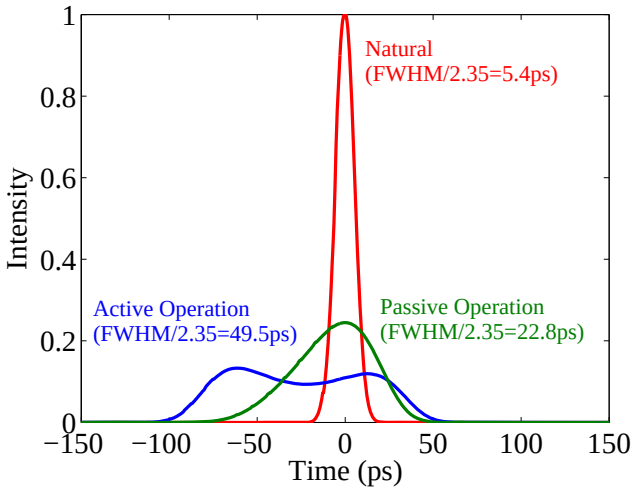

Figure 5.15: Calculation of the bunch lengthening in active and passive operations of the harmonic cavity.

stored. Note that even if the initial alignment of magnets is imperfect, say, the initial random errors of sextupole magnets are more than ±10 μm, the beam is still able to be stored as far as the electron orbit is properly guided to the center of each sextupole within the tolerance in a beam commissioning. Therefore, the challenging issue is how we should integrate the whole strategy, including not only the alignment of magnets but also the commissioning procedure, to guide the electron orbit to the center of all sextupoles within the tolerance.

Our first strategy to approach the issue is to align neighboring magnets as precisely as possible by making use of a vibrating wire technique [29] and others. Note that not only sextupole but also quadrupole magnets need to be precisely aligned to some extent in our case, because undesirable dipole kicks from the off-axis field of the strong quadrupoles may produce an unacceptable closed orbit distortion for the initial commissioning [1]. The bottom line is that magnets should be aligned as precisely as possible whatever the following commissioning procedure is. Based on our experience with the current SPring-8 and the results at other sites, we expect to achieve about the same order of accuracy as required ($\sim \pm 10$ μm), but still need a backup. Further, the initially aligned magnets may eventually move due to temperature shift or other drifts in circumstances.

Therefore, the second strategy is to prepare beam position monitors (BPM's) that allow us to measure *absolute* beam positions against magnetic center of each sextupole. We mean by the term "*absolute* beam position" that precise measurements of relative positions, or movement, of beam positions are not enough. We have to precisely know the relation between the center of magnet and the BPM position, so that beam positions against the magnetic center are to be measured with an adequate resolution. This capability enables us to adjust an electron orbit to the magnets, either in commissionings or daily operations.

The accuracy of the *absolute* beam position measurement is determined by a convolution of several factors, such as residual errors in the BPM calibration, a nominal (instinsic) spatial resolution of BPM, and systematic error like beam current dependence of electronics. In addition, mechanical stability of BPM chambers and electrodes as well as the stability of BPM electronics are also essential to sustain the precise absolute measurement in continuous operation. An overall resolution contributed by these factors has to be kept below as small as ± 10 μm, unless another approach to meet the requirement, such as a new commissioning scheme, would be introduced.

Another scenario of the commissioning may be to observe tune shifts due to the off-axis field of sextupoles, since the tune shift is more sensitive to the misalignment than the position shift is. The challenging issue is still under consideration and more confirmation is needed. Detailed monitoring schemes as well as commissioning strategies are further discussed in Ref. [1], or will come later.

BPMs would be equipped not only nearby sextupoles but also on both sides of insertion devices and long straight sections. The number of BPMs for SPring-8-II is listed in Table 5.6.

Table 5.6: The number of BPMs for SPring-8-II

Sextupole	1012
ID sides	120
LSS	16
Total	1148

In addition to the BPM system, varieties of instruments, such as current monitors, beam size monitors and bunch length monitors, are indispensable for reliable and stable beam operations. At the same time, reuse of instruments of the SPring-8 facility is also important from a perspective of cost effectiveness and environmental consideration. Since developments of these monitors other than the BPM are unlikely critical, existing instrumentations would be reused as far as it is possible.

New vacuum enclosures and in-vacuum insertion devices will have smaller apertures than the existing ones. It results in larger resistive wall impedance and other collective effects, which may cause transverse and longitudinal instabilities of beams. We have been developing a transverse bunch-by-bunch feedback system based on a new concept in order to overcome the high growth rate of the multi-bunch and single-bunch instabilities [1].

Timing Systems

As discussed in the previous chapters, the synergy of the new storage ring and the XFEL is one of unique features for the upgrade plan. The electron beam is planned to be injected from the XFEL linac to the new storage ring, and pump-and-probe experiments using X-rays provided from the two extreme light sources are supposed to give new opportunities to users. For the purpose, it should be made sure that the two light sources work together.

One of concerns is that master oscillators of the two accelerators have different frequencies; the XFEL linac is based on 2,856 MHz and other sub- and higher harmonics such as 5,712 MHz (C-band), whereas the new storage ring is designed on a 508.58 MHz basis. It should be emphasized that the situation on the frequency relation exactly happens at the current storage ring of SPring-8 and its injector. The current storage ring and the booster synchrotron are operated at 508.58 MHz, while the linac runs on a 2,856 MHz basis. Yet, a precise injection timing system from the injector to the ring successfully functions (see Ref. [30].) It is therefore expected that the similar timing system should work for the new coupling between the SPring-8 II and the XFEL linac, although further study continues.

A timing jitter is one of important issues for the design of timing systems. An acceptable timing jitter is first determined by a length of injection bucket. As described in the section of RF system, superconducting harmonic cavities are installed in order to simultaneously store short and long bunches. Since the resulting bunch length of the short one is 4 ps, the requirement for the timing jitter should be a fraction of the bunch length. Another factor that may limit the timing jitter is a requirement for pump-and-probe experiments. An overall time resolution of the pump-and-probe experiment is determined by a convolution of pump and probe pulse lengths and the timing jitter in between. Thus, it is again desirable to suppress the timing jitter below the pulse lengths. As a result, we set a goal that the timing jitter should be a few picosecond or less.

The timing jitter of the injection system is not only generated from its electronics and related devices, but also from that of synchronous phase, at which electron bunches stays as a result of radiation damping and RF acceleration. Since the synchronous phase changes as gaps of insertion devices are independently altered by users, or accelerating voltages are shifted by bunch charge fluctuation, it is also demanded to adjust a beam injection timing based on a measurement of actual bunch arrival time.

Since the accuracy of timing system in the order of a few picosecond is generally not brand-new in today's accelerator technologies, we expect that such a timing system would be feasible with existing technologies. Further study and development will continue [1].

5.3 Short Pulse Options

Short pulse options are prepared for time-resolved experiments of pico-second order and fast pump-and-probe experiments with high repetition rate. Short X-ray pulses from a storage ring have very wide spectral range and would allow us to observe dynamic evolutions of microscopic systems in various time scales from pico- to several seconds. Basic strategies of short X-ray pulse generation have been considered as follows:

(1) A target pulse width is in a range of subpico- to pico-second.
(2) Only selected bunches are shortened, leaving others untouched to avoid deterioration of the ultra low emittance. (see Fig. 5.16)
(3) Short X-ray pulses are available at all beamlines.

Subpico- to pico-second X-ray pulses are expected to fill a gap of almost three orders of magnitude in bunch lengths between several tens of femtosecond available by the SACLA linac and several tens of picosecond by the SPring-8 II. In addition, the time range of pico-second or less will be of essential importance for temporal resolution of novel pump-and-probe experiments such as a method using synchronization with SACLA called X-ray pump and X-ray probe experiments (see Chapter 4).

Figure 5.16: Short bunches are trapped in some specific buckets. Other buckets are dedicated for long bunches with the ultra low emittance.

As methodologies to generate short X-ray pulses at a storage ring, there are two types of schemes; bunch compression and bunch slicing. In general, the former is supposed to yield higher peak brilliance/flux than the latter does, because the slicing schemes extract a part of a pulse energy. The slicing, on the other hand, may enable us to generate shorter radiation pulses, some of which are even synchronized with external laser pulses. More precisely, the two types of schemes may differently affect the transverse emittance, energy spread, and other characteristics of stored beams, especially for a very low emittance ring. Note that the combination of the compression and the slicing may also work. Thus, it is necessary to thoroughly study what is a best option to generate short X-ray pulses at the upgraded SPring-8.

The bunch compression in the subpico-second range requires a very strong RF potential

to confine all electrons of a bunch. The RF potential needs to have the frequency of mm-wave range and a peak power of Giga-watt level to beat a wake potential derived from the coherent synchrotron radiation (CSR). One possible solution to apply the strong confinement potential to the electron bunches may be a mm-wave inverse free electron laser (mm-iFEL) [31] as discussed in the supplementary volume [1]. Simulation studies show that the mm-iFEL leads to the equilibrium bunch length of 0.6 ps (r.m.s.), when a bunch charge is 479 pC corresponding to a bunch current of 0.1 mA.

Another way to compress bunches is to make use of the higher harmonic RF system. Though the system is mainly supposed to lengthen stored electron bunches by modifying the main RF potential, it can also be applied to shorten the bunches once the RF phase of the higher harmonic is optimized for bunch compression. As discussed in the section of RF systems, the harmonic number of 3.5 is chosen for effective bunch lengthening. The half-integer gives an opportunity to simultaneously store short and long bunches bucket by bucket. This scheme for storing the short bunches will not require any additional installation of hardware. The shortest bunch length achieved by the 3.5th harmonic system is several picosecond longer than that by the mm-iFEL scheme, but it may still be useful for some experiments.

In the case of bunch slicing, a laser slicing technique [32] is as well one of the candidates for our purpose. The biggest advantage is the synchronization with a pump laser below a picosecond, since the X-ray pulse is sliced by the laser itself. The electron energy of 6 GeV requires a big laser with the peak power of Tera-watt region, but it is already available in a market. The peak brilliance tends to be lower compared with other schemes that compress bunches instead of slicing bunches. It is necessary to investigate whether the slicing technique is suitable for the SPring-8 II user experiments as well as is feasible at the site.

The main features of the three schemes mentioned above are summarized in Table 5.7. More detailed discussion is found in Ref. [1].

Table 5.7: Comparisons of pulse length, repetition rate and peak brilliance of three possible schemes. Peak brilliances are values relative to that from an ultra low emittance bunch of 35 pm·rad which is stretched to 40 ps (r.m.s.).

	pulse length (r.m.s.)	repetition rate	relative peak brilliance
mm-wave iFEL	$\sim$ 0.6 ps	$>$ 208 kHz	2 $\sim$ 5
3.5th harmonic RF	3 $\sim$ 4 ps	$>$ 208 kHz	4 $\sim$ 5
laser slicing	$<$ 1 ps	$\sim$ 1 kHz	$<$ 0.1

5.4 Design Alternatives

The baseline design has been presented in this chapter. The new lattice features 6 bend achromat with damping wigglers at the electron energy of 6 GeV. The stored current is assumed to be 300 mA at maximum based on the heat load estimation. In order to achieve the extremely small emittance under constraints such that the ring circumference is the same as the current one, we do not necessarily rely on existing technologies; instead, we take into consideration extensive technology developments in almost every key component so that we try to push the limit of the storage ring as further as possible.

Through the overall study via design iteration between lattice and hardwares, we have addressed technical challenges that are critical to our goal. The major challenges are listed below;

- Strong multipole magnets
- Alignment precision of magnets and new commissioning strategy for sending electron beams at the center of magnets
- Vacuum chambers equipped with radiation slots that accommodate strong magnets with small bore radii
- New injection scheme based on a fast kicker
- New RF systems including superconducting higher harmonic apparatus

The parameters presented in the report may change in detail as the design study is further proceeded. For example, the stored current could be decreased if lower emittance, i.e., smaller IBS effect, with smaller current would be preferred by users. Collective effects may also limit an acceptable maximum current when it is thoroughly studied. The RF frequency might be changed as well. The current setting, 508.58 MHz, is based on a cost effectiveness, because it allows us to continue using the existing RF systems. Another frequency, e.g., 476 MHz, might be picked up if the harmonic relation between the new storage ring and the XFEL linac, which runs at 2,856 MHz and its sub/higher harmonics, should be taken. The detailed parameters will be determined from perspectives of both accelerator and experiment sides. In addition, some of *major* parameters might be modified, if necessary. We shall here briefly overview design alternatives that may be eventually necessary to overcome the above challenging issues.

One of the possibilities is to change an electron energy. So far we have chosen 6 GeV to reduce the natural emittance. More precisely, the emittance including the IBS effect starts to increase below the electron energy of 4 to 6 GeV for a bunch current of 0.1 to 1 mA. Since the SPring-8 II aims to cover the spectral range of up to 100 keV as the current SPring-8 does, the electron energy of 6 GeV is chosen. As indicated in Section 5.2, the decrease of the electron energy relies on recent and future advances in insertion devices. Depending on demands from

Table 5.8: Comparison of power consumption (rough estimation). For SPring-8, the power consumption by the linac and the booster ring are included, while the new design does not because the two injectors will not be used. Accelerator voltages of 16, 12, and 4 MV are respectively assumed for SPring-8, new design, and the alternative. Power consumption for the higher harmonic system is assumed to be 0.4 MW for the new design and the alternative.

	Energy[GeV]/Current[mA]	Magnets [MW]	RF system [MW]	Total [MW]
SPring-8	8.0 / 100	4.1	7.7	11.8
New design	6.0 / 300	2.0	5.9	7.9
Alternative	4.5 / 300	1.5	1.9	3.4

future experiments, it may be required to increase the energy back to higher value to push the spectral range into even harder X-rays. So far, we have not found a strong reason to go beyond 8 GeV, though. Another candidate is to decrease the energy at the expense of especially flux at high photon energies above 100 keV. First, the lower energy effectively serves experiments at soft X-rays to X-rays of about tens of keV. The motivation from the accelerator point of view is that the lower energy helps relax some of accelerator parameters, including the above major challenging issues; the required magnetic field of magnets and kicker field of the injector are proportional to the electron energy, and the RF system could be smaller. The requirement for damping wigglers and the related apparatus such as absorbers would be also relaxed. Since the electron emittance is proportional to the square of the electron energy, the coherent fraction is also improved by decreasing the electron energy. Moreover, the electron energy of lower than about 5 GeV starts to bring the Touschek lifetime to a new regime where the Touschek lifetime is expected to quickly increase as the emittance becomes small [33].

Another concern is a power consumption. The expected power consumptions of current and planned accelerator complex are compared in Table.5.8. Here, accelerator voltages of 16, 12, and 5 MV are respectively assumed for the current SPring-8, the new design, and the alternative, for the similar over-voltage factor. See the figure caption for other assumptions. One can see that the energy consumption is suppressed at 6 GeV even with the average current of 300 mA. It should be emphasized, therefore, that the newly designed ring already indicates the energy efficiency. Since the new ring is expected to yield higher brilliance than the current one by two to three of orders of magnitude (see Chapter 6 in detail), it follows that the energy efficiency would be significantly improved. The possibility of decreasing the electron energy below 6 GeV should even assist it as is shown in Table.5.8. The power consumption for the 4.5 GeV/300 mA ring would be less than half of the current one. At present the energy of 6 GeV is the best compromise for our purpose, which may be adjusted more at later stages.

Another important design alternative is related to a combined function magnet, especially that combines dipole and quadrupole fields. The combined function magnets have been employed at MAX-lab [34], especially for the MAX-IV storage ring, for example. Such a magnet can decrease the packing factor, therefore a lattice with bending magnets combined with quadrupoles has been as well designed. The known challenging issue with the combined magnet is an alignment error. The dipole magnets should be carefully aligned in order to avoid undesirable kick of an orbit by quadrupole fields [1]. Another type of combined function magnet, such as sextupole magnets coupled with quadrupole fields, are also being considered.

References

[1] The SPring-8 Upgrade Plan Working Group, *Preliminary Accelerator Design of SPring-8 II*, to be published.

[2] T. Watanabe *et al.*, Proc. of IPAC'11 (Sep. 4–9, 2011), San Sebastián, Spain (2011).

[3] A. Ropert, *et al.*, Proc. of EPAC'00, Vienna, Austria, p. 83 (2000).

[4] H. Wiedemann, *Particle Accelerator Physics*, Third Edition, Springer (2007).

[5] S.Y. Lee, *Accelerator Physics*, World Scientific (1999).

[6] D. Einfeld *et al.*, Proc. of EPAC'96, Sitges, Spain, p. 638 (1996); D. Einfeld and M. Plesko, Nucl. Instrum. Meth. A **335**, 402 (1993).

[7] L. Emery and M. Borland, Proc. of PAC'03, Portland, Oregon, USA, p. 256 (2003).

[8] M. Borland, Nucl. Instrum. Meth. A **557**, 230 (2006).

[9] K. Tsumaki and N. Kumagai, Nucl. Instrum. Meth. A **565** , 394 (2006); K. Tsumaki and N. Kumagai, Proc. of EPAC'06, Edinburgh, UK, p. 3362 (2006).

[10] S.C. Leemann *et al.*, Phys. Rev. ST-AB **12**, 120701 (2009).

[11] R. Hettel *et al.*, Proc. of EPAC'08, Genoa, Italy, p. 2031 (2008); *PEP-X Status Report* (2008); K. Bane *et al.*, *A Design Report of the Baseline for PEP-X: an Ultra-Low Emittance Storage Ring*, SLAC-PUB-13999 (2010).

[12] Y. Shimosaki, "*Nonlinear Resonance Analysis for Correction of Off-Momentum Dynamic Aperture*", 2nd Workshop on Nonlinear Beam Dynamics in Storage Rings (Nov. 2–4, 2009), DIAMOND, United Kingdom (2009).

[13] K. Soutome *et al.*, Proc. of IPAC'10, Kyoto, Japan, p. 2555 (2010).

[14] Y. Shimosaki *et al.*, "*Lattice Design of a Very Low-emittance Storage Ring for SPring-8-II*", Proc. of IPAC'11 (Sep. 4-9, 2011), San Sebastián, Spain (2011).

[15] Y. Shimosaki and K. Takayama, Phys. Rev. E **62**, 2797 (2000).

[16] H. Tanaka *et al.*, Nucl. Instrum. Meth. A **431**, 396 (1999); Erratum, *op. cit.*, A **440**, 259 (2000).

[17] M. Takao, Phys. Rev. E **72**, 046502 (2005); M. Takao *et al.*, Phys. Rev. E **70**, 016501 (2004).

[18] K. L. Brown, IEEE Trans. Nucl. Sci. **NS-26**, 3490 (1979).

[19] L. Emery, Proc. of PAC'89, Chicago, USA, p. 1225 (1989).

[20] K. Oide and H. Koiso, Phys. Rev. E **47**, 2010 (1993).

[21] T. Harada, Y. Kobayashi, T. Miyajima and S. Nagahashi, Phys. Rev. ST-AB **10**, 123501 (2007).

[22] T. Naito *et al.*, Proc. of PAC'09, Vancouver, BC, Canada, p. 1620 (2009).

[23] M. Borland *et al.*, AIP Conf. Proc. **1234**, 501 (2010).

[24] Y. Kawashima, H. Ego, Y. Ohashi, and M. Hara, Proc. EPAC'08, Genoa, Italy, p. 1485 (2008).

[25] H. Ego *et al.*, Nucl. Instrum. Meth. A **400**, 195 (1997).

[26] M. Borland, "*elegant: A Flexible SDDS-Compliant Code for Accelerator Simulation*", Advanced Photon Source LS-287 (2000).

[27] P. Marchand, Proc. of the 18th Particle Accelerator Conference, New York, USA, p. 989 (1999).

[28] A. Hofmann and S. Myers, CERN ISR-TH-RF/80-26 (1980).

[29] A. Temnykh, Proc. of PAC'97, p. 3218 (1997).

[30] Y. Kawashima, T. Asaka, and T. Takashima, Phys. Rev. ST-AB **4**, 082001 (2001).

[31] V. N. Litvinenko, "*Femtosecond e-beams in storage rings*", Femtosecond Beam Science edited by M. Uesaka, Imperial College Press, p. 80 (2005).

[32] R. W. Schoenlein *et al.*, Appl. Phys. B **71**, 1 (2000).

[33] V. N. Litvinenko, ICFA Workshop (1999).

[34] http://www.maxlab.lu.se/

Chapter 6

Light Sources and X-ray Optics

6.1 Light Sources

In this section, an overview of light sources available in SPring-8 II is presented. Firstly, the basic policy on how to define the specifications of insertion devices (IDs) to be installed in the storage ring is described. Secondly, details of IDs in several typical beamlines are presented together with expected light source performances to compare with the current values. Finally, a couple of technical issues are addressed, which are crucial for the upgrade plan and operation of the new storage ring.

6.1.1 Basic Policy on ID Specification

The insertion device (ID) is one of the most important components in a synchrotron radiation (SR) facility, which actually produces high-quality SR from the electron beam accumulated in the storage ring. The quality of SR is generally characterized by three physical quantities, i.e., the brilliance, flux, and spatial coherence. In order to discuss the comprehensive performance of a SR beamline, however, we need to consider another important characteristics, i.e., the radiation power, which denotes the photon intensity obtained by integrating the photon flux over the entire energy range. In most of the experiments using a monochromatized photon beam, only the photons contained in the bandwidth and angular acceptance of the monochromator are irradiated to the sample. The other photons are absorbed by front-end components and optical elements in the beamline and then turn to heat sources in the respective devices. If the cooling capability of a particular component is not sufficient, the component can be significantly damaged or at least deformed. Such a heat load problem is especially serious for the optical elements such as monochromators and mirrors, because the deformation of these devices results in a fluctuation of the photon beam position at the sample and a variation of the energy resolution, which can lead to a significant reduction in the effective brilliance and flux. In this sense,

specifications of IDs should be defined not only to optimize the brilliance and flux but also to reduce the radiation power or heat load, especially on the optical elements.

It is well known that IDs can be classified into two types, i.e,, undulators and wigglers. As discussed in the followings, the undulator is much more advantageous than the wiggler, toward improvement of the brilliance and reduction of the heat load. This is more noticeable in the ultra-low emittance storage ring, which is one of the important keywords for the upgrade plan of SPring-8.

Let us first consider the selection of IDs in terms of the brilliance. Roughly speaking, the brilliance is evaluated by dividing the total flux by the effective optical emittance, i.e., the product of the source size and angular divergence. Because the total flux is simply proportional to the number of ID periods, the total flux from a wiggler is close to that from an undulator having the same number of periods. As long as the SR emitted from a single electron is concerned, the effective optical emittance of undulator radiation (UR) is always equal to the natural optical emittance (emittance of diffraction-limited light) and is independent of the number of periods. On the other hand, the effective optical emittance of wiggler radiation (WR) grows as the number of periods increases, and thus the brilliance of WR is usually a couple of orders of magnitude less than that of UR.

Next let us discuss the issue on how to reduce the heat load. The radiation power can be reduced by intercepting the off-axis photons by the so-called XY slit placed in the front-end section. This scheme, when applied to UR, works well because the angular spread of the photon flux at the fundamental energy (and high-harmonic energies) is much smaller than that of the radiation power, which can be eliminated effectively by the XY slit having an appropriate opening angle, without significantly sacrificing the flux. This is not the case for WR, because the angular profiles of the photon flux and radiation power are close to each other and thus narrowing the slit aperture to reduce the heat load results in the loss of available flux.

It is worth noting that the validity of the above discussions largely depends on the electron beam emittance. If it is much larger than the natural optical emittance, the brilliance does not largely depend on the type of ID any more, and the heat load reduction using the XY slit is not so advantageous because the flux angular profile is broadened by the convolution with the electron beam distribution. This in turn means that the lower the electron beam emittance becomes, the more advantageous the undulator is over the wiggler.

Summarizing the discussions above, undulators are supposed to be the main IDs in SPring-8 II and wigglers are to be selected only when the users request special optical properties that cannot be provided by undulators, such as a white spectrum or broad spatial profile.

In the following sections, specifications of IDs to be installed in several typical beamlines are presented together with the calculation results of expected light source performances.

6.1.2 Hard X-ray Beamline

Firstly, specifications of IDs for hard X-ray beamlines (HXBLs) are described. In terms of the available brilliance and flux, the magnetic period should be as short as possible. In SPring-8, in-vacuum undulators (IVUs) have been aggressively adopted in pursuit of shortening the magnetic period. In SPring-8 II, the cryogenic undulator (hereinafter cryo-undulator), which is an extension of IVU, is supposed to be the standard ID for HXBL toward further shortening of the magnetic period. In order to cover the photon energy region down to 5 keV, which is similar to that of the existing SPring-8 standard beamline, the possible shortest magnetic period is found to be 14.4 mm with the minimum gap being assumed to be 2 mm (see Section 5.2.1).

If the energy region can be confined to a more narrow one, the magnetic period can be shorter to improve the brilliance. This concept has been already applied to several beamlines in SPring-8. For example in BL35XU, an IVU with a magnetic period of 20 mm, which is the shortest one in SPring-8, is installed, and covers the photon energy region from 14.4 to 26 keV. If we would apply the same concept to SPring-8 II, the magnetic period could be shortened down to 10.2 mm. As shown later, this would result in an enhancement of the brilliance three times and flux twice. If a more broad energy region is required to the contrary, we need to lengthen the magnetic period and the high-energy region should be covered by high-harmonic radiation. It should be noted, however, that we would lose the brilliance overall, especially in the high energy region because of two effects. One is the reduction of the number of periods and the other is the shrinkage of the energy region covered by the fundamental radiation. The most straightforward way to fix the problem is to adopt a revolver undulator, which accommodates more than one magnet arrays with different magnetic periods on a rotary girder. It should be noted, however, that applying this concept to the cryo-undulator requires a lot of efforts. Instead, we consider a new cryo-undulator scheme that enables a wide-band energy coverage with the fundamental radiation, which is based on a "composite-period undulator" concept recently proposed in SPring-8.

In SPring-8 BL08W, the wiggler is used as a light source to provide hard X-ray photons with energies up to 300 keV. As stated in Section 6.1.1, wigglers would not be adopted in SPring-8 II without any special reason. For hard X-ray applications like those in BL08W, utilization of high-harmonic UR would be recommended instead of WR. As shown later, high-harmonic UR is expect to provide much better performances than WR does in terms of both the brilliance and flux with much less heat load. If a variable polarization option is requested as in BL08W, we need to consider a novel undulator magnet configuration together with its operation, because the phasing motion (moving the undulator magnet array in the longitudinal direction) under the ultra-high vacuum condition is not feasible with the existing undulator magnet configuration. Note that this is not applied to the energy region below 30 keV, where a polarization control technique based on a crystal phase retarder using the Bragg diffraction has been realized and

routinely used.

6.1.3 Soft X-ray Beamline

The soft X-ray beamline (SXBL) covers the photon energy region between 250 eV and 2 keV. The electron beam energy of 6 GeV would be so high that a high K value would be required to lower the fundamental energy of UR down to 250 eV. Assuming a conventional undulator, this results in a significant increase in the intensity of high harmonic radiation, which turns to heat sources in optical elements. The undulator specification should be defined to avoid such a heat load problem especially in SXBLs. In addition, the ID should have a capability to control or at least select the polarization state unlike those in HXBLs, because the polarization control technique, such as the crystal phase retarder in the hard X-ray region, is not yet established in the soft X-ray region. In general, the so-called APPLE-II undulator can be selected as an ID to produce a variety of polarization states. It should be noted, however, that the heat load in the linear polarization mode of this type of undulator can be significantly large when a high K value is applied, and thus it is impractical to be adopted in SXBL for polarization control.

In order to solve the problem, special undulators designed to reduce the heat load have been installed in SPring-8 and successfully operated for many years: the helical undulators for circular polarization and figure-8 undulators for linear polarization, which are supposed to be the main IDs as well in SXBLs in SPring-8 II. In the former, the helicity of circular polarization can be flipped by the phasing motion. In the latter, the vertical and horizontal linear polarization can be switched by changing the undulator gap and an adequate selection of the photon energy. It is not possible, however, to switch from the linear to circular polarization only with these undulators, and thus each SX beamline in SPring-8 is currently confined to either of the linear- or circular-polarization application except a few exceptions.

Recently, a new undulator scheme, which enables the polarization control with the heat load being kept low, has been proposed in SPring-8. In this scheme, it is possible to switch the device from the helical undulator to the figure-8 undulator with a simple procedure. Furthermore, the linear polarization angle is selectable in the figure-8 undulator mode. In SPring-8 II SXBLs, this undulator scheme could be introduced for a flexible control of polarization states.

The helicity switching speed in the above scheme cannot exceed 0.1 Hz at the moment, because it is carried out mechanically, namely by the phasing motion. In several experiments such as those with magnetic circular dichroism, the signal-to-noise ratio of the measurement strongly depends on the switching speed. For the purpose of improving the speed, a fast helicity switching system, composed of two undulators with opposite helicity and five kicker magnets, has been developed in SPring-8 and implemented in BL25SU, which is currently operated at the maximum switching speed of 10 Hz. In order to install the same system in the normal straight section of SPring-8 II, which is about 2 m shorter than that of SPring-8, we would need to make

the kicker magnets much more compact than the current ones.

Although the above helicity switching system with kicker magnets has been operated for more than 10 years and is reliable enough, it is not easy to achieve a switching speed higher than the current maximum value of 10 Hz. In order to aim at a much higher switching speed, a new helicity switching system called a segmented crossed undulator, which has been installed and under commissioning in SPring-8 BL07LSU, is considered to be an option for the faster helicity switching. It is composed of several undulator segments, half of which produce linear polarization and the rest produce vertical polarization, and electromagnet phase shifters placed in between. In order to apply this concept to the normal straight section of SPring-8 II, down-sizing the electromagnet phase shifters and shortening the magnetic period would be crucial, because all these components should be packed into the limited space of 3.7 m. If necessary, a possibility of modifying them to in-vacuum devices needs to be considered.

6.1.4 New Category Beamline

In addition to the IDs installed in the normal straight sections, two new types of IDs are supposed to be installed in the storage ring, with which new category beamlines would be available to users in SPring-8 II. One is a mini undulator to be installed in the arc section of the storage ring and the other is a damping wiggler to be utilized as a mean to reduce the beam emittance. Detailed specifications of these IDs are described in the followings.

Mini Undulator Beamline

In one of the drift spaces between magnets in the arc section, there is a slot where a short ID may be installed as a light source for a new beamline, which is referred to as Mini Undulator Beamline (MUBL). The maximum space allowed for the ID, which is decided from the geometrical condition of the adjacent magnets, is supposed to be about 0.5 m and the minimum vertical aperture is expected to be 9 mm. Considering the fact that IVUs require extra spaces with a length of several hundreds of millimeters for installation of RF transitions to connect the magnet end with the vacuum duct smoothly and electrically, out-vacuum undulators (OVUs) are more attractive than IVUs in terms of the net magnet length, even at the expense of the minimum gap. As an example, we assume an OVU with a period of 38 mm. The net magnet length is supposed to be 0.4 m and thus we have a number of periods of 10. The minimum gap and the resultant maximum K value are expected to be 13 mm and 2.3, respectively, which is large enough to smoothly connect the brilliance and flux curves between UR harmonics. Note that the possibility of adopting IVUs should be explored if the RF transitions can be much more compact than the current design.

Damping Wiggler Beamline

As mentioned in Section 5.2.1, damping wigglers are planned to be installed in the storage ring in order to reduce the emittance, which also could work as light sources for new beamlines referred to as Damping Wiggler Beamlines (DWBLs). For an efficient emittance reduction, the magnetic field and period of the damping wiggler should be as strong and short as possible (see Section 5.2.1 for details). Assuming a permanent magnet wiggler operated at room temperature, the possible magnetic field strength is at most 2.1 Tesla. The shortest period to achieve the maximum field of 2.1 Tesla at the gap of 12 mm is 200 mm, resulting in the K value of 37. The total wiggler length is decided to satisfy the requirement on the radiation damping for the emittance reduction and supposed to be several tens of meters, which is too long to be constructed in a single body and thus divided into several units with a typical length of 3 m. The arrangement and locations of these wigglers should be carefully decided with many points taken into account, such as the number of beamlines and handling of the large radiation power.

6.1.5 Expected Light Source Performances

In this section, the light source performances expected in the typical beamlines described in the previous sections are presented. The accelerator and ID parameters to be used in the calculations are summarized in Tables 6.1 and 6.2. Note that the stored current of the SPring-8 II is assumed to be 300 mA, while that of the current SPring-8 is 100 mA.

As shown in Table 6.2, two sets of parameters have been prepared for HXBL. "HXBL-A" is an alternative to the standard undulator beamline of SPring-8, while "HXBL-B" is a beamline dedicated to the confined energy region (14.4~26 keV), and, to be specific, is an alternative to BL35XU.

The light source performances have been calculated with these parameters and compared with those in SPring-8 BL03XU (standard beamline), BL35XU, BL25SU (soft X-ray beamline), BL08W (wiggler beamline), BM1 (bending magnet beamline). All the calculations have been carried out using the SR calculation code SPECTRA [1].

Brilliance

Figure 6.1 shows the brilliance available in the existing beamlines in SPring-8 and proposed beamlines in SPring-8 II as a function of the photon energy. The current values in SPring-8 are indicated by dashed lines, while those expected in the corresponding beamlines in SPring-8 II are indicated by solid lines with the same colors. We expect an improvement of brilliance by 2 and 3 orders of magnitude in SXBL and HXBL, respectively. Also note that even in MUBL, the brilliance is expected to be higher than that of the standard beamlines in SPring-8. On the other hand, almost no improvement is found in the wiggler beamline. This is a consequence of the

Table 6.1: Accelerator parameters used in the calculations. "Section" in the twiss parameter list denotes the location in the storage where a light source is installed.

(a) Beam Parameters

Beam Energy (GeV)	6
Natural Emittance (pm·rad)	35
Coupling Constant	0.02
Energy Spread	0.0011
Stored Current (mA)	300

(b) Twiss Parameters

Section	β_x (m)	β_y (m)	α_x	α_y	η_x (m)	$\eta_{x'}$
(a)	1.07	1.43	0	0	0	0
(b)	9.09	12.3	-8.40	7.15	0.020	0.018
(c)	1.07	1.43	0	0	0	0
(d)	0.29	17.1	-0.54	-0.055	0.0035	-0.0047

fact that the wiggler is an incoherent light source and the reduction of the beam emittance does not necessarily result in the improvement of brilliance. It is now clear that the use of wiggler as a light source in SPring-8 II should be avoided as long as possible, if no special reason exists.

Available Flux

Figure 6.2 shows the comparison of the available flux, i.e., the total flux integrated over the whole solid angle. In the bending magnet beamline, a horizontal angular acceptance of 0.1 mrad has been assumed for the photon beam extraction. Note that the same angular acceptance has been assumed in the wiggler beamline as well, because the angular divergence of WR is extremely large and it is thus impractical to gather all the photons and irradiate to the sample.

The improvement of the available flux from the existing values is not so significant compared to that of the brilliance, because it is independent of the electron beam emittance. Even so, we can expect an improvement by one order of magnitude in the undulator beamlines thanks to the increase in the average current and number of magnetic periods. Note that the flux available in MUBL is much larger than that in BM1 in SPring-8 under the supposed condition, and thus we can conclude that the construction of MUBL is useful in terms of the available flux as well as the brilliance.

Table 6.2: ID parameters used in the calculations. See the caption of Table 6.1 for the meaning of "Section".

Beamline	Source Type	Period (mm)	Min. Gap (mm)	Max. K	Length (m)	Section
HXBL-A	cryo-undulator	14.4	2	2.74	3	(a)
HXBL-B	cryo-undulator	10.2	2	1.61	3	(a)
SXBL	Helical Undulator	75	12	4.15	3	(a)
MUBL	Planar Undulator	38	13	2.3	0.38	(b)
DWBL	Damping Wiggler	200	12	37	3	(c)
BM	Bending Magnet	-	-	(0.7 T)	-	(d)

Spatial Coherence

The spatial coherence of SR is usually characterized by the so called coherent fraction $p_{x,y}$ defined as

$$p_{x,y} = \frac{\lambda/4\pi}{\sqrt{\sigma_r^2 + \sigma_{x,y}^2}\sqrt{\sigma_{r'}^2 + \sigma_{x',y'}^2}},$$

where σ_r and $\sigma_{r'}$ denote the source size and angular divergence of radiation emitted from a single electron when passing through an undulator, $\sigma_{x,y}$ and $\sigma_{x',y'}$ denote the beam size and angular divergence of the electron beam in the horizontal and vertical directions at the source point (undulator center), respectively. The coherent fraction corresponds to the M^2 factor in the laser optics and has the maximum value of 1, with which radiation can be focused to the size determined by the diffraction limit using the ideal optics.

Figures 6.3(a) and (b) show the comparison of the coherent fraction in the horizontal and vertical directions, respectively. In the horizontal direction, we can expect an improvement by one (SXBL) or two (HXBL) orders of magnitude. On the other hand, the improvement is not so significant in the vertical direction, because the coherent fraction is already close to 1 especially in the lower energy region. It should be noted that the wiggler beamline has a coherent fraction much lower than 1 in any case, reflecting the fact that the wiggler is an incoherent light source.

Heat Load

In addition to the light source performances described above, the heat load should be also investigated as explained in Section 6.1.1, in particular, in the undulator beamline. Figure 6.4 (a) shows the total radiation power as a function of the fundamental energy in the undulator beamlines except MUBL. Similar to the available flux, the radiation power would increase by nearly

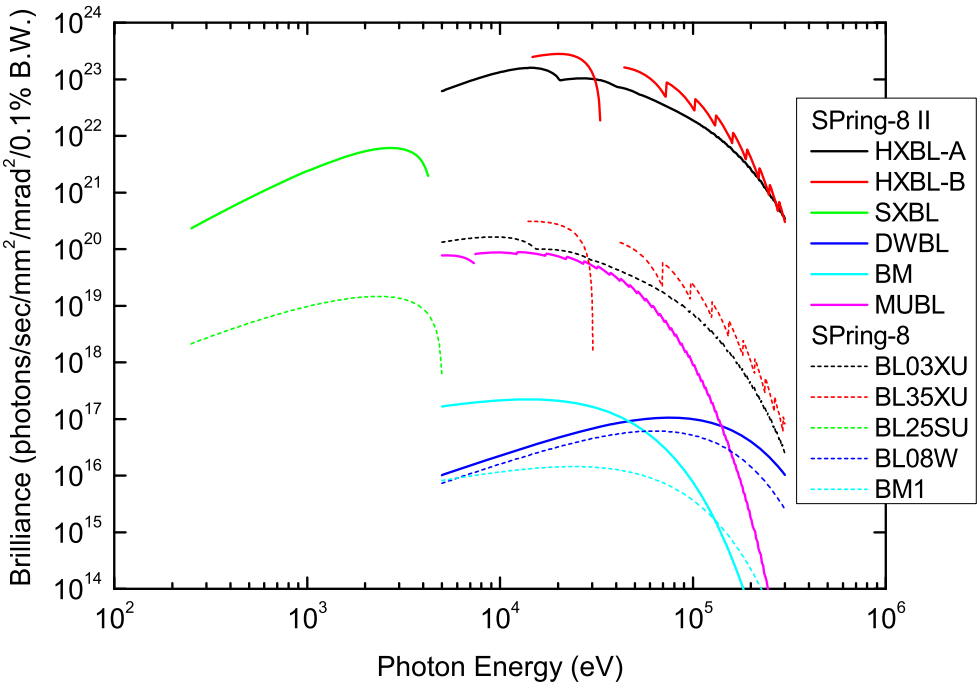

Figure 6.1: Comparison of the brilliance curve available in the existing beamlines in SPring-8 and proposed ones in SPring-8 II. Peak values at respective harmonics are plotted in the undulator beamline, while a spectrum obtained at the maximum K value is plotted in the wiggler beamline. The stored current of 300 and 100 mA are respectively assumed for SPring-8 II and SPring-8.

one order of magnitude because of the increase in the average current and number of periods. It is thus important to carefully design the high-heat load components in the front end section.

Concerning the heat load on optical elements such as the mirror and monochromator, we need to check the partial radiation power passing through the XY slit to eliminate the off-axis power. The calculation results are plotted in Fig. 6.4 (b) as a function of the fundamental energy. The aperture size of the XY slit is assumed to be four times the photon beam size at the fundamental energy so as not to lose the available flux too much. The partial radiation power in SPring-8 II beamlines is found to be at most double of that in the corresponding beamlines in SPring-8, which means that the heat load on optical elements is less problematic than that in the front end section. From the above discussions, it is clear that the heat load reduction using the XY slit works better in SPring-8 II than in SPring-8 thanks to the lower electron beam emittance. It should be noted, however, that the heat load is still larger than the current values and the cooling system of optical elements should be considered carefully.

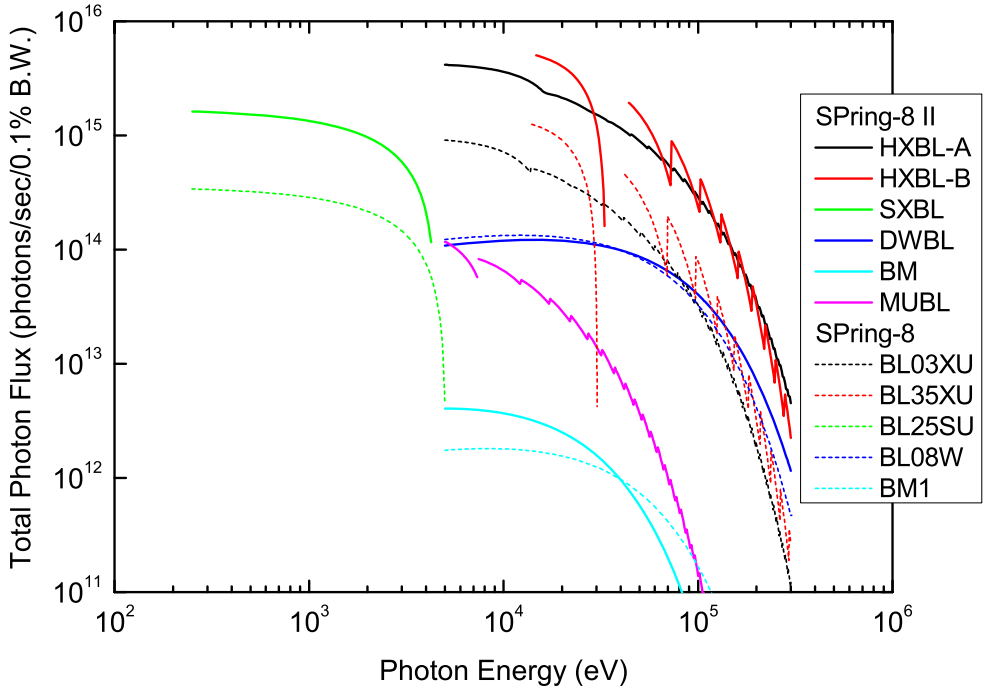

Figure 6.2: Comparison of the flux available in the existing beamlines in SPring-8 and proposed ones in SPring-8 II. The stored current of 300 and 100 mA are respectively assumed for SPring-8 II and SPring-8.

6.1.6 Recycle of the Existing IDs

Although more than 30 IDs have been installed in SPring-8, they cannot be reused in SPring-8 II without modifications mainly because of two reasons. Firstly, the straight section length, which is 5.7 m in SPring-8, will be shortened to 3.7 m to allow the multi-bend lattice configuration for the ultra low emittance ring. Secondly, undulator parameters such as the magnetic period and minimum gap are supposed to be changed. For the total cost reduction, however, we have to recycle the components of existing IDs as much as possible. For example, the SPring-8 ID mechanical frame is composed of three units with a length of 1.5 m, and thus can be decomposed and reassembled to a new mechanical frame with the total length of 3.0 m using two of three units. For this to be applicable, the length of the space in the both ends of the ID, which is occupied by several components and currently 1.2 m long, should be shrunk down to 0.7 m. In particular, beam position monitors (BPMs), which are now working as part of an interlock system for the electron beam trajectory error, are to be excluded from the components installed in the ID straight section, by integrating their functions into other BPMs being distributed over the storage ring.

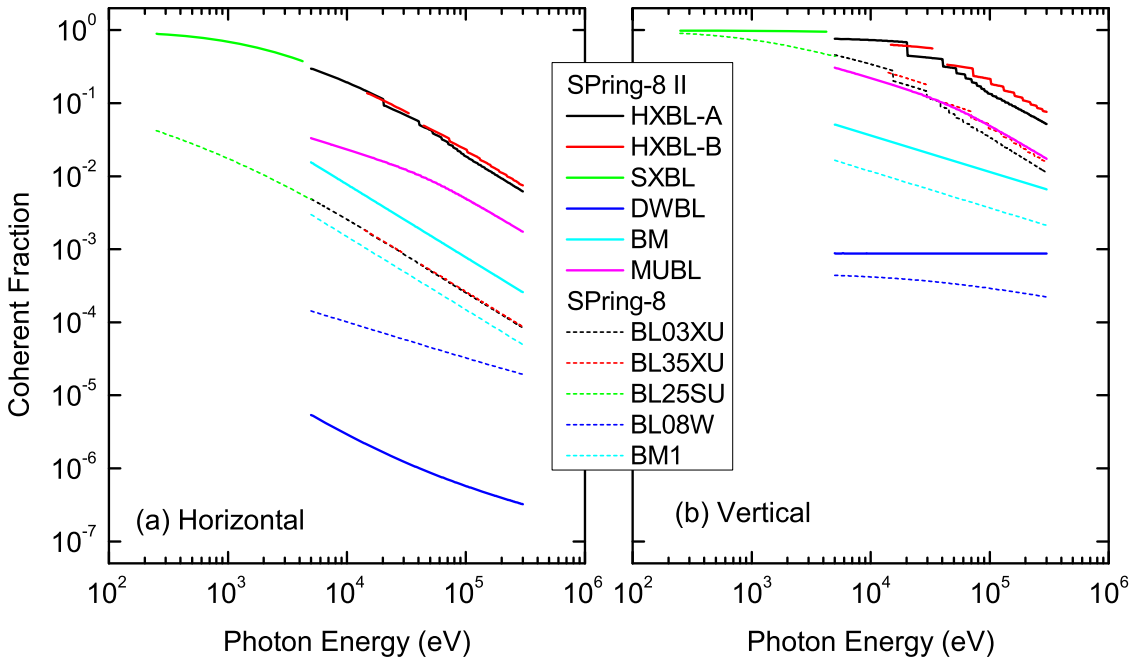

Figure 6.3: Comparison of the coherent fraction in the (a) horizontal and (b) vertical directions.

6.1.7 Beam Stabilization

It is expected in SPring-8 II that a high-flux and nano-focusing beam will be available by introducing a nanometer-focusing mirror and de-magnifying the light source directly without any virtual source in the beamline (see Section 6.3.3). On the other hand, this would impose that the electron beam characteristics at the source point (undulator center) should be extremely stable not to spoil the focusing performance. We have three relevant factors to take care concerning the undulator operation: residual field integral, natural focusing and radiation loss, which can be varied when opening and closing the undulator gap.

The variation of field integral leads to the beam-orbit fluctuation and thus spoils the pointing stability of the photon beam. In SPring-8, it is already corrected by adjusting the current of the steering coil installed in the both ends of the ID based on a feed-forward table created in advance and we shall investigate the scheme to improve the correction resolution and reliability if necessary. The variations of natural focusing and radiation loss cause fluctuations in betatron function and beam emittance, which result in the variations of the beam size and angular divergence. In principle, they can be compensated by adjusting the current of the quadrupole magnets and the gap of the damping wigglers. It is thus important to discuss the correction procedures and its implementation, including its necessity.

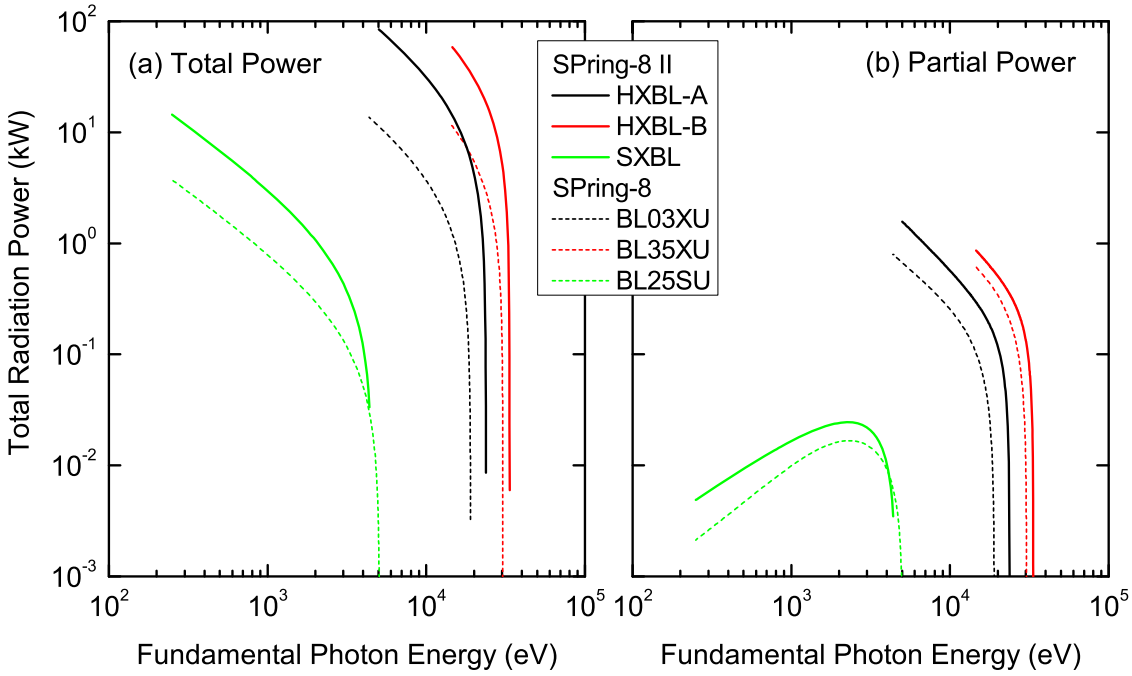

Figure 6.4: Comparisons of the heat load: (a) total radiation power and (b) partial radiation power passing through the XY slit. See text for details. The stored current of 300 and 100 mA are respectively assumed for SPring-8 II and SPring-8.

6.1.8 Summary

In this section, the basic policy to define the ID specifications and expected optical performances have been presented. It should be noted that they are based on the state-of-the-art technologies and ideas currently available, and thus can be modified further according to the progress of the ID technology and theory.

6.2 Front end

The photon beams are transported through the front-end section connecting the light source and the X-ray optics of the beamline, where unwanted heat components in the original radiation is eliminated. Another important function of the front-end section is to monitor the beam position of the radiated X-rays. In the SPring-8 upgrade plan, two key developments in the front-end components will be indispensable: (1) high-heat-load handling, and (2) fast beam-position monitoring technologies.

6.2.1 Handling of high heat load

Newly-developed cryogenic undulators with a short period and a narrow gap would be installed in the upgraded SPring-8 storage ring to dramatically enhance the photon flux. These new undulators would considerably increase the total radiation power as well. Therefore, the front-end section of SPring-8 II beamlines should be designed to eliminate the higher heat load adequately. Otherwise, the heat load onto the downstream X-ray optics would be too high and their designs would be severely restricted. Thus the increase of the heat-load capacity of the front-end components is an unavoidable issue. We are currently performing studies on the following issues.

1. Thermal limitation of the existing high heat load components, made of dispersion-strengthened copper with ultra-fine particles of aluminum oxide and oxygen-free copper
2. Volumetric heating technology
3. Reducing the thermal contact resistance in junctions of photon absorbers
4. Development of multifunctional components (e.g. integration of a fixed mask and a photon absorber)
5. Development of "speckle-free" X-ray windows with a high heat-load resistance

These investigation will be continued until a solution is achieved where the heat load from the high-power undulators could be safely handled. Another important issue is to tune the performances of the high-heat-load components for different light sources, *i. e.* standard undulator, mini-undulator, and bending magnet. The light source of each beamline is optimized to the required photon energy range, energy bandpass, photon polarization, and so on. The period, number of period, total length, minimum K values, correspondingly the resulting radiation power, are different at each beamline.

6.2.2 Pulse-by-pulse monitoring of X-ray beam position

As discussed in Section 3.1, clarification of the time-evolution of physical and biological phenomena would be one of the main scientific targets using the upgraded SPring-8. These studies use the short-pulse characteristics of the X-ray beam and a pump-probe scheme. For such studies, "pulse by pulse" stability of the X-ray beams would be required in addition to the long-term stability that has been established in SPring-8. For pulse-by-pulse diagnostics of the X-ray beam position, a fast beam-position-monitor device is needed. We have been developing a new detector head with a photocathode made of a micro-strip line structure that is capable to work in the GHz range. With the detector, the beam position of individual X-ray pulses (separation

of 2 ns) was successfully measured. An evaluation study at a bending magnet beamline showed a good performance with resolutions in position of $\lessapprox 10$ μm, in intensity of $\lessapprox 1\%$, and in time of $\lessapprox 10$ ps. The heat load resistance of the device remains to be an unresolved issue. When the heat load resistance is improved, the detector with a micro-strip line structure would be a promising fast beam-position monitor device that may be installed in the undulator beamlines at SPring-8 II.

Further, correlation analysis between the electron and photon beam positions would allow us to stabilize the X-ray beam more accurately and reliably. A beam position diagnostic system that simultaneously determines the positions of the electron beam in the storage ring and the X-ray beam at the beamline would be introduced at SPring-8 II.

6.3 X-ray optics

SPring-8 II will allow pioneering studies in a wide range of research fields as discussed in Chapters 3 and 4. The enhanced brilliance and flux of the X-ray beam will push the studies requiring high sensitivity and efficiency. Development in optics for the upgraded SPring-8 is important to efficiently deliver high quality radiation to the sample. A mission of the optics in SPring-8 II is to concentrate as many photons as possible into real or reciprocal space with the appropriate size for each experiment. The X-ray beam should be highly tunable since the required beam sizes may range from square millimeter to square nanometer. To provide an extremely stable beam is another big issue. In this section, we describe the basic specifications of the X-ray optical components for SPring-8 II standard undulator beamlines. Requirements for optics in mini-undulator beamlines and bending-magnet beamlines would be much more relaxed. Optical components for these beamlines may be designed with small modifications of those in the standard undulator beamlines.

6.3.1 Monochromator

Double-crystal monochromators will be used in most standard undulator beamlines in SPring-8 II, as have been in SPring-8. Silicon- or diamond-single crystals are selected as the monochromator crystals, producing monochromatic X-rays between 4 and 40 keV with an energy bandwidth of $\Delta E/E \approx 10^{-4}$. The basic mechanical design of the monochromator remains unchanged from that currently adopted in SPring-8. The stability and radiation tolerance would be the major issues that needs to be improved to an ultimate level for various scientific research to be successfully conducted.

Mechanical stability

Excellent mechanical stability in the monochromator is highly required, particularly for experiments using a nano-focused X-ray beam. At SPring-8 II standard undulator beamlines, an X-ray flux of 10^{14} photons/s could be focused in an area of 50×50 nm^2 by directly demagnifying the light source using KB mirrors (see Section 6.3.3). There would be a great progress in photon flux density of 70,000 times from the case of SPring-8, where the beam size was too large and a demagnification of a small virtual source, slits or pinholes, is often used for X-ray focusing. In the direct demagnifying scheme, the monochromator is the only optical component between the light source and the focusing mirror. Angular vibration of the monochromator crystals, if exists, could significantly affect the effective focused beam size. The angular vibration of a monochromator crystal has to be suppressed to within 0.1 μrad (0.02") for 50×50 nm focusing. Possible sources of the angular vibration are, for example, circulation of coolant inside crystals, vibrations of vacuum systems, air conditioners, and the vibrations of the floor. Currently, the angular vibration of the monochromator was estimated to be approximately 1 μrad in June 2011, still one order of magnitude larger than the required level. Further R&Ds to improve the mechanical stability are ongoing.

Thermal stability

Various kinds of heat transfer occur inside and outside of a monochromator chamber. The strategy to tackle thermal stability problems is divided into two approaches, namely, an effective cooling of the monochromator crystals and a stable temperature control of the whole equipment.

Most of the power from the incident radiation is transformed into heat in a narrow area on the irradiated surface of the first monochromator crystal. Without sufficient cooling, thermal deformation of the crystal lattice would result in a deteriorating performance of the monochromated X-ray beam. Cooling systems must be designed with a careful consideration on the following three important factors; thermal conductivity, thermal expansion, and heat transfer. In SPring-8 undulator beamlines, the cooling of the silicon crystals is carried out by two kinds of coolant: cryogenic liquid nitrogen or water at room temperature. In the cryogenic cooling system, silicon crystal blocks are mounted on copper plates cooled with liquid nitrogen. Silicon crystals have a good performance with respect to thermal conductivity and thermal expansion near the liquid nitrogen temperature. However heat transfer from the crystal is not very good as the crystals are cooled indirectly. On the other hand, in the water-cooling system, the crystal has a pin-post shaped water channel just beneath the irradiated surface for efficient heat exchange. The pin-post channel causes a turbulent water flow that increases the heat transfer rate. Both cooling systems could effectively work for an incident radiation power of 500 W and a power density of 500 W/mm^2. However, the power and power density expected from the light sources of SPring-8 II is twice of this level, 1 kW and 1 kW/mm^2, therefore an enhancement of cooling

power is required.

All three processes, thermal conductivity, thermal expansion, and heat transfer, need to be optimized in the crystal cooling system adapted for SPring-8 II. A simple solution is to use both the cryogenic cooling and the heat-transfer channel. A new design, different from the conventional pinpost shape, would be required. Additionally, the flow rate of liquid nitrogen needs to be increased from the current level of 4 L/min to 10 L/min, to reduce the pressure drop within the transport pipes inside and outside of the monochromator.

When the temperature inside a monochromator is not stable, thermal deformation of the stepper stages in the monochromator results in a drift in beam intensity over time. Secondary radiation generated at the first crystal also acts as a heat source, while liquid nitrogen works as a negative heat source. We have successfully controlled the temperature of SPring-8 monochromators with a fluctuation of only 0.1 °C (peak-to-valley) using additional heaters and radiation shields. Further improvement would be needed.

Radiation torelance

Since the monochromators in SPring-8 II will be subjected to exposure of the X-ray flux several times higher than that of current SPring-8, the radiation damage to various parts of the monochromator would be considerably higher. Especially, the resistance to high-energy radiation of coating on electric wires would be one of the most serious problems. To solve this problem, we plan to cover the wires with effective radiation shields and to use wires coated with polyimide.

6.3.2 Mirrors for higher-harmonic rejection

X-ray beams obtained with a crystal monochromator inevitably contain higher-order harmonic X-rays aside from the first-order X-rays. Total reflection mirrors are widely used to remove the higher-harmonic X-rays. The glancing angle of an incident beam is as small as a few milliradians when a total reflection mirror is used. This results in a large irradiation footprint at the surface of the mirror, significantly reducing the power density on the mirror surface. For this reason, the cooling of such a total-reflection mirrors is much easier than that of monochromator crystals. A configuration of beamline optics, in which a total reflection mirror is placed in front of a monochromator, is a reasonable solution for SPring-8 II to handle the high power radiation, instead of the present configuration, in which the monochromator is used as the first optical component, in SPring-8 beamlines.

6.3.3 Nanometer-focusing mirror optics

Focusing of X-rays down to a size of 1 nm is a challenge of the current synchrotron radiation facilities. The present record in the smallest X-ray beam size is 7×8 nm [2], which RIKEN and Osaka University have recently accomplished at SPring-8 using the precise multilayer mirrors in the Kirkpatric and Baez (KB) configuration. SPring-8 is one of the leading center for the X-ray nano-focusing techniques [3]. The diffraction limited light source available at SPring-8 II would accelerate the developments to realize the ultimate X-ray nanobeams, aiming towards the size of molecules.

In addition to the benefit for the ultimate nanofocusing, the extremely high brilliance of SPring-8 II light source will significantly increase the photon flux in an X-ray focus spot with the size of a few tens of nanometer. Figure 6.5 illustrates the remarked difference of the photon flux obtained in a beam spot, from 40×40 nm^2 to 1×1 μm^2, before and after the upgrade. Calculation was made assuming the X-ray energy of 15 keV and the X-ray optics similar to those at present SPring-8 undulator beamline, where a 100 nm focusing has been recently achieved. The optics include the standard double-crystal monochromator and the KB focusing mirrors. It is assumed that crossed-slits would be inserted as the virtual source downstream of the monochromator when the source size is too large for focusing by demagnifying itself. In the figure, the flux curves suddenly drop at the focus size thresholds of 100×100 nm^2 for SPring-8 and at 50×50 nm^2 for SPring-8 II. These threshold sizes are determined by the source size. Direct focusing (demagnifying) of the light source is used for the focus size larger than these thresholds, where nearly all the flux from the source could be collected in the focus spot. A small virtual source (a few micrometer square), on the other hand, is needed to achieve the focus size smaller than these thresholds, significantly reducing the flux in the focus spot. The focus size achieved by demagnifying the source is much reduced from 1 μm to 50 nm in horizontal direction due to the much smaller source size after the upgrade. Thus, the increased brightness and the reduced source size of the SPring-8 II significantly enhances the X-ray intensity at the focus spot. The enhancement of the flux is estimated to be 300 times for the 100 nm square-focusing, 70,000 times for 50 nm square, and 14 times for 40 nm square.

Developments of new focusing optics is currently ongoing: multilayer KB mirrors [3] and a single mirror with an ellipsoidal surface profile, with an enlarged numerical apertures, will be promising to further reduce the focus size and enhance the available focused beam flux. Additionally, multilayer mirror would offer an option for a wide-bandpass monochromator to increase the photon flux by one order of magnitude with a reasonable bandpass. In addition, we shall continue to make every effort to stabilize the optical components. For focusing systems, a stability of pico-meter-order is needed for providing the stable nanometer-size of X-ray focused beams.

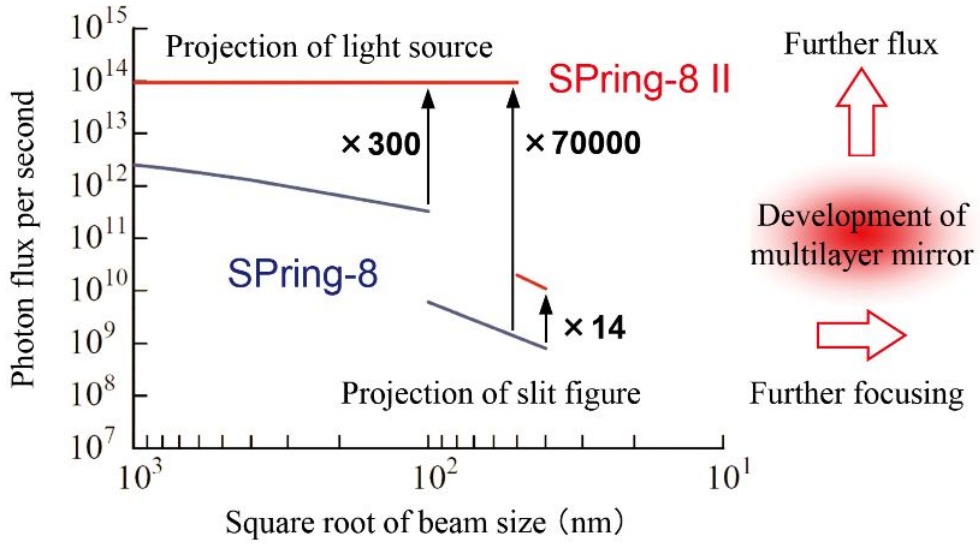

Figure 6.5: Comparison of the X-ray photon flux available in a nanometer-focused spot at the standard undulator beamlines of SPring-8 and SPring-8 II (left). Development of multilayer fabrication will be a key issue to further enhance the flux and to reduce the focused spot size (right).

6.3.4 X-ray beam position monitor

The angular vibration of a monochromatic X-ray beam has to be be suppressed within 0.1 μrad for nano-focusing experiments, as shown in Section 6.3.1. Real-time detection of the position and direction of the X-ray beam with a feedback stabilization system is planned to be installed at SPring-8 II standard undulator beamlines. This system consists of two X-ray beam position monitors placed just behind the monochromator and just before the focusing mirrors, at a typical distance of 30 m. The required angular resolution of 0.1 μrad may be achieved using the two monitors that have a positional resolution of 1 μm separated by this distance.

References

[1] T. Tanaka and H. Kitamura, J. Synchrotron Rad. **8**, 1221 (2001).

[2] K. Yamauchi, H. Mimura, T. Kimura, H. Yumoto, S. Handa, S. Matsuyama, K. Arima, Y. Sano, K. Yamamura, K. Inagaki, H. Nakamori, J. Kim, K. Tamasaku, Y. Nishino, M. Yabashi, and T. Ishikawa, J. Phys: Cond. Mat. **23**, 394206 (2011).

[3] H. Mimura, S. Handa, T. Kimura, H. Yumoto, D. Yamakawa, H. Yokoyama, S. Matsuyama, K. Inagaki, K. Yamamura, Y. Sano, K. Tamasaku, Y. Nishino, M. Yabashi, T. Ishikawa, and K. Yamauchi, Nat. Phys, **6**, 122 (2010).

Appendix A

Outline of the Upgrade Project

The discussion on the SPring-8 upgrade plan was initiated in 2007, and in October, 2008, the SPring-8 upgrade working group (WG) was organized by about 50 staffs. The first result of the discussion done by the working group came out as an internal report in December, 2008, which defined "boundary conditions and expected light source performance of the upgraded SPring-8" from the viewpoint of scientific requirements. The internal report started with setting the time schedule and the target cost range; the upgrade is supposed to be executed in 2019 with one-year dark time, and the budget should be around 40 billion Japanese yen. Another specific 'boundary condition' is that existing buildings with accelerator tunnels as well as experimental hutches should be reused for the cost-effectiveness. Regarding the light source performance, it was claimed that the brilliance should be increased by multiple orders of magnitude by significantly reducing the horizontal emittance, while covering a similar spectral range of X-ray and keeping the stability that the current SPring-8 has.

Upon the requirements, the WG soon started looking through many possibilities, such as the Energy Recovery Linac (ERL) and the minimal upgrade of the existing storage ring. Simultaneously, future scientific cases were extensively discussed, of which result was summarized in the next internal report on "future scientific cases" in March, 2009. The discussion on the expected scientific cases has been continued, and is summarized in the preliminary report as well.

Since the middle of 2009, symposiums and workshops have been held almost annually. The symposiums mainly focus on scientific perspective of future photon sciences that is expected to be explored at the SPring-8 II, or even beyond that. The discussions are not necessarily limited to scientific or industrial areas that are already connected to the photon sciences executed at the SPring-8. Instead, the discussions are open to various possibilities at new scientific frontiers. The workshops, on the other hand, focus on accelerator design for the SPring-8 II. The purpose is to find out an optimum accelerator design that best matches scientific studies and industrial applications discussed at the symposiums and other opportunities.

The first workshop was held in December, 2009. First, the WG showed the ultimate goal of

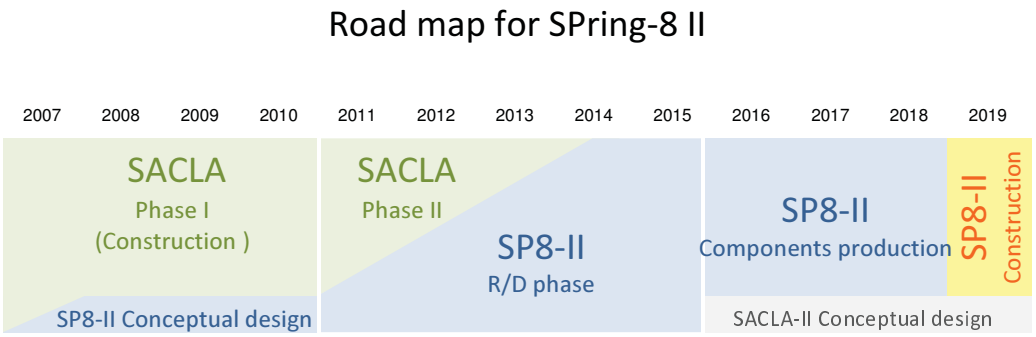

Figure A.1: Planned Schedule for SPring-8 II.

Table A.1: Milestones

Date	Events
Oct. 10, 2008	Kick-off of the SPring-8 Working Group
Dec. 18, 2008	Release of Internal Report on "Boundary Condition and Expected Light Source Performance of the Upgraded SPring-8"
Mar. 24, 2009	Release of Internal Report on Future Scientific Cases
Jun. 19, 2009	1st Symposium on SPring-8 Future Ugprade 2019
Dec. 12, 2009	1st Workshop on SPring-8 II Accelerator Design
Dec. 4, 2010	2nd Symposium on SPring-8 Future Upgrade 2019
Apr. 25, 2011	2nd Workshop on SPring-8 II Accelerator Design

the SPring-8 II plan, and the basic accelerator strategy was introduced. However, the presentation did not go into detail at the stage. Six speakers from KEK and JAEA then talked about accelerator developments and current status at each facility, such as the KEKB, the cERL, and J-PARC.

In December, 2010, and April, 2011, the second symposium and workshop were held. Through the second series of the meetings, the scientific perspective of future photon sciences at the SPring-8 and the resulting requirements to the light source performance had been made clearer, and the further developed accelerator design, not only in lattice but also in hardwares, was presented and was intensively discussed. Although there are still critical issues remained for securing the new accelerator design, the basic strategy was briefly fixed. The accelerator design described in this report is based on the result of the 2nd workshop.

In addition to the two series of symposiums and workshops, the WG members have presented the upgrade plan at public conferences, workshops, and meetings. The presentations are listed in the following.

Presentation Lists

1st Symposium on SPring-8 Future Upgrade 2019 (Tokyo, Jun. 19, 2009)

M. Yabashi, “Overview of the SPring-8 upgrade”
M. Suzuki, “Perspective on future photon sciences with the upgraded SPring-8”
K. Soutome, “Accelerator design approach toward the SPring-8 upgrade”
H. Yamazaki, “Strategy of beamline developments for the future plan”
K. Maejima, “X-ray bioimaging: possibilities and future”
S. Matsui, “Cutting-edge nano-technology and photon science”
Y. Tokoro, “Photo-induced phase transition dynamics”
S. Fujioka, “Future perspective of high-energy density science”
(All in Japanese.)

1st Workshop on SPring-8 II Accelerator Design (SPring-8, Dec. 22, 2009)

M. Yabashi, “Introduction of SPring-8 upgrade plan”
T. Watanabe, “Future strategy of accelerator development for the upgrade”
M. Yoshida, “Improvement of beam quality of Linac and its application”
H. Sakai, “Development status of ERL linac and super-conducting cavities”
Y. Ohnishi, “Current status of KEKB and the upgrade plan”
M. Kinsho, “Current status of J-Parc accelerators and the power upgrade plan”
K. Oide, “Suggestions to the SPring-8 upgrade plan - round beam, second-floor ring etc -”
(All in Japanese.)

2nd Symposium on SPring-8 Future Upgrade 2019 (Tokyo, Dec. 4, 2010)

M. Yabashi, “Current status of SPring-8 upgrade plan”
M. Suzuki, “Future photon sciences enabled by the SPring-8 II”
T. Watanabe, “Next generation light source development for future sciences”
R. Kainuma, “Discovery of magnetic shape memory alloy and its exotic behavior”
S. Kobata, “Light-driven controllable molecules and crystals”
T. Fukada, “Elucidation of functions of bio-essential elements and its future clinical applications”
(All in Japanese.)

2nd Workshop on SPring-8 II Accelerator Design (SPring-8, Apr. 25–26, 2011)

T. Watanabe, “Overview of SPring-8 upgrade plan”
K. Soutome, “New lattice design of ultimate storage ring”

K. Fukami, “New designs and developments of magnet and vacuum systems”
T. Fujita, “Challenges of monitor systems for SPring-8 II”
T. Nakamura, “Proposal of new injection systems”
H. Ego, “Development of fundamental and higher harmonic RF systems”
M. Masaki, “Study on short X-ray pulse generation from storage ring”
Y. Shimosaki, “Numerical result of detuned lattice” etc.
(All in Japanese.)

2nd Workshop on Nonlinear Beam Dynamics in Storage Rings (Oxford, Nov. 2–4, 2009)

Y. Shimosaki, “Nonlinear resonance analysis for correction of off momentum dynamic aperture”.

Workshop on Low Emittance Ring (CERN, Jan. 12-15, 2010)

T. Watanabe, “SPring-8 upgrade plan and short bunch options”
K. Soutome, “Feasibility study of very low emittance rings at SPring-8”

ICFA Advanced Beam Dynamic Workshop on Future Light Sources (SLAC, Mar. 1–5, 2010)

T. Watanabe, “SPring-8 upgrade plan”

International Particle Acceleartor Conference 2010 (Kyoto, May 23–28, 2010)

K. Soutome, “Design study of a very low-emittane storage ring for the future upgrade plan of SPring-8”

7th Annual Meeting of Particle Accelerator Society of Japan (Himeji, Aug. 4–6, 2010)

K. Fukami, “Beam transport from XFEL-linac to storage-ring in SPring-8”
Y. Shimosaki, “Correction of off-momentum dynamic aperture” (All in Japanese.)

Joint Meeting of High-Pressure Materials Science Group and Planetary Science Group (SPring-8, Jan. 5–6, 2011)

M. Suzuki, “Introduction of SPring-8 upgrade plan” (in Japanese).

24th Annual Meeting and General Assembly of the Japanese Society for Synchrotron Radiation Research (Tsukuba, Jan. 7–10, 2011)

Y. Shimosaki, "Design study of very low-emittance lattice for SPring-8 II storage ring" M. Masaki, "SPring-8 upgrade plan: Study on short X-ray pulse generation" (All in Japanese.)

Meeting of Industrial Users Society of SPring-8 (Kobe, Jun. 9, 2011)

M. Suzuki, "Overview of SPring-8 upgrade plan" (in Japanese).

The 14th Annual Meeting of Japanese XAFS Society (UVSOR, Sep. 9, 2011)

Y. Tamenori, "Introduction of SPring-8 upgrade plan" (in Japanese).

ICFA Beam Dynamics Mini Workshop on Low Emittance Rings 2011 (Crete, Greece, Oct. 3–5, 2011)

K. Soutome, "SPring-8-upgrade: Lattice design of a very low emittance storage ring"
K. Fukami, "SPring-8 upgrade: Strong magnets for ultimate storage ring"

8th Annual Meeting of Particle Accelerator Society of Japan (Tsukuba, Aug. 1–3, 2011)

Y. Shimosaki, "Dynamic aperture correction for very low-emittance storage ring of SPring-8 II"
C. Mitsuda, "Construction of beam transport magnets from SACLA linac to SPring-8 storage ring"
M. Masaki, "Simulation study of short bunch generation using mm-wave inverse FEL at the SPring-8 storage ring"
(All in Japanese.)

SPring-8 Conference 2011 (Tokyo, Nov. 1–2, 2011)

M. Suzuki, "Contribution to cost-effective society through ultimate storage Ring (1)"
T. Watanabe, "Contribution to cost-effective society through ultimate Storage ring (2)"
(All in Japanese).

Meeting of SUNBEAM Consortium (SPring-8, Nov. 7, 2011)

M. Suzuki, "Introduction of SPring-8 upgrade plan" (in Japanese).

The 2nd Meeting on High-Pressure Applications of Future Light Source (Okinawa, Nov. 8, 2011)

N. Hirao, “SPring-8 upgrade plan” (in Japanese).

International Particle Accelerator Conference 2011 (San Sebastian, Spain, Nov. 11, 2011)

T. Watanabe, “Current status of SPring-8 upgrade plan”
Y. Shimosaki, “Lattice design of a very low-emittance storage ring for SPring-8 II”
M. Masaki, “A proposal of short X-ray pulse generation from compressed bunches by mm-wave iFEL in the SPring-8”
C. Mitsuda, “The construction status of beam transport line from XFEL-linac to SPring-8 storage ring”
K. Tsumaki, “Design of a beam transport line from the SACLA linac to the SPring-8 storage ring”
T. Watanabe, “Measurement of longitudinal dynamics of injected beam in a storage ring”

Note: In above, only speakers are shown without co-authors or the on-behalf-of descriptions, and some of Japanese titles were translated into English not by the speakers, but by the editors of the preliminary report.